Engineering View of Gravitation

by

Carver Mead

DOI: 10.7907/me3d-6f20

ISBN-13: 9781600490149

ISBN: 160049014X

Contents

Chapter 1

Introduction

1.1 Personal Note

I became interested in gravitation in 2004, when I attended the launch of the Gravity-Probe B satellite[27]. The evening before the launch, Francis Everitt, the principal investigator on the project, gave a delightful presentation describing in simple terms what was being measured, and how the measurement was done. I had just finished my "Little Green Book"[44] a few years earlier, and the effect they were looking for sounded just like the four-vector coupling in that book, *but with gravitation instead of magnetism.* When I got home, I started working on the problem, to see if I could use four-vector gravitational coupling to analyze it. Of course I went down several rat-holes, as one always does in a new field, but within a year or two I had a really clean solution, which I wrote up while it was still fresh in my mind. That writeup appears as Chapter 11 in this document. Then, of course, I wondered if I could get the "tests of GR" with my approach. After a long struggle I was able to get a clean understanding of planetary orbits, and, by incorporating both a relativistic wave function and vector-potential coupling, came up with exactly Einstein's orbital precession formula at first order beyond Newton. I wrote that one up as I went along because figuring out something like that in a new way is *very satisfying!* It appears in this document as Chapter 10.

In both these cases I realized that my approach was *much simpler* than GR, and I could describe it *conceptually.* As the years passed, I tried to develop a conceptual understanding of various phenomena involving gravitation and Quantum matter waves. Whenever I would get a clean understanding of one, I would write it up so I could remember it later. So my file system accumulated a decent number of these writeups, and I thought about making them into a book. The first attempt got bogged down, so I gave up, and it lay fallow for some years.

When I would try to talk to anyone about it, there would be either a blank stare, or some statement like:
"It has been shown that GR is the unique formulation that encompasses:

1. The principle of relativity as expressed by general covariance
2. The principle of equivalence."

When I would reply that those proofs only applied to metric theories, and

1. G4v is not a metric theory—it has a variable speed of light.
2. G4v incorporates both principles at the fundamental level.

the conversation would be politely steered to a different topic, as if I had uttered an indecency. I realized that the only people that might be open to a new approach are the young people, just starting their technical careers.

Opportunity came in 2022 when I was awarded the Kyoto Prize in Advanced Technology, for work I had done in the 1960's and 70's:

`https://www.kyotoprize.org/en/2022/carver_mead/`

I was asked to give two talks: The first, primarily for the Kyoto people, was to share the background and meaning of the work being recognized. The second, for the Kyoto organization in San Diego, CA, could be on any topic, and the audience was primarily young people interested in science and technology.
I chose to give the talk **Engineering Concepts Clarify Physical Law**. As I thought about it, it was clear that a number of young people at the event might get interested in learning more about the approach, and would need something that gave more details. So I grabbed these chapters out of my files. They are not finished works, and have not had the benefit of any review or editing process. The style changes from one to the next, and my use of various methods of adding emphasis may irritate some readers. I often refer to "recently" meaning shortly before that file was written. There are bound to be errors and duplications. But it's what I have—a Very Rough Draft!
The whole theory can be falsified by an experiment using today's technology: See Section 7.6.
I am eager to do that experiment! Or perhaps one of you can do it, or help me do it.
Readers who get seriously interested and would like to act as reviewers are encouraged to send their findings to my admin Donna Fox, `dfox@caltech.edu` who keeps things organized. I will treasure what you come up with.
You can find more on my web site: `carvermead.caltech.edu`

1.2 Background

Students today are told that our understanding of Fundamental Physical Law is embodied in Three Great Theories: Quantum Mechanics, General Relativity, and Classical Electrodynamics.

Upon enquiry they find that Quantum Mechanics (QM) is formulated in $3n$ dimensions, where N is the number of interacting elements (*e.g.* Electrons) involved in the problem of interest. The mathematics used involves the manipulation of $3N$ dimensional mathematical structures, and the result is expressed in $3N$ spatial dimensions plus an intrinsic spin degree of freedom for each electron. The multi-dimensional "wave function" of space and spin must also satisfy the Pauli exclusion principle (anti-symmetry with respect interchange of electron degrees of freedom.) Furthermore, since the complexity of the problem of calculating anything in $3N$ dimensions grows exponentially with N, even the growth of computing power with Moore's Law has not enabled first-principles solution of any but the simplest quantum systems. The student is assured that no one *understands* QM at an intuitive level, and all attempts to do so have been futile—all physical law is embodied in the mathematical formalism, limited only by the intrinsic complexity of its calculation—so *just Shut Up and Calculate!*[1]

An enquiry into General Relativity (GR) reveals that it has been universally successful in predicting the results of numerous gravitational experiments, many of which seemed counter-intuitive. It is formulated in curved space-time, so the space and time coordinates of any given point depend on the distribution of matter in the space. Calculations in such a space are inherently self-referential, and require sophisticated mathematical techniques for their solution. Most problems require certain simplifications to produce solutions that are useful in practice. However that may be, the student is assured that all physical law associated with gravitation (with the exception of quantum systems) is embodied in GR, and what remains is to apply it to ever more "interesting" gravitational arrangements.

An enquiry into Electrodynamics reveals that Maxwell's Equations were not derived by Maxwell, but by his followers who, along with Maxwell, were determined to base electromagnetic phenomena on disturbances in what they called the *Luminiferous Ether*—a substance that was postulated to pervade all of space, and to follow the laws of classical mechanics, thereby enabling light to propagate through it. The equations themselves are expressed in vector calculus, and require a number of auxiliary classical mechanics relations, most noticeably a mechanical *force law* by which electrical charges and currents interact. Much of our modern electrical technology is based on specializations of Maxwell's Equations, simplified and highly tuned for specific applications like electrical machinery (motors, generators, transformers), wireless transmission (radio, television, cellular, satellite, deep space communication), transmission *via* conductors (cable, ethernet, power transmission lines).

These three Great Theories all developed in the scientific culture of classical mechanics, and are expressed in constructions that were leading-edge at the time. But that was a century or more ago, and technology has since evolved from the mechanical/geometric age to the electrical/electronic age. Concepts that have made electrical technology successful had very different connotations in the mechanical view of a century ago than they do in the context of todays ubiquitous electrical and electronic reality. In particular, electromagnetic waves are everywhere, and propagate in empty space—a concept that no longer causes any consternation. So the fact that fundamental elements of matter like electrons, protons and neutrons are waves that also propagate in empty space is easily visualized by anyone familiar with radio waves. Likewise the notion of a potential is built into our electrical culture at the bottom level—the electrical potential is called the Voltage, and no discussion of electrical phenomena can proceed without it. The fact the potential is defined with respect to some reference "zero" is obvious—every Voltmeter has two terminals! Yet these two fundamental concepts are largely absent from the way the three Great Theories are taught.

Viewed through the engineering concepts of waves and potentials,
modern experiments give a clear and intuitive view of fundamental physical law.

[1] David Mermin phrase

I have selected the following historic experiments because they directly illuminate the *conceptual* connection between quantum waves and gravitational and electromagnetic potentials:

1. 1927 - Direct observation of the wave nature of free electrons.[12]
2. 1929 - The expanding universe, containing the enormous energy from the cosmic expansion.[31]
3. 1961 - Quantized flux experiments showed that a superconducting ring6 had a coherent collective wave function which had an integer number of 2π phase advance in its path around the ring[14][16].
   Such macroscopic wave functions provide our most direct access to the 3-dimensional wave nature of matter.
4. 1964 - The Superconducting Quantum Interference Device (SQUID) showed unequivocally that the superconducting collective wave function was coupled *via* the electromagnetic vector potential $\vec{A}$, not the Maxwell magnetic field $\vec{\mathcal{B}}$[34].
5. 1964 - The London Moment 6 in a rotating superconducting ring showed directly that the free-floating collective electron wave function finds a delicate balance between opposite electromagnetic and cosmic gravitational vector potentials.[29]
6. 1965 - The Cosmic Microwave Background (CMB) was detected and identified.[75]
7. 1967 - The Shapiro Delay 7.3 of radar signals passing close to the Sun was the first direct demonstration of the effect of the gravitational scalar potential on the measured speed of light.[64][56][15]
8. 1975 - Direct measurement 4 of gravitational scalar potential effect on Neutron wave functions.[9]
9. 1976 - The Fiber-Optic Gyroscope (FOG)5.3 - Direct effect of gravitational vector potential on electromagnetic propagation (Sagnac Effect), and the cosmic zero of rotation.[71]
10. 1977 - Convincing observation of the CMB frame of reference.[66]
11. 1979 - Direct measurement of the effect of gravitational vector potential 5.4 on Neutron wave functions.[73]
12. 2010 - Direct measurement of atomic clock frequency *vs* gravitational scalar potential.[8]

I strongly advocate introducing students to physical law *via* these great modern experiments rather than dragging them through endless repetition of centuries-old classical mechanics ideas.

This document is written for non-specialists, who will almost certainly prefer a more historical introduction. These readers can skip the expert section for now and go directly to Section 1.5.

1.3 For Experts

This document contains a highly practical approach to the conceptual formulation of Physical Law.
The result is a simplified and unified quantum treatment of Electromagnetism and Gravitation.

I have found that readers who are already expert in these subjects tend to skip all the introductory material and scan the equations in order to find the "meat" of the document. In the process they completely miss the entire purpose of doing physics this way. So I have provided a special introduction just for them.

1.3.1 Electromagnetism (E&M)

The most fundamental formulation of E&M deals with two four-vectors, shown in bold-face type (SI units):

$$\mathbf{J} = \left\{ \vec{J}, c\rho \right\} \qquad \text{the four current density} \tag{1.1}$$

which represents the density ρ and flow $\vec{J}$ of charged matter, and

$$\mathbf{A} = \left\{ \vec{A}, \frac{\mathcal{V}}{c} \right\} \qquad \text{the four potential} \tag{1.2}$$

which contains the scalar potential $\mathcal{V}$ and the vector potential $\vec{A}$, representing the scalar (electrostatic) and vector (magnetic) interaction between elements or aggregations charged matter.

The four-current-density $\mathbf{J}$ is the source of the four-potential $\mathbf{A}$:

$$\mathbf{A}(0,t) = \frac{\mu_0}{4\pi}\int \frac{\mathbf{J}(\vec{r}, t \pm r/c)}{r} \quad \longleftrightarrow \quad \Box^2\mathbf{A} = -\mu_0\mathbf{J} \tag{1.3}$$

The equivalence follows from Green's representation theorem, and $\Box^2$ is the four-vector Laplacian:

$$\Box^2 = \nabla^2 - \frac{1}{c^2}\frac{\partial^2}{\partial t^2} \tag{1.4}$$

The effect of the vector potential on matter is represented, at the most fundamental level, by the presence of the four-potential in the four-momentum $\mathbf{p}$ of each element of charged matter:

$$\mathbf{p} = \hbar\mathbf{k} - q\mathbf{A} \quad \longrightarrow \quad \mathbf{J} = \frac{qn}{m}\left(\hbar\mathbf{k} - q\mathbf{A}\right) \tag{1.5}$$

where $\mathbf{k} = \left\{\vec{k}, \omega/c\right\}$ is the propagation four vector of the matter wave function, and the current density four-vector is just the aggregation of n per unit volume elements of matter of charge q.

So the four-potential approach to electromagnetism, and the wave representation of matter, together give a direct coupling of the momentum of the elementary "source" charges to the momentum of the elementary "affected" charges without any use of the classical notion of "force." The potentials are merely bookkeeping devices, and do not imbue the intervening space with degrees of freedom of its own.

As detailed in CE[44], this succinct, self-contained and intuitive formulation captures, in a relativistically correct manner, the behavior of electromagnetic phenomena all the way from the radiation of individual atoms up through superconductors, transmission lines, radio antennæ, electric motors and generators.

1.3.2 Gravitation

For GR, Einstein chose, quite arbitrarily, to assume that the Speed of Light c is the same constant in all inertial frames of reference—quite at odds with his 1911 and 1912 theories. Unfortunately he did not have the hindsight provided by the direct observation of the gravitational slowing of Radar pulses by Shipiro in 1967, and many that followed into the present. However that may be, GR must work in frames of reference whose space and time axes are constantly warped by the presence of matter.

A mathematical theorem: Sylvester's Law of Inertia, shows that there is always a free-fall frame of reference, but it does not specify what the speed of light will be in that frame of reference. GR assumes that value will always be the "Universal Speed of Light in Vacuum" $\sim 3\times10^8$ meters/sec. G4v does Not make that assumption.
In G4v the value of the speed of light c at any point depends on the location and energy of other matter relative to that point. However Special Relativity remains valid locally, in any free-fall frame of reference, provided this local value of c is used.

G4v works in frames of reference where lengths are independent of Gravitational Scalar Potential, and the speed of light is, as directly observed, proportional to the Gravitational Scalar Potential. To avoid duplication of variables,
In G4v the Speed of Light c itself is used as the Gravitational Scalar Potential.
The quantity of matter is Not the mass m but the Compton wave number $k_0 = \frac{mc}{\hbar}$.
Thus, for example, the mass m_e of the electron is not a fixed number of kilograms,
but the electron's Compton wave number k_0 is always 2.589605×10^{12} meters^{-1}.

Note about units: G4v is formulated in wave units, where energies have the units of frequency ω, and momenta have the units of a propagation vector k, *i.e.,* inverse length. The units of both k_0 and $\vec{k}$ are inverse length, therefore the gravitational vector potential $\vec{A}$ is dimensionless. The product of k_0 and the gravitational potential c is a frequency ω_0. In mechanical units, the rest momentum $\hbar k_0 = mc$, which, when multiplied by the gravitational potential c is equal to the rest energy $\hbar\omega_0 = mc^2$. See Section 3.1 for details.

The proper use of four-vector quantities assures us of Lorentz-invariance in free-fall (Inertial) "flat" frames of reference in which the coordinates do not depend on the contents—an *enormous* simplification!

Relation to GR

The Einstein Field Equations of GR can be written as:

$$G_{\mu\nu} = \frac{8\pi G}{c^4} T_{\mu\nu} \qquad T_{\mu\nu} = \begin{pmatrix} T_{00} & T_{01} & T_{02} & T_{03} \\ T_{10} & T_{11} & T_{12} & T_{13} \\ T_{20} & T_{21} & T_{22} & T_{23} \\ T_{30} & T_{31} & T_{32} & T_{33} \end{pmatrix}. \tag{1.6}$$

Where G is Newton's gravitational constant and $T_{\mu\nu}$ is the Stress-Energy Tensor. The element T_{00} is the energy per unit volume divided by c, and T_{01}, T_{02}, T_{03} are the momentum per unit volume in, for example, the x, y, z directions. Thus the units of all elements are momentum per unit volume.

It is well known that, for weak gravity, Eq. 1.6 reduces to a vastly simpler linear equation[2] of the form:

$$\Box^2 A_{\mu\nu} = \left[\nabla^2 - \frac{\partial^2}{\partial t^2}\right] A_{\mu\nu} \approx \frac{-4\pi G}{c^3} T_{\mu\nu} \tag{1.7}$$

where $A_{\mu\nu}$ is the Tensor Gravitational Potential and the $T_{\mu\nu}$ is slightly different from the one in Eq. 1.6. Since lengths in G4v do not change when the gravitational potential c changes, we need to express the gravitational constant G as a length. By definition the Planck length

$$\ell_p = \sqrt{\frac{\hbar G}{c^3}} \quad \Rightarrow \quad G = \frac{\ell_P^2 c^3}{\hbar} \tag{1.8}$$

Since G4v works strictly with a wave description of elements of matter; let's check the units of Eq. 1.7: m=meter, s=second, $\hbar\omega$=energy, $\omega \sim 1/s$, $\hbar k$=momentum, $k \sim 1/m$, $\alpha = [x, y, z]$:

$$\begin{aligned} G &= \frac{\ell_P^2 c^3}{\hbar} \quad \Rightarrow \quad \frac{G}{c^3} = \frac{\ell_P^2}{\hbar} \\ T_{00} &= \frac{1}{c}\frac{\hbar\omega}{\text{vol}} \quad \Rightarrow \quad \frac{G}{c^3} T_{00} = \frac{\ell_P^2}{\hbar} \cdot \frac{1}{c}\frac{\hbar\omega}{\text{vol}} = \frac{\ell_P^2}{c}\frac{\omega}{\text{vol}} \propto \frac{1}{m^2} \\ T_{0\alpha} &= \frac{\hbar k_\alpha}{\text{vol}} \quad \Rightarrow \quad \frac{G}{c^3} T_{0\alpha} = \frac{\ell_P^2}{\hbar} \cdot \frac{\hbar k_\alpha}{\text{vol}} = \ell_P^2 \frac{k_\alpha}{\text{vol}} \propto \frac{1}{m^2} \end{aligned} \tag{1.9}$$

We may now express Eq. 1.7 using our wave representation of matter:

$$\Box^2 A_{\mu\nu} \approx \frac{-4\pi\ell_P^2}{\hbar} T_{\mu\nu} \quad \Rightarrow \quad A_{\mu\nu} \approx \frac{-\ell_P^2}{\hbar} \int \frac{T_{\mu\nu}(x, y, z, t \pm t_t)}{r(t \pm t_t)} \, d\text{vol} \quad \text{where} \quad t_t = \int_{\text{path}}^{r} s/c(s) \, ds \tag{1.10}$$

Since the d'Alembertion operator $\Box^2 = \left(\nabla^2 - \frac{1}{c^2}\frac{\partial^2}{\partial t^2}\right)$ has the units of $1/m^2$, the tensor gravitational potential $A_{\mu\nu}$ is dimensionless. The integral form follows from Green's theorem, as Einstein indicated in *Meaning of Relativity*, Eq.101, and the discussion that follows. As written, Eq. 1.10 can utilize all components of $T_{\mu\nu}$. When we only include the first column, or, equivalently, the top row, we arrive at a four-vector version.

The top row and left column of the stress-energy tensor contain the components of the energy-momentum four-vector, which are attributes of any fundamental element of matter. The diagonal elements $T_{\alpha\alpha}$ represent the moments of inertia of a binary, and are the largest source of the Gravitational Waves that directly alter the spacing of the LIGO mirrors—a fact that that I bungled in my arXiv:1503.04866 paper, but was handled properly in my collaborators' arXiv:1502.00333 paper. For gravitational arrangements where elements of matter like Electrons and Neutrons, and massive objects like stars, planets, etc. can be approximated as discrete elements, we can ignore the blue and green $T_{\alpha\beta}$ elements, and a straightforward four-vector formulation becomes, as long as the curvature is small, an excellent approximation.

[2] See, *e.g.* Wikipedia: **Linearized Gravity.**

The quantities in Eq. 1.10 are, with $\alpha = [x, y, z]$ and 4-vector quantities in **bold**:

$$\begin{aligned} T_{00} &= \frac{1}{c}\frac{\hbar\omega}{\text{vol}} = \frac{\hbar\omega}{c}\Psi^*\Psi \\ T_{0\alpha} &= \frac{\hbar k_\alpha}{\text{vol}} = \hbar k_\alpha \Psi^*\Psi \\ \text{Using } \mathbf{T} &= \Big[T_{00}, T_{0x}, T_{0y}, T_{0z}\Big] = \hbar\Big[\frac{\omega}{c}, k_x, k_y, k_z\Big]\Psi^*\Psi = \hbar\mathbf{k}\Psi^*\Psi \\ \textit{Eq. 1.10 becomes } \Box^2\mathbf{A} &\approx \frac{-4\pi\ell_P^2}{\hbar}\hbar\mathbf{k}\Psi^*\Psi = -4\pi\ell_P^2\mathbf{k}\Psi^*\Psi \end{aligned} \tag{1.11}$$

$$\Box^2\mathbf{A} \approx -4\pi\ell_P^2\mathbf{k}\Psi^*\Psi \quad \Rightarrow \quad \mathbf{A} \approx -\ell_P^2\int \frac{\mathbf{k}\Psi^*\Psi(x,y,z,t\pm t_t)}{r(t\pm t_t)}\,d\text{vol} \quad \text{where} \quad t_t = \int_{\text{path}}^{r} s/c(s)\,ds \tag{1.12}$$

We have thus shown that, in weak gravity, where only the Energy-Momentum elements of the Stress-Energy tensor play a significant role, we have a four-vector version of Einstein's field equation that is parallel to, and integrated with CE[44] four-vector, quantum-based electromagnetism. We call this formulation G4v.

1.4 G4v

G4v has the following positive attributes:

- It is parallel to, and integrated with CE [44] four-vector electromagnetism.
- It is based on 4-vector properties of matter waves, and thus has a fundamental Quantum basis.
- It is formulated with 4-vector relations in ordinary "flat" space-time, and is easy to work with.
- It uses the gravitational 4-potential, not merely "fields" which are derivatives of the potential. For that reason it can treat the full scalar and vector relations of Mach's Principle: **Inertia and Rest Energy of an element of matter are due to its Gravitational 4-Vector coupling to all matter inside the Horizon of the Universe!**
- It predicts all the observed post-Newtonian phenomena normally attributed to GR with the exception of Gravitational Waves, which require the diagonal elements $h_{\alpha\alpha}$.
- Its predictions are quantitatively in accord with observations, as far as have been determined.
- It is based on Mach's principle, and provides a basis for the Equivalence Principle.
- Being based on Mach's principle, it provides a *Cosmic* basis for Special Relativity.
- Its solution for a massive "Black Hole" is free of singularities.
- A simple cosmology based on G4v predicts a universe consistent with observation without requiring "dark energy."

G4v has the following limitations:

- It does not include the diagonal spatial elements in the stress-energy tensor, so misses the largest contribution to the separation of the LIGO mirrors by gravitational waves. The Green's Function of binary systems, containing diagonal tensor elements that are 4 times the amplitude of the G4v vector element, is easily added, and this addition gives the same prediction for LIGO results as linearized GR. This *ad hoc* addition is not satisfying, as a full tensor-potential based theory would be. It might be prudent to await the outcome of the Section 7.6 experiment before undertaking the effort involved in such a development.
- It is an engineering approach, and employs different logic than main-stream theoretical physics.
- It is not nearly as highly evolved and mathematically sophisticated as GR.

1.5 History

Building on the work of Cavendish and Coulomb, the parallel between electromagnetism and gravitation became obvious to many scientists. Both Maxwell and Heaviside attempted theories of gravitation based on their electromagnetic equations. They were discouraged by the fact that, due to the opposite sign of coupling, gravitational energies were invariably negative.

In 1911, Einstein [23], reasoning solely from the *equivalence principle*, which he called "the happiest thought of his life," put forth a theory in which the speed of light decreased near a massive body. In that paper he predicted three of the modern post-Newtonian effects due to this decrease in the speed of light with gravitational potential:

- Gravitational redshift
- Dependence of the speed of light on the gravitational potential
- Gravitational deflection of light by massive bodies

His expression for the redshift gives the accepted modern value, which was not observed experimentally until 1960. He ended the paper with the following historic passage:

> A ray of light going past the Sun would accordingly undergo deflection to the amount of $4 \times 10^{-6} = 0.83$ seconds of arc. The angular distance of the star from the center of the Sun appears to be increased by this amount. As the stars in the parts of the sky near the Sun are visible during total eclipses of the Sun, this consequence of the theory may be compared with experience... It would be urgently wished that astronomers take up the question here raised, if though the considerations presented above may seem insufficiently established or even bizarre. For, apart from any theory, there is the question whether it is possible with the equipment at present available to detect an influence of gravitational fields on the propagation of light.

Although the results of observation would not be known for another 9 years, his analysis led to 1/2 the observed bending. This factor of two seems to be the only reason modern authors refer to this remarkable landmark paper.

It was clear to Einstein that, if the parallel between electric and gravitational interactions were a reliable guide, there must be more to the story. In 1912, in a short paper in an obscure journal[19], he explored the question: *Is There a Gravitational Effect which is Analogous to Electrodynamic Induction?*
The predictions of this paper are even more far-reaching than those of the 1911 paper:

- Proximity Increase in Inertia
- Gravitational Influence on Frame of Reference
- Mechanism for Mach's Principle

Shortly after his 1912 paper, Einstein struck out in a totally new direction, leading to General Relativity (GR) in 1915. This new theory absorbed the change in the speed of light with gravitation potential into dilation of the spacetime metric. He postulated that the velocity of light was the same constant in any local Lorentz frame. Including both the time and spatial variation of the spacetime metric in GR led to the correct prediction for the bending of light, as reported by Eddington and his colleagues [17] in 1920.

We return here to Einstein's original 1911/12 formulation: that the speed of light depends on the gravitational potential, and that gravitation includes an inductive coupling. This approach was extended with several deep insights by Max Abraham [57] in what he called "a constructive competition with A. Einstein." That work might have led to a Minkowski-type four-vector theory of gravitation based on the obvious parallel with electromagnetism. However, at the time, attempts to use gravitational potential invariably led to negative energy. Also, Abraham had extended the *Lorentz force law* to include damping in the electromagnetic field. The application of the Abraham-Lorentz law to gravitation led to an apparent runaway instability, which, along with the negative-energy problem, put an abrupt end to the development of four-vector theories of gravitation.

From our modern perspective, these pioneering workers were lacking a number of centrally important insights which, taken together, provide a clear guide to a unification of Electromagnetic and Gravitational interaction of Quantum Matter Waves. We have used this new set of insights to clarify the solution space in the following ways:

- The negative gravitational potential energy presents no problem when it is viewed as subtracting from the enormous kinetic energy of the cosmic expansion.
- The coupling of matter wave functions *via* the electromagnetic vector potential appears directly, and does not involve the Maxwell field quantities $\vec{\mathcal{E}}$ and $\vec{\mathcal{B}}$. No force equation is needed, and hence the Abraham-Lorentz confusion does not arise.
- In 1951 Callen & Welton[7] showed that Abraham's damping addition to the Lorentz force was due to coupling to a continuum of quantum levels, and hence depended on the *square* of the coupling constant, not to the coupling constant itself as Abraham had assumed. For that reason the term results in damping for both gravitation and electromagnetism, rather than in an instability for gravitation.
- Collective Electrodynamics [**CE**] [44] provides full Quantum-based articulation of electromagnetics based solely on the four-vector potential[3]. Practical problems from electric motors, permanent magnets, antenna patterns, and atomic transitions are all worked in a significantly simpler manner than with the traditional Maxwell's Equations and their concomitant force equations. In addition, the theory correctly treats interaction with superconductors, whereas the Maxwell approach does not.
- Sagnac effect demonstrations with light[71], with superconducting Electrons[29], and with Neutrons[73], have all, within their accuracy, demonstrated that the coordinate system in which the Wave Function has zero rotation is identical to the observed coordinate system of matter in the Universe. Because none of the present consensus theories work at the level of potential, they cannot make this connection, but it is a natural consequence of Mach's Principle, which inspired Sciama's *Origin of Inertia*[62]. At the end of Einstein's *Meaning of Relativity*[21], he outlines his approach to obtaining Mach's Principle, which uses a gravitational vector potential, but he does not carry it through. We adopt Sciama's 4-vector potential coupling between all elements of matter in the Universe, and apply it at the Quantum level.
- This being an Engineering approach, we take the obvious interpretations of the experimental results, rather than superimpose some belief coming from previous history. From the numerous observations of Shapiro Delay[64][65][56][15], the obvious conclusion is that the Speed of Light is directly proportional to the gravitational potential—a conclusion Einstein reached in 1911. GR has taken the position that the length of rigid rods is proportional to the gravitational scalar potential, as are the speed of clocks. That combination then predicts that the speed of light slows by twice the gravitational scalar potential, which accounts for the factor of 2 in the bending of light, observed in 1919, and verified in the Shapiro Delay. We take the view that photons carry momentum, and therefore have vector as well as scalar coupling to matter—the sum of the two effects accounting for the factor of two. This difference in the origin of that factor of 2 is testable using current technology—see Section 7.6.

[3] Poincaré, Minkowski, Sommerfeld, Abraham and Lewis all made noble attempts to develop such a theory, but only Lewis produced a conceptually simple four-vector electromagnetic theory [36]. All these efforts predated both Schrödinger's papers and London's insights into the quantum nature of superconductivity, so none of them were able to develop a wave-vector based theory free from force-law coupling

1.6 Present Approach

We describe here an internally-consistent, Quantum coupled treatment of gravitation and electromagnetism. The electromagnetic part is put forth in Collective Electrodynamics—Quantum Foundations of Electromagnetism [44], hereinafter referred to as CE, and described briefly in Section 1.3.1. The Gravitational theory described in this document, which we call G4v, is a direct extension of Einstein's 1911/12 approach. It differs from previous attempts in a number of important ways:

- Neither the electromagnetic nor gravitational fields are quantized.
  The wave functions and four-potentials are continuous functions of space and time.
  Quantization results from the interaction of matter and field wave functions.
- The theory is based on Mach's Principle and provides a conceptual base for the Equivalence Principle.
- It is not a metric theory; it is formulated in flat space-time.
  Lengths are constant and do not vary with gravitation potential
- **The speed of light c is equal to the gravitational scalar potential.**
  It is not constant, but varies with position and time.
- The quantity of matter coupled gravitationally is not the mass m.
  It is the Compton wave number $k_0 = mc/\hbar$.
- The theory is based on four-vector coupling.
  It is thus locally Lorentz-invariant in regions where the speed of light can be considered constant.
- The source of the electrical four-potential is the charge–current density four-vector, and that for the gravitational four potential is the energy-momentum four-vector. Both quantities are defined for the wave function of the source matter, and appear as terms in the affected matter wave function.
  The concept of force is not necessary, but can be computed if desired.

This approach allows a unified treatment that avoids the historical stumbling blocks caused by force-law based coupling. We obtain, in a simple and straightforward manner, all of the canonical experimental "tests of GR." In particular we observe that, in 1911, Einstein included only the scalar part of the interaction, neglecting the vector part. As noted above, his 1912 paper [19] provides the key element that was missing in 1911: Because the photon is traveling at the speed of light, the vector contribution to the speed and deflection of light is equal to that of the scalar part, and the two effects add. Thus the total deflection of light predicted in this manner agrees with GR and with observation. He was thus within a day's work of having a correct solution to the light-deflection problem. It is ironic that this "near-miss" diverted the entire evolution of gravitational theory onto a completely different path. Our approach to the speed of light can be tested using today's technology—see Section 7.6.

In addition to obtaining the correct value for the light-deflection problem, we also obtain exactly the same expressions as GR, to the first order beyond Newton, for perihelion precession, Gravity Probe B, gravitational redshift, Shapiro delay, and the gravitational bending of light.

For gravitational waves, it is now clear that those that affect the spacing between the LIGO mirrors are primarily polarized by "strain" modes—the "stretching of spacetime." These are represented by the diagonal modes of the source tensor[33]. Expanding the G4v gravitational potential approach to include these linearized GR Green's Function potentials from binary systems is straightforward, and produces the same results as GR. That insight, which is not part of G4v proper, was missed in my arXiv:1503.04866 posting, which therefore gave the wrong location and amplitude for the historic 2017 LIGO sighting [38][37]. To properly incorporate tensor elements beyond the first row/column is a future project, and only worthwhile if the Section 7.6 experiment succeeds. Meanwhile we can rely on the Green's Function "hack."

Chapter 2

Waves as the Foundation of Physics

There is a tendency to teach science concepts in the order in which they were discovered. Such an approach would not pose a problem if scientific discovery were perfectly well-ordered, so that each new discovery was an extension of the prior knowledge. The actual evolution of our knowledge is, however, much more chaotic than this simple idealization: New findings always modify our understanding of older ideas.

The dangers of unwillingness to give up historical viewpoints has been most prominent in the recent development of quantum physics. Specifically, it is common practice to teach classical mechanics as the foundation of physics. Subsequently, quantum phenomena are introduced in a manner that tries to avoid admitting that classical mechanics is not fundamental, whereas in fact it derives from quantum mechanics as a special case. A key defect of this approach is the introduction of point-particles which are described as interacting in a mechanical manner, leading to infinite energy density and further difficulties.
Ernst Mach[41] foresaw the problem long before it had become acute. He said:

> The view that makes mechanics the basis of the remaining branches of physics, and explains all physical phenomena by mechanical ideas, is in our judgment a prejudice ... The mechanical theory of nature, is, undoubtedly, in an historical view, both intelligible and pardonable; and it may also, for a time, have been of much value. But, upon the whole, it is an artificial conception.[1]

Classical mechanics is inappropriate as a starting point for physics because the elements out of which it is constructed—force, mass, position, velocity, etc.—are not fundamental; rather they are properties that emerge in the limit of an incoherent aggregation of an enormous number of quantum elements, each of which has the nature of a *wave*. Feynman (FLP vol. II Sec. 15-5) [25] expressed it this way:

> There are many changes in what concepts are important when we go from classical to quantum mechanics... Instead of forces, we deal with the way interactions change the wavelength of waves.

So, to have a unified approach to physics, we start with the wave nature of elements of matter, and derive the behavior of macroscopic systems by treating them as aggregations of a large number of these elements. The phenomena of electromagnetism arise directly from the *coherent* aggregation of *charged* elements, as discussed at length in CE [44]. We find that, at the fundamental level, gravitation couples matter waves with other matter waves *via* the gravitational four-potential in exactly the same manner that one charged matter wave couples to another charged matter wave *via* the electrodynamic four-potential.

The phenomena of ordinary macroscopic gravitation, mechanics and thermodynamics arise directly from the *incoherent* aggregation of *uncharged* elements. The unified approach presented here accommodates the full range of interactions.

2.1 Mechanics of Matter Waves

We begin with the connection between the wave nature of matter and mechanics. Every element of matter has a **wave function** ψ, as first put forth by de Broglie[13].
The most elementary wave function ψ is of the form:

$$\psi = a\, e^{i\phi} = a\, e^{i(\mathbf{k}\cdot\mathbf{r})} = a\, e^{i(\vec{k}\cdot\vec{r}-\omega t)} \tag{2.1}$$

The amplitude envelope a, and the propagation vector $\vec{k}$ are assumed to be slowly varying functions of the spatial location $\vec{r}$ and the time t. Such wave functions are solutions of some wave equation: the most common being the Riemann–Sommerfeld Equation for electromagnetic waves and the Schrödinger, Klein-Gordon, and Dirac Equations for matter waves. The density of energy or charge carried by the wave is proportional to the absolute square $\psi^*\psi$ of its wave function.

[1] The quote appears in Ch. V, pg. 495 of the final (1919) edition of reference [41].

For some reason that is only postulated and not yet understood at the fundamental level, the integral over all space of $\psi^*\psi$ for each element of matter is equal to unity. This quality is called the **normalization** of the wave function, and, when multiplied by the elementary charge q, is called the **quantization of charge**; it is responsible for the particle-like properties of matter. It can be thought of as the mechanism by which each element of matter keeps its "identity" even though it is distributed in space and time.

In Eq. 2.1 the **phase** ϕ is the dot product of the **propagation four-vector**[2] $\mathbf{k} = \vec{k}, \omega/c$ and the corresponding **interval** $\mathbf{r} = \vec{r}, ct$. The dot product of any two four-vectors is a scalar—it is invariant under a Lorentz transformation, *i.e.,* it has the same value in any inertial coordinate system. Thus the phase ϕ has the same value in any inertial coordinate system. We can derive other relativistically correct laws from such dot products: Taking the dot product of $\mathbf{k}$ with itself we obtain:

$$\mathbf{k} \cdot \mathbf{k} = \vec{k} \cdot \vec{k} - \frac{\omega^2}{c^2} = k^2 - \frac{\omega^2}{c^2} \tag{2.2}$$

Defining $k_0^2 = \mathbf{k} \cdot \mathbf{k}$ where k_0 is the **Compton wave number** or **standing-wave number** of the wave function and the scalar magnitude k of the propagation vector $\vec{k}$ of the wave is called the **wave number**, we obtain

$$\omega^2 = \left(k_0^2 + k^2\right) c^2. \tag{2.3}$$

Thus, using the relation between the wave variables and their mechanical counterparts: momentum $\vec{p} = \hbar\vec{k}$ and energy $E = \hbar\omega$ we obtain the final form:

$$E^2 = \left(p_0^2 + p^2\right) c^2. \tag{2.4}$$

where the final form is obtained from the relation between the wave variables and their mechanical counterparts: momentum $\vec{p} = \hbar\vec{k}$ and energy $E = \hbar\omega$. The scalar magnitude k of the propagation vector $\vec{k}$ of the wave is called the **wave number**. The quantity k_0 is called the **Compton wave number** or **standing-wave number** of the wave function, and $p_0 = \hbar k_0$ is the corresponding **rest momentum**. The quantity $\omega_0 = k_0 c$ is called the **rest frequency** of the matter wave and $E_0 = \hbar\omega_0 = \hbar k_0 c$ is the corresponding **rest energy**. The frequency ω is the change in phase per unit time. The propagation vector $\vec{k}$ is the change in phase per unit distance. It may seem strange for a stationary element of matter to have a momentum, but a standing wave can have a phase that changes with distance, which then becomes its rest momentum. Electromagnetic waves in free space have $k_0 = 0$.

Two fundamental postulates of *G4v* are:

1. **The speed of light c is the local gravitational potential.**
2. **The Compton wave number k_0, not the "mass", is the quantity of matter.**

so their product is the rest frequency ω_0.

In *G4v*, the entire rest energy of electrically neutral matter is gravitational in origin!

Eq. 2.3 is called a **dispersion relation** between the frequency ω (energy $E = \hbar\omega$) and the propagation vector $\vec{k}$ (momentum $\vec{p} = \hbar\vec{k}$) of the matter wave. As we will see shortly, the path of propagation of a matter wave is governed by its dispersion relation.

We note here that this formulation is quite different from the familiar Newtonian one, and is the source of many effects normally associated with GR. Although it takes a little getting used to, we will find that the entire relativistic dynamics of an electromagnetic wave, and that of any matter wave, including gravitational interaction, can be derived simply from its dispersion relation. The power of this method can only be appreciated by way of examples, to which the remainder of this volume is dedicated.

All familiar elements of matter have some restriction on their wave functions at the **Compton** scale, almost certainly associated with an internal degree of freedom called **spin**. That restriction is, in some way that has not yet been clearly conceptualized, responsible for the rest standing-wave-number k_0, called the **Compton wave number**: the inverse of the **reduced Compton wavelength** of the matter wave function. In G4v k_0 is the fundamental quantity of matter, not the mass m.

[2] See Section 2.2 of [44] or Susskind Lecture Notes for an introduction to four-vector notation.

The wave view of matter allows us to visualize many physical phenomena in an extraordinarily powerful way: Instead of visualizing a "particle" of matter having a "mass" with a "position" at every "time," we visualize it in the same way we view a ray of light—extended along some **path of propagation**. The path is determined by conservation of energy and angular momentum, as appropriate, and by the environment, given by the gravitational and electromagnetic potentials in the neighborhood. For example the orbit of a planet can be treated as the path of propagation of a "ray" of matter with the same dispersion relation as the planet, carried out in Chapter 10. In that case the orbit is totally determined by the gravitational potentials and the dispersion relation— *The path is exactly the same if the planet is a wave stretched around the orbit as it is if the planet is a compact sphere whose center-of-mass is tracing out the orbit!*

2.2 Phase Integrals

Most of the important properties of waves derive from the **phase** ϕ. The propagation four-vector $\mathbf{k}$ is defined as the four-gradient of the phase:

$$\mathbf{k} = \Box\phi = \left\{\nabla\phi, -\frac{1}{c}\frac{\partial\phi}{\partial t}\right\} = \left\{\vec{k}, \frac{\omega}{c}\right\} \tag{2.5}$$

The wave propagates in the $\vec{k}$ direction along its path of propagation, which is perpendicular to the contours of equal phase. When the interval is taken along this path, it follows immediately from the definition of gradient that the phase between two space-time points is a minimum.

$$\phi_{12} = \int_1^2 \nabla\phi \cdot d\vec{r} - \omega\, dt \;=\; \text{minimum} \tag{2.6}$$

This principle defines **ray optics** in terms of **wave optics**, where it is called **Fermat's Principle**.

Applied to matter waves, the phase is called the **action**; many problems can be solved using Eq. 2.6, which is then a simplified form of **path integral**, and its solution called the **principle of least action**.

The form in which we will most often use this principle will be to view a "snapshot" of the wave around the entire path at one point in time. We then integrate the wave vector $\vec{k}$ along the path to get the phase.
The correct path will have stationary phase (not changing to first order with small changes to the path).

This method was clearly described by Leonhard Euler in 1744, in very recognizable terms[24]:

> Let the mass of the projectile be M, and let its speed be v while being moved over an infinitesimal distance ds. The body will have a momentum Mv that, when multiplied by the distance ds, will give $Mv\,ds$, the momentum of the body integrated over the distance ds. Now I assert that the curve thus described by the body to be the curve (from among all other curves connecting the same endpoints) that minimizes $\int Mv\,ds$.

Identifying Euler's momentum with our wave vector:

$$\phi_{12} = \int_1^2 \vec{k} \cdot \vec{ds} \tag{2.7}$$

Notice that there is no time anywhere in this formulation—and it works for any set of potentials to which the projectile is subjected, provided only that the potentials are not explicit functions of time. So Euler anticipated the result of the wave view of matter 180 years before de Broglie and Schrödinger put it forth in a more tangible form. Examples of our application of the method are given in Sections 2.5, 5.1, 7, 7.4, and 12.5.3.

2.3 Classical from Quantum

The classical limit emerges from the incoherent aggregation of a large number of quantum objects. The initial aggregation of individual matter (Fermi) wave functions requires that the wave function of each additional element of matter be orthogonal to that of all others present. The most elementary attribute of a stationary aggregation will be manifest by every element of matter being paired with another element with equal and opposite wave vector, thereby making a standing wave. As we add more and more such standing waves in different directions, we build up a composite structure that has no net momentum, but has a **position** as observed for macroscopic objects. The total momentum vector $\vec{k}$ of a stationary object is zero, because the momentum of each element is precisely cancelled by that of another. But the scalar Compton standing wave numbers of all the elements are independent, do not cancel each other, and so they add up. So the Compton wave number $k_0 = \frac{mc}{\hbar}$ of the aggregate, and therefore its rest energy $k_0 c = \frac{mc^2}{\hbar}$, is not a separate thing at all—it is simply the aggregation of all the orthogonal standing-wave vectors of the individual constituent elements of matter. The rest energy is just the sum of all the Compton standing waves subject to the local gravitatenal potential c. And the reason we can use the wave properties of a moving aggregation of matter, even when the matter involved is a big, messy, incoherent aggregation of individual quantum elements, is that *all its constituent elements share a common motion, and therefore a common wave vector, which emerges as the momentum of the object.*

Any wave structure transports matter (or energy) with its **group velocity** $v = \partial\omega/\partial k$, so, to make the connection with ordinary mechanics, we differentiate Eq. 2.3 with respect to k:

$$2\,\omega\frac{\partial\omega}{\partial k} = 2kc^2 \quad \Rightarrow \quad \frac{\omega}{c^2}\frac{\partial\omega}{\partial k} = k \quad \Rightarrow \quad \frac{\hbar\omega}{c^2}\,v = \hbar k \quad \Rightarrow \quad \frac{E}{c^2}\,v = p \tag{2.8}$$

We see that the momentum is proportional to the velocity, but the "constant" of proportionality E/c^2 depends on velocity (because E does) and on the gravitational potential c. It is only for small velocities ($v \ll c$), and gravitational potentials whose relative change during the motion is negligible, that the proportionality constant E/c^2 in Eq. 2.8 can be considered constant.

Only in this limiting case we can define a **mass** $m = E_0/c^2 = \hbar\omega_0/c^2 = \hbar k_0/c = p_0/c$, and the result approximated:

$$mv \approx p \qquad \text{where} \qquad m = \frac{\hbar k_0}{c} \tag{2.9}$$

The idea that mass is somehow a "fundamental" property of an element of matter, although familiar from classical mechanics, has been one of the principle stumbling blocks in the search for a unified treatment of gravitation, as we will see more clearly in the following sections. In this document we will use wave variables in all our calculations, and only translate our results into familiar mechanical units at the end.

2.4 Dispersion Relations

The familiar form of Eq. 2.9 in terms of the variables used in classical mechanics prepares us for the more important case where the gravitational potential, equal to the speed of light, is a function of position.
The relationships involved can be visualized with the aid of the dispersion curves of Fig. 2.1.

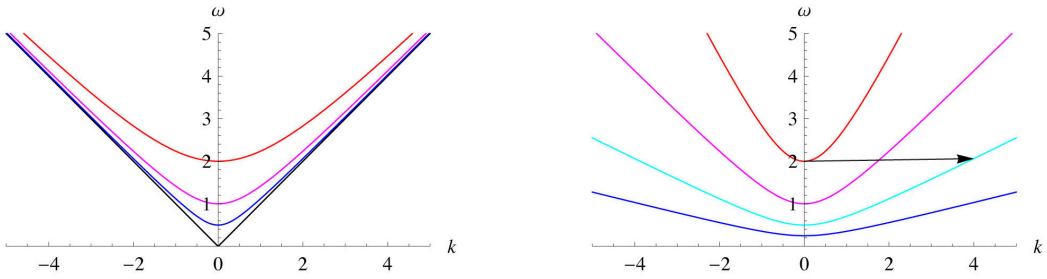

Figure 2.1: Dispersion relations of Eq. 2.3 for Left: elements of matter with $k_0 = 0$(black), 0.5(blue) 1(magenta) and 2(red), all in an environment of $c = 1$. Right: Single element of matter with $k_0 = 1$ in environments of different gravitational potentials $c = 0.25$(blue), 0.5(cyan), 1.0(magenta) and 2(red). The y-axis intercept is the rest energy $k_0 c$, the slope at large k is c, and the curvature at $k = 0$ is $\hbar/m$, as can be seen in Eq. 2.10. It is k_0 that is coupled by gravitation, and is constant when the gravitational potential, equal to the speed of light, is changed. The black arrow is the trajectory of an element of matter in free-fall moving in the $+k$ direction.

As before, differentiating Eq. 2.3 with respect to k at a particular value of c yields

$$\omega\frac{\partial\omega}{\partial k} = kc^2 \quad \Rightarrow \quad \omega\frac{\partial^2\omega}{\partial k^2} + \left(\frac{\partial\omega}{\partial k}\right)^2 = c^2$$
$$\left.\frac{\partial^2\omega}{\partial k^2}\right|_{k=0} = \frac{c^2}{\omega_0} = \frac{c}{k_0} = \frac{\hbar}{m} \tag{2.10}$$

Max Abraham discovered already in his 1913 paper (page 353 in [57]) that mc, not the mass m, is the most natural representation of the gravitational **quantity of matter** of a massive object, which does not change as the gravitational potential, equal to the speed of light c, changes.

Abraham also adopted the assumption that the lengths of material objects do not change with gravitational potential, already introduced in Einstein's 1911 and 1912 papers. Those facts were rediscovered independently nearly 100 years later in the course of the present investigation, and are incorporated in the scaling laws upon which G4v is based.

2.5 Gravitational Field

Changes in the gravitational potential c with position in space occur *e.g.* near massive bodies. The spatial gradient of the gravitational potential c is called the **gravitational field** g. To derive the dynamics of a matter wave in a gravitational field, we use the group velocity $\vec{v} = \partial\omega/\partial k$ in Eq. 2.8:

$$\frac{\omega}{c^2}\vec{v} = \vec{k} \qquad \Rightarrow \qquad \frac{\omega^2}{c^4}v^2 = k^2 \tag{2.11}$$

Using this result in Eq. 2.3 yields the energy and momentum as a function of velocity:

$$\begin{aligned} \omega^2 = \left(k_0^2 + \frac{\omega^2}{c^4}v^2\right)c^2 = k_0^2c^2 + \omega^2\frac{v^2}{c^2} \qquad &\Rightarrow \qquad \frac{k_0^2c^2}{\omega^2} = 1 - \frac{v^2}{c^2} \\ \omega = \frac{k_0 c}{\sqrt{1 - v^2/c^2}} = \frac{mc^2}{\hbar\sqrt{1 - v^2/c^2}} \qquad &\text{and} \qquad \vec{k} = \frac{\omega}{c^2}\vec{v} = \frac{k_0\,\vec{v}/c}{\sqrt{1 - v^2/c^2}} = \frac{m\vec{v}}{\hbar\sqrt{1 - v^2/c^2}} \end{aligned} \tag{2.12}$$

On the surface, Eq. 2.12 looks just like the standard relativistic expressions for energy and momentum as functions of velocity. However, in G4v the speed of light c is also the gravitational potential.
So, if c is a function of position, each of the curves shown in the right side of Fig. 2.1 will be that of an element of matter at a different position, and an energy-conserving wave which was stationary at a position where $c = c_0$ will accelerate to wave vector $\vec{k}$ and hence velocity $\vec{v}$ at a position where $c = c_0 - \delta$, as shown by the black arrow. The energy ω and the Compton wave number k_0 are both constant, so

$$\omega = k_0c_0 = \frac{k_0(c_0 - \delta)}{\sqrt{1 - v^2/\left(c_0 - \delta\right)^2}} \qquad \Rightarrow \qquad 1 - \frac{\delta}{c_0} = \sqrt{1 - \frac{v^2}{\left(c_0 - \delta\right)^2}} \tag{2.13}$$

In the Newtonian limit where $\delta \ll c_0$, Eq. 2.13 reduces to

$$\delta \approx \frac{v^2}{2c_0} \qquad \Rightarrow \qquad k_0\delta \approx \frac{k_0v^2}{2c_0} \qquad \Rightarrow \qquad mc_0\delta = \frac{mv^2}{2} \tag{2.14}$$

So the decrease in gravitational potential energy $mc_0\delta$ has been converted into the kinetic energy $mv^2/2$.

Now let us see how the velocity v changes with time. Differentiating the first expression in Eq. 2.14, and noticing that the velocity $v = \frac{\partial z}{\partial t}$, and that the local gravitational field $g = c_0\,\frac{\partial\delta}{\partial z}$,

$$\frac{v}{c_0}\frac{\partial v}{\partial t} = \frac{\partial\delta}{\partial t} = \frac{\partial\delta}{\partial z}\frac{\partial z}{\partial t} \qquad \Rightarrow \qquad \frac{\partial v}{\partial t} = g \tag{2.15}$$

Thus our matter wave is accelerated by the local gravitational field in exactly the way we would expect from Newton's law. We are reminded that in Newtonian physics Eq. 2.15 would read

$$m_{\text{grav}}\,g = m_{\text{inertial}}\frac{\partial v}{\partial t} \quad \text{and} \quad m_{\text{grav}} = m_{\text{inertial}} \qquad \Rightarrow \qquad \frac{\partial v}{\partial t} = g \tag{2.16}$$

Since there is no fundamental reason in Newtonian theory why the gravitational mass m_{grav} should be equal to the inertial mass m_{inertial}, we see just how artificial and contrived the force-law view of elementary physics really is. From these relations we also see just how misleading the idea of "mass" is. It is neither the quantity coupled by gravitation, nor the quantity conveying inertia to the matter wave function, nor is it the invariant quantity when the gravitational potential is changed. It has been the subject of endless debate in the context of special relativity, but the problem with the concept goes much deeper than that.
It is only in the context of gravitation as the origin of inertia that the resolution becomes clear.
Throughout this treatment, when we express results in terms of standard mechanical variables, the mass M and the gravitational constant G will mean their values at the average cosmic gravitational potential c_0.

Chapter 3

Basic G4v Formulation

3.1 Mach's Principle

Mach's principle (Section 9.17) is a central tenet of **CE** [44] and G4v:

> Every element of matter derives its dynamical properties from interactions with every other element of matter on its past and future light cones.

More specifically, in a matter-wave context, this statement can be made quantitative by describing its propagation four-vector elements ω and k in a coordinate system in which the element is at rest:

$$\vec{k} = -k_0 \chi \sum_i \frac{\vec{k}_i}{r_i} \qquad \omega = k_0\, c = k_0 \left(c_\infty - \chi \sum_i \frac{\omega_i}{r_i} \right) \tag{3.1}$$

where r_i is the distance, along the light cone, from the ith element of matter to the point where the potential is being evaluated, χ is the gravitational coupling constant, and c_∞ is the speed of light in a fully-dispersed universe, as described in detail in Chapter 9.

We can see just how deeply this theory is a true theory of *relativity*. Momentum is the result of propagation *relative to* everything in the universe. Eq. 3.1 includes not only the scalar potential c that we have discussed in the previous section, but also the vector interaction due to the propagation of other matter with which our local element is coupled.

The interactions in the summations in Eq. 3.1 decrease inversely with the distance r_i, but, in a uniform universe, the amount of matter in any spherical shell is proportional to r^2, so the sum is dominated by matter in the far-distant universe. Thus the matter that governs our local inertia and speed of light is the matter farthest away. So, instead of embarking in a futile attempt to keep track where all that matter is, we define **potentials** that describe the big sum: The gravitational vector potential $\vec{A}$ and scalar potential c are given by the Mach's Principle sum of contributions from all other elements of matter in the universe[1].

$$\vec{A} = -\chi \sum_i \frac{\vec{k}_i}{r_i} \qquad c = c_\infty - \chi \sum_i \frac{\omega_i}{r_i} \tag{3.2}$$

In a region where c can be considered approximately constant, $\vec{A}$ and c can be made into a four-vector, whereupon these equations are of exactly the same form as those of electrodynamics, but with the opposite sign of coupling coefficient.

$$\mathbf{A} = \left\{ \vec{A}, c \right\} \quad \text{and} \quad \mathbf{k} = \left\{ \vec{k}, \omega \right\} = k_0\, \chi\, \mathbf{A} \tag{3.3}$$

Eq. 3.2 is the basis for G4v cosmology, as detailed in Chapter 9. However, in the vast majority of cases, we are concerned with gravitational phenomena involving a few local massive bodies in the background potential of the rest of the universe.

In this most common case, we factor the terms in Eq. 3.2 into those from distant(dis) and local(loc) sources:

$$\begin{aligned} \vec{A} &= -\chi \sum_j^{\text{dis}} \frac{\vec{k}_j}{r_j} - \chi \sum_i^{\text{loc}} \frac{\vec{k}_i}{r_i} \\ c &= c_\infty - \chi \sum_j^{\text{dis}} \frac{\omega_j}{r_j} - \chi \sum_i^{\text{loc}} \frac{\omega_i}{r_i} \end{aligned} \tag{3.4}$$

[1] The potentials determine the energy and momentum per unit k_0 of a free-floating element of matter. This simple relationship is strictly true only when the k_0 of the "test element" has a k_0 that is much less than the k_0 of the matter elements i responsible for the potential. In many cases we shall encounter, such as planets around the Sun, gyroscopes in the GPB satellite, mirrors in the LIGO interferometer, etc., this approximation is satisfied by many orders of magnitude. However, when we consider the interaction of objects of comparable k_0, such as binary star and "black hole" systems, the potential must be properly apportioned among the interacting elements.

Except in the case of cosmology, we do not know the value of c_∞, but we can directly observe the local speed of light c_0 in the background of the universe at large, corresponding to the first two terms in the expression for c in Eq. 3.4, which thus becomes:

$$\begin{aligned} \vec{A} &= -\chi \sum_j^{\text{dis}} \frac{\vec{k}_j}{r_j} - \chi \sum_i^{\text{loc}} \frac{\vec{k}_i}{r_i} \\ c &= c_0 - \chi \sum_i^{\text{loc}} \frac{\omega_i}{r_i} \end{aligned} \tag{3.5}$$

In a coordinate system that is at rest with respect to the universe at large, for every distant element of matter with propagation vector k_j there will be another element with equal and opposite propagation vector $-k_j$, and the distant sum for $\vec{A}$ in Eq. 3.5 will be zero. In fact, that is the definition of "at rest with respect to the universe at large." In that special coordinate system, Eq. 3.5 becomes:

$$\begin{aligned} \vec{A} &= -\chi \sum_i^{\text{loc}} \frac{\vec{k}_i}{r_i} \\ c &= c_0 - \chi \sum_i^{\text{loc}} \frac{\omega_i}{r_i} \end{aligned} \tag{3.6}$$

It is this formulation we shall adopt for the rest of the present treatment. Because the effect of distant matter has been taken into account, we can henceforth omit the "loc" notation, and all $\vec{k}_i$ and ω_i will be understood to refer to local massive bodies.

3.2 Matter at Rest

Let us consider a "test object" of Compton wave-number k_0 at rest in the coordinate system of the universe at large. Because the element is not moving, its propagation vector $\vec{k}$ will be only that contributed by other local matter moving with respect to it, as represented by the gravitational vector-potential $\vec{A}$, and its frequency ω will be only that contributed by the potential due to other matter, as represented by the gravitational scalar-potential $\vec{c}$.

$$\begin{aligned} \vec{k} &= k_0 \vec{A} = -k_0 \chi \sum_i \frac{\vec{k}_i}{r_i} \\ \omega &= k_0 c = k_0 \left(c_0 - \chi \sum_i \frac{\omega_i}{r_i} \right) \end{aligned} \tag{3.7}$$

If the matter also carries a charge q and is subject to electromagnetic vector and scalar potentials $\vec{A}_e$ and $\mathcal{V}$, as discussed at length in [44], Eq. 3.7 becomes

$$\vec{k} = k_0 \vec{A} + \frac{q}{\hbar} \vec{A}_e \qquad \omega = k_0 c + \frac{q}{\hbar} \mathcal{V} \tag{3.8}$$

Note about units: G4v is formulated in wave units, where energies have the units of frequency, and momenta have the units of a propagation vector, *i.e.,* inverse length. The units of both k_0 and $\vec{k}$ are inverse length, therefore the gravitational vector potential $\vec{A}$ is dimensionless. The product of k_0 and the gravitational potential c is a frequency. In mechanical units, the rest momentum $\hbar k_0 = mc$, which, when multiplied by the gravitational potential c is equal to the rest energy $\hbar\omega_0 = mc^2$.

Thus the coupling constant χ has dimensions of length squared. In G4v

$$\chi = \ell_P^2 = \frac{\hbar G}{c^3} \tag{3.9}$$

where ℓ_P is the **Planck Length**. In G4v, lengths do not change when the gravitational potential changes, so the coupling constant χ is indeed constant. Planck's constant $\hbar$ is merely a translation from frequency to energy, both of which scale directly with c, so $\hbar$ is also constant. The ordinary "gravitational constant" $G = \ell_P^2 c^3/\hbar$ thus is not constant at all, but scales as the cube of the gravitational potential c.
Wherever we refer to G, we will mean its value in the average potential c_0 of the present universe.

3.3 Interacting Elements of Matter in Motion

All interesting gravitational problems involve the interaction of two or more elements of matter.
Part of the energy and momentum of each element comes from its own motion, and part from its electrical and gravitational interaction with other elements. We will adopt the following notation:

- The total energy and momentum of element j are ω_j and k_j
- The isolated rest energy and momentum of element j are ω_{0j} and k_{0j}
- The gravitational scalar and vector potentials at the position of element j are c_j and A_j
- The electrical scalar and vector potentials at the position of element i are $\mathcal{V}_j$ and A_{ej}
- The electrical charge of element j is q_j
- The (positive) distance between element j and element i is $r_{ji} = r_{ij}$
- The velocity of element j in the chosen coordinate system is $\vec{v}_j$

The relativistically correct values for ω_j and k_j due to the motion of a "test object" are given by Eq. 2.12, with $\vec{A}_j$ and c_j defined in Eq. 3.7, and the electromagnetic terms from Eq. 3.8:

$$\begin{aligned} \omega_j &= k_{0j}\frac{c_j}{\sqrt{1-v_j^2/c_j^2}} + \frac{q_j}{\hbar}\mathcal{V}_i \\ \vec{k}_j &= k_{0j}\frac{\vec{v}_j/c_j}{\sqrt{1-v_j^2/c_j^2}} + k_{0j}\vec{A}_j + \frac{q_j}{\hbar}\vec{A}_{ej} \\ \text{where} \quad c_j &= c_0 - \chi\sum_{i\neq j}\frac{\omega_i}{r_{ij}} \quad \text{and} \quad \vec{A}_j = -\chi\sum_{i\neq j}\frac{\vec{k}_i}{r_{ij}} \end{aligned} \tag{3.10}$$

As always, c_j is the local speed of light, equal to the local gravitational scalar potential.
We see that this system of equations is self-referential, with the solution for each element dependent on the contributions of all the others. It includes both gravitational and electromagnetic interactions. As noted above, the simple form of the potentials given here is only correct when the k_0 of the "test object" j is much less than that of the objects i creating the potential.

In a region where the speed of light c can be considered constant, the three-vector $\vec{k}$ and the scalar ω/c form the elements of a proper four-vector, which transforms (locally) according to the local Lorentz transformation. However the dispersion relation (Eq. 2.12) seems to be valid over a wider range of circumstances, and renders the Lorentz transformation largely unnecessary.

3.4 Weak Gravity Limit

Many problems, including almost all the "tests of GR" that have been carried out thus far, operate in the regime where the potential c is not too different from the average background potential c_0 and, in addition, the velocities involved are much less than c. It is thus desirable to develop a simplified procedure that is suitable for such weak-gravity situations. In this "non-relativistic, weak-gravity" limit for uncharged matter, we expand the radical in Eq. 3.10, keeping only terms of lowest order in v/c. In this limit the energy and momentum become:

$$\begin{aligned} \omega_j &\approx k_{0j}c_j\left(1+\frac{v_j^2}{2c_j^2}\right) \\ \vec{k}_j &\approx k_{0j}\left(\frac{\vec{v}_j}{c_0}\frac{c_0}{c_j}+\vec{A}_j\right) \end{aligned} \tag{3.11}$$

Next we take the case, which often accompanies the low-velocity case, where the coupling terms involving χ are small as well: The corresponding approximations for the potentials then become:

$$\begin{aligned} c_j &\approx c_0 \left(1 - \frac{\chi}{c_0}\sum_{i\neq j}\frac{\omega_{0i}}{r_{ij}}\right) = c_0\left(1 - \frac{\chi}{c_0}\sum_{i\neq j}\frac{c_0 k_{0i}}{r_{ij}}\right) = c_0\left(1 - \chi\sum_{i\neq j}\frac{k_{0i}}{r_{ij}}\right) \\ \frac{c_0}{c_j} &\approx 1 + \chi\sum_{i\neq j}\frac{k_{0i}}{r_{ij}} \\ \vec{A}_j &\approx -\chi\sum_{i\neq j}\frac{k_{0i}}{r_{ij}}\frac{\vec{v}_i}{c_0} \end{aligned} \tag{3.12}$$

After which the approximations for energy and momentum in Eq. 3.11 become

$$\begin{aligned} \omega_j &\approx \omega_{0j}\left(1 - \chi\sum_{i\neq j}\frac{k_{0i}}{r_{ij}} + \frac{v_j^2}{2c_0^2}\right) \\ \vec{k}_j &\approx k_{0j}\left(\frac{\vec{v}_j}{c_0}\left(1 + \chi\sum_{i\neq j}\frac{k_{0i}}{r_{ij}}\right) - \chi\sum_{i\neq j}\frac{k_{0i}}{r_{ij}}\frac{\vec{v}_i}{c_0}\right) = k_{0j}\left(\frac{\vec{v}_j}{c_0} + \chi\sum_{i\neq j}\frac{k_{0i}}{r_{ij}}\frac{(\vec{v}_j - \vec{v}_i)}{c_0}\right) \end{aligned} \tag{3.13}$$

Multiplying by $\hbar$ and using $m = \hbar k_0/c_0$ from Eq. 2.9 and $\chi = \hbar G/c_0^3$ from Eq. 3.9 to convert our results into familiar mechanical units, the energy $E = \hbar\omega$ and momentum $\vec{p} = \hbar\vec{k}$ of our object become:

$$\begin{aligned} E_j &\approx m_j c_0^2\left(1 - \frac{G}{c_0^2}\sum_{i\neq j}\frac{m_i}{r_{ij}}\right) + \frac{m_j v_j^2}{2} \\ \vec{p}_j &\approx m_j\left(\vec{v}_j + \frac{G}{c_0^2}\sum_{i\neq j}\frac{m_i}{r_{ij}}(\vec{v}_j - \vec{v}_i)\right) \end{aligned} \tag{3.14}$$

We can see a number of things much more clearly from the "post-Newtonian" approximation in Eq. 3.14 than we could see from the fully relativistic form in Eq. 3.10:

- The energy contains the rest energy $m_j c_0^2$ in addition to the Newtonian potential energy $-m_j m_i G/r_{ij}$ and kinetic energy $m_j v_j^2/2$.
- The fraction contributed by the coupling term $m_i G/r_{ij}c_0^2$ is the same for both energy and momentum, as it must be for the equivalence principle to hold.
- The potential energy contributed by m_i to m_j is exactly equal to that contributed by m_j to m_i.
- The momentum contains the Newtonian term $m_j v_j$ and the vector coupling term $\frac{m_j m_i G}{r_{ij}c_0^2}(v_j - v_i)$. The momentum contributed by m_i to m_j is exactly equal and opposite that contributed by m_j to m_i.

Even with the extreme simplifications we have adopted to obtain Eq. 3.14, we still retain the momentum coupling term that allows us to treat the first-order corrections beyond the Newtonian limit, and obtain results for the standard "tests" that are in agreement with experiment and with GR.

Again we see just how deeply this theory is a true theory of *relativity*. Momentum is the result of motion *relative to* everything in the universe. Said another way, each of the masses m_i has contributed its fraction $m_i G/r_i c^2$ to the **frame of reference** of mass m. G4v thus fully embodies Mach's Principle at the most fundamental level.

The application of these methods to real problems will help clarify the principles involved.

3.5 Whence Special Relativity?

We have in Eq. 3.10 a general method of determining the propagation vector (momentum) $\vec{k}$ and frequency (energy) ω for a moving element of matter subject to any combination of gravitational and electromagnetic interactions. This formulation is firmly rooted in Mach's principle, by which the inertia and rest energy of a body are induced by its gravitational interaction with *all* of the (primarily distant) matter in the visible universe, as depicted in Eq. 3.5.

Any such formulation based on Mach's principle, by its very nature, makes local interactions dependent on the nature of the entire visible universe: *i.e.,* on its **cosmology**. A simple G4v cosmology is detailed in Chapter 9. We have seen already that local quantities heretofore treated as "fundamental constants" (such as the speed of light c) are determined by the universe at large. There are other important properties of physical law that have their origin in cosmology: The most obvious of these is the **equivalence principle**, postulated by Einstein as "the happiest thought of his life." The G4v formulation above makes it clear that this "equivalence" property—that inertia and gravitational attraction have a common origin—is expressed directly by the four-vector nature of gravitation, together with Mach's principle, as Einstein had expected it to be.

Other, less obvious properties of physical law are also deeply rooted in cosmology. An important example is brought center-stage by Eq. 3.10. Our development of this equation was done in the frame of reference of the universe at large. In modern treatments this frame is well-defined by the cosmic microwave background (CMB). The motion of a frame of reference with respect to the CMB is evidenced by the Doppler shift of CMB radiation being dependent on the direction of observation. From such measurements it is known that our solar system is moving with respect to the CMB at more than 600 km/sec (See [66] and references therein).
So none of our experiments are done in the frame of the universe.

In 1905 Einstein[18] introduced another postulate, the **principle of relativity**, governing the local properties of physical law. That principle, in the present context, is equivalent to the statement that a relation such as Eq. 3.10 is valid in any coordinate frame having the following properties:

1. The coordinate frame is moving at a constant velocity (not rotating) with respect to the universe at large.
2. The speed of light (gravitational potential) can be considered approximately constant over the range of motion considered.

Such coordinate frames are called **inertial frames**.
The postulate is equivalent to the statement that the four-vectors in one such frame are related to the corresponding four-vectors in another such frame by a Lorentz transformation.

By now there is overwhelming evidence, principally from electromagnetic propagation and high-energy particle physics experiments, that the principle of relativity is valid. Physicists have grown accustomed to it, and it is now expressed in elegant mathematics. Nonetheless, there is no *conceptual* basis for such a principle as it is presented in elementary classes and textbooks.

Our G4v cosmology has a property that helps us understand *conceptually* the origin of the principle of relativity in the same way it helped us see the origin of the principle of equivalence. The interaction responsible for inertia and rest energy is mediated by space-time paths called **light cones.** Because the universe is expanding with a velocity proportional to the distance from us, both the forward and backward light cones have **horizons**, where distant matter is receding from us at the speed of light. Matter beyond these horizons is effectively decoupled from us, and has no effect on local physics. The distance to the horizon is called the **Hubble radius**, and the volume of the universe within the horizon is called the **Hubble volume**.

If we are moving in a straight line toward one horizon and away from the opposite horizon, our velocity relative to distant matter ahead of us decreases, and that relative to distant matter behind us increases. The net result is that the horizon expands ahead of us, in the direction we are moving, and shrinks behind us. So, if the average energy density of the universe is constant for an additional Hubble radius beyond the horizon, the average contents of the universe with which we interact will stay the same, no matter what direction and speed we are moving, so long as we are just moving in a straight line and not accelerating.

So here we have the cosmic origin of the principle of relativity.

3.6 Some Further Details

This section is largely redundant and most readers will prefer to skip to Section 4.

Many problems, including almost all the "tests of GR" that have been carried out thus far, operate in the regime where the potential c is not too different from the average background potential c_0 and, in addition, the velocities involved are much less than c. It is thus desirable to develop a simplified procedure that is suitable for such weak-gravity situations. In this "non-relativistic, weak-gravity" limit for uncharged matter, we expand the radical in Eq. 3.10, keeping only terms of lowest order in v/c:

$$\begin{aligned} \omega_i &= k_{0i}\frac{c_i}{\sqrt{1-v_i^2/c_i^2}} + q_i\mathcal{V}_i \\ \vec{k}_i &= k_{0i}\frac{\vec{v}_i/c_i}{\sqrt{1-v_i^2/c_i^2}} + q_i\vec{A}_{ei} \\ \text{where}\quad c_i &= c_0 - k_{0i}\chi\sum_{j\neq i}\frac{\omega_j}{r_{ij}} \end{aligned} \tag{3.15}$$

$$\begin{aligned} \omega_i &\approx k_{0i}c_i\left(1+\frac{v_i^2}{2c_i^2}\right) = \omega_{0i} + \frac{k_{0i}v_i^2}{2c_i} \\ \vec{k}_{mi} &\approx k_{0i}\frac{\vec{v}_i}{c_i} \end{aligned} \tag{3.16}$$

We also neglect the second-order coupling term in Eq. 3.17

$$\begin{aligned} \omega_i &\approx \omega_{mi} + \omega_{0i} - k_{0i}\chi\sum_{j\neq i}\frac{\omega_j}{r_{ij}} + q_i\mathcal{V}_i \\ \vec{k}_i &\approx \vec{k}_{mi} - k_{0i}\chi\sum_{j\neq i}\frac{\vec{k}_j}{r_{ij}} + q_i\vec{A}_{ei} \end{aligned} \tag{3.17}$$

$$\begin{aligned} \vec{k} &\approx k_0\left(\frac{\vec{v}}{c}+\vec{A}\right) + \frac{q}{\hbar}\vec{A}_e \\ \omega &\approx k_0 c\left(1+\frac{v^2}{2c^2}\right) + \frac{q}{\hbar}\mathcal{V} \end{aligned} \tag{3.18}$$

The effect of local perturbing matter is represented by c and $\vec{A}$ from Eq. 3.6:

$$\begin{aligned} \vec{A} &= -\chi\sum_i\frac{\vec{k}_i}{r_i} \\ c &= c_0 - \chi\sum_i\frac{\omega_i}{r_i} \end{aligned} \tag{3.19}$$

Using these substitutions and neglecting products of small quantities, Eq. 3.16 becomes

$$\begin{aligned} \vec{k} &\approx k_0\left(\frac{\vec{v}}{c_0} - \chi\sum_i\frac{\vec{k}_i}{r_i}\right) + \frac{q}{\hbar}\vec{A}_e \\ \omega &\approx k_0\left(c_0 - \chi\sum_i\frac{\omega_i}{r_i}\right)\left(1+\frac{v^2}{2c^2}\right) + \frac{q}{\hbar}\mathcal{V} \\ &\approx k_0c_0 - k_0\chi\sum_i\frac{\omega_i}{r_i} + \frac{k_0v^2}{2c_0} + \frac{q}{\hbar}\mathcal{V} \end{aligned} \tag{3.20}$$

Next we multiply through by $\hbar$ and use $m = \hbar k_0/c_0$ from Eq. 2.9 and $\chi = \hbar G/c_0^3$ from Eq. 3.9 to convert our results into mechanical units, the momentum $\vec{p} = \hbar\vec{k}$ and energy $E = \hbar\omega$ of our object are:

$$\begin{aligned} \vec{p} &\approx m\left(\vec{v} - \frac{G}{c_0^2}\sum_i \frac{m_i\vec{v}_i}{r_i}\right) + q\vec{A}_e \\ E &\approx m\left(c_0^2 + \frac{v^2}{2} - G\sum_i \frac{m_i}{r_i}\right) + q\mathcal{V} \end{aligned} \tag{3.21}$$

Even with the extreme simplifications we have adopted to obtain Eq. 3.21, we still retain the unification with electromagnetism, and the momentum coupling term that allows us to treat the first-order corrections beyond the Newtonian limit. This term is all that is required to obtain results for the standard "tests" that are in agreement with GR.

Again we see just how deeply this theory is a true theory of *relativity*. Momentum is the result of motion *relative to* everything in the universe. Said another way, each of the masses m_i has contributed its fraction m_iG/r_ic^2 to the **frame of reference** of mass m. G4v thus fully embodies Mach's Principle at the most fundamental level.

The application of these methods to real problems will help clarify the principles involved.

In this "non-relativistic, weak-gravity" limit for uncharged matter, we expand the radical in Eq. 3.10, keeping only terms of lowest order in v/c and taking $c_i \approx c_0$ except where the difference is first-order, and dropping products of small quantities:

$$\begin{aligned} \omega_i &= k_{0i}\frac{c_i}{\sqrt{1 - v_i^2/c_i^2}} \approx k_{0i}c_i\left(1 + \frac{v_i^2}{2c_i^2}\right) \approx \omega_{0i} + \frac{k_{0i}v_i^2}{2c_0} - k_{0i}\chi\sum_{j\neq i}\frac{\omega_j}{r_{ij}} \\ \vec{k}_i &= k_{0i}\frac{\vec{v}_i/c_i}{\sqrt{1 - v_i^2/c_i^2}} + k_{0i}\vec{A}_i \approx k_{0i}\frac{\vec{v}_i}{c_i} - k_{0i}\chi\sum_{j\neq i}\frac{\vec{k}_j}{r_{ij}} \end{aligned} \tag{3.22}$$

It is instructive to explicitly deal with the purely gravitational interaction of two uncharged elements.
In the coordinate system of the universe at large, the first has energy ω_1 and momentum $\vec{k}_1$, and the second has energy ω_2 and momentum $\vec{k}_2$. Eq. 3.17 for the energies then becomes:

$$\begin{aligned} \omega_1 &= \omega_{m1} + \omega_{01} - k_{01}\chi\frac{\omega_2}{r_{12}} \\ \omega_2 &= \omega_{m2} + \omega_{02} - k_{02}\chi\frac{\omega_1}{r_{12}} \end{aligned} \tag{3.23}$$

which has solutions

$$\begin{aligned} \omega_1\left(1 - \frac{k_{01}\chi}{r_{12}}\frac{k_{02}\chi}{r_{12}}\right) &= \omega_{01} + \omega_{m1} - \frac{k_{01}\chi}{r_{12}}(\omega_{02} + \omega_{m2}) \\ \omega_2\left(1 - \frac{k_{02}\chi}{r_{12}}\frac{k_{01}\chi}{r_{12}}\right) &= \omega_{02} + \omega_{m2} - \frac{k_{02}\chi}{r_{12}}(\omega_{01} + \omega_{m1}) \end{aligned} \tag{3.24}$$

Similarly, Eq. 3.17 for the momenta then becomes:

$$\begin{aligned} \vec{k}_1 &= \vec{k}_{m1} - k_{01}\chi\frac{\vec{k}_2}{r_{12}} \\ \vec{k}_2 &= \vec{k}_{m2} - k_{02}\chi\frac{\vec{k}_1}{r_{12}} \end{aligned} \tag{3.25}$$

which has solutions

$$\begin{aligned} \vec{k}_1\left(1 - \frac{k_{01}\chi}{r_{12}}\frac{k_{02}\chi}{r_{12}}\right) &= \vec{k}_{m1} - \frac{k_{01}\chi}{r_{12}}\vec{k}_{m2} \\ \vec{k}_2\left(1 - \frac{k_{02}\chi}{r_{12}}\frac{k_{01}\chi}{r_{12}}\right) &= \vec{k}_{m2} - \frac{k_{02}\chi}{r_{12}}\vec{k}_{m1} \end{aligned} \tag{3.26}$$

They appear linear in that superposition applies, once the energy, momentum and light-cone distance for each of the sources are known. The system of elements is, however, a dynamical system requiring self-consistent solution.

- The vector and scalar potentials appear directly in the momentum and energy of each element. The momentum and energy are also the sources for the vector and scalar potentials.
  So any solution is self-referential.
- The gravitational scalar potential is equal to the speed of light c, which determines the light cone and therefore the distance r_i in Eq. 3.2. This additional self-referential dependence necessarily creates non-linearity.

Examples of highly non-linear gravitational problems we shall encounter in later sections are:

- The neutron star/black hole is analyzed, in Chapter 12, in which the gravitational potential can vary by a large factor within very short distances.
- Cosmological calculations, in which the entire universe must be considered, and a substantial fraction of its total energy is tied up in the mutual gravitational attraction of its elements, as in Section 9.

Chapter 4

Gravity and Wave Functions

For many years it was thought that gravity might be a phenomenon confined to macroscopic classical objects *i.e.* incoherent aggregations of large numbers of quantum elements as discussed in Section 2.3. An end was put to all such discussions by the historic 1975 experiment of Colella, Overhauser and Werner [9][72]. They constructed an interferometer from a single Silicon crystal, as shown in Fig. 4.1.

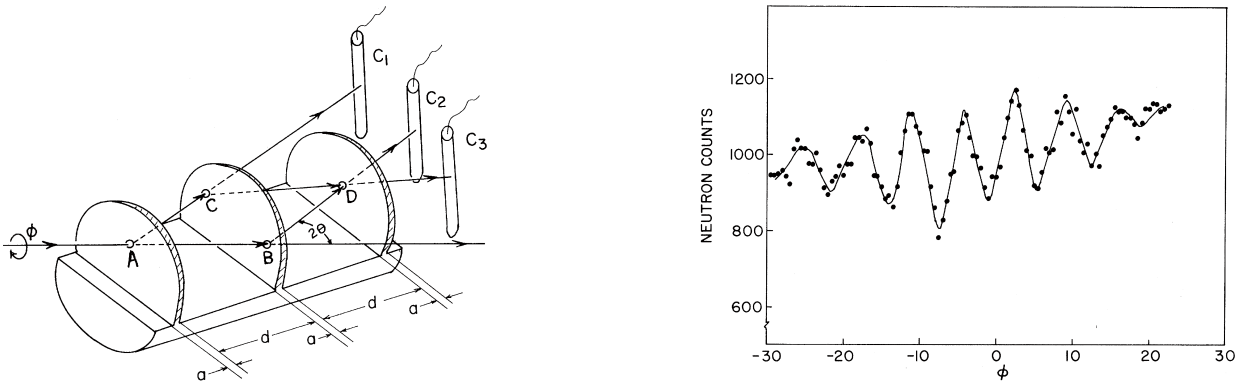

Figure 4.1: Left: Neutron interferometer hewn from a single dislocation-free Silicon crystal.
Right: Interference pattern, as evidenced by the difference in the number of Neutron counts in counters C_2 and C_3 as the apparatus is rotated by angle ϕ around the AB axis in the Earth's gravitational field.

A collimated beam of Neutrons impinges from the left along path AB, striking the first thin crystal fin at point A. The Neutron wave is diffracted by the crystal, so part of it travels to point C from whence part is diffracted to point D and part continues to counter C_1. From point A, the remaining part of the incident wave continues to point B, from whence part is diffracted to point D where the CD path and the BD path interfere, creating an amplitude pattern at counters C_2 and C_3. The probability to count each Neutron in these two counters is proportional to the square of that amplitude, which varies as the cosine of the relative phase of paths ACD and ABD. As the apparatus is rotated by the angle ϕ in the direction shown, point C is moved to higher potential in the Earth's gravitational field, and point B is moved to lower potential. The dependance of wavelength with gravitational potential is worked in Section 2.5. Because the Neutron speed is much less than the speed of light and the gravitational field is small, we can use the simple formulation: The Neutron mass m, velocity v, height h and the gravitational field is g, and the total Neutron energy $E >> mgh$:

$$
\begin{aligned}
p = mv = \hbar k_0 = \frac{2\pi\hbar}{\lambda} \quad &\Rightarrow \quad v = \frac{2\pi\hbar}{m\lambda} \\
E = \frac{\hbar^2(k_0+\Delta k)^2}{2m} + mgh \approx \frac{\hbar^2(k_0^2+2k_0\Delta k)}{2m} + mgh &= \text{Constant} \\
\frac{\hbar^2 k_0 \Delta k}{m} = -mgh \quad &\Rightarrow \quad \Delta k = \frac{-m^2gh}{\hbar^2 k_0} = \frac{-m^2gh\lambda}{2\pi\hbar^2}
\end{aligned}
\tag{4.1}
$$

The Neutron mass $m \approx 1.675 * 10^{-27}$ kg, and its wavelength is given as $\lambda = 1.445 \times 10^{-10}$ meter, so their velocity $v \approx 2700$ meter/sec, a factor of 10^5 less than the speed of light, so our approximation is good.

Looking at the interferometer in Fig. 4.1, the height of path AB does not change with rotation angle ϕ, and the two diagonal path segments AC and BD change by exactly the same amount, so all the relative phase change occurs in path segment CD, which, spaced $\approx .03$ meter from segment AB, will rise by $h \approx .03 \sin\phi$. Path segment CD is $\approx .035$ meters long, so the maximum number of cycles phase shift going from $+h$ to $-h$ will be $\Delta k.035/\pi \approx 19$ cycles, in agreement with the papers. At any given angle, the phase shift $\beta \approx 9.4 \sin\phi$ cycles.

The actual data shown in the right side of Fig. 4.1 is the difference between the counts in counters C_2 and C_3, so we need a way to estimate the count rate in these two counters as the phase β. Each encounter a neutron makes with one of the Silicon fins results in an amplitude to go straight-through and an amplitude to Bragg reflect from

the 220 plane of the Si crystal. The process is complicated, and analyzed in detail in reference [72]. We can make a rough estimate by modeling the amplitude to reflect as R and the amplitude to go directly through as S. From the left drawing in Fig. 4.1, Paths have the following amplitudes:

Path	Amplitude Count Rate	Sum
$ABDC_2$	S R S	
$ACDC_2$	R Rcos(ϕ) R	S^2 R + cos(ϕ) R^3
$ACDC_3$	R Rcos(ϕ) S	
$ABDC_3$	S R R	S R^2 + cos(ϕ) S R^2

The papers tell us that the part of the count rate that is independent of ϕ for C_2 is 2.6 times that for C_3, which leads to R ≈ 0.53, S≈ 0.85. When we allow S to be imaginary, indicating a 90 degree phase shift on the transmitted wave relative to the refracted wave, we obtain:

$$\begin{aligned} C_2 &= -RS^2 + R^3\cos(\phi) \quad \Rightarrow \quad I_2 = C_2C_2^* = R^2S^4 - 2R^4S^2\cos(\phi) + R^6\cos^2(\phi) \\ C_3 &= iR^2S\big(1+\cos(\phi)\big) \quad \Rightarrow \quad I_3 = C_3C_3^* = R^4S^2\big(1+2\cos(\phi)+\cos^2(\phi)\big) \end{aligned} \tag{4.2}$$

The count rates I_2 and I_3, given in the right-hand expressions in Eq. 4.2 are given in [72] as:
$I2 = \gamma - \alpha\cos(\phi)$, $I_3 = \alpha(1+\cos(\phi))$, $\gamma/\alpha = 2.6$ with which we are in agreement with $\gamma = R^2S^4$, $\alpha = 2R^4S^2$ except for a factor of 2 in the first term in parentheses in I_3, and the second order terms containing $\cos^2(\phi)$, which are down by a factor of $R^2/2S^2$ in I_2 but equal in I_3, and are very evident in their Fig.3. It is not clear why they left them out of their analysis.

The difference in counting rates, which is plotted in Fig. 4.1 is

$$I_2 - I_3 = R^2S^4 - R^4S^2 - 4R^4S^2\cos(\phi) + (R^6 - R^4S^2)\cos^2(\phi) \tag{4.3}$$

For the values of R and S given, the expected gravity modulated rate $4R^4S^2$ is 2.5 times the background rate $(R^2S^4 - R^4S^2)$, which is much larger than observed in Fig. 4.1. If we had taken S to be real, the cos(ϕ) terms in I_2 and I_3 would have cancelled, so the phase-shift I assumed for S was wildly optimistic. Although, except for the optimistic modulation, this rough-and-ready analysis seems to agree with the observation, I have not been able to follow the extensive analysis in reference [72] well enough to determine where I went wrong. They did, however, comment on the low level of modulation. Interested readers are encouraged to get to the bottom of this.

Independent of the details, this *Historic Experiment* showed, for the first time in history, that the gravitational scalar potential directly enters the frequency ω of the wave function $[\omega, \vec{k}]$ four-vector. In another four years, this heroic group was able to show that the gravitational vector potential directly enters the propagation vector $\vec{k}$ of the wave function $[\omega, \vec{k}]$ four-vector, thereby verifying that the gravitational vector potential $\mathbf{A}$=$[c, \vec{A}]$ affects wave functions in exactly the same way as does the electrodynamic four-potential $\mathbf{A}_e$=$[\mathcal{V}, \vec{A}_e]$.
That *Even More Historic Experiment* is the subject of Chapter 5 .

Chapter 5

Rotation

The most familiar display of the existence of a frame of reference outside the earth is the Foucault Pendulum (1851). It swings back and forth in a plane fixed with respect to "the fixed stars", what we today would call the distant Universe. The puzzle of what is responsible for the ultimate reference for physical law has troubled "natural philosophers" for centuries. Today the history and makeup of the Universe as a whole is a respectable scientific subject.

5.1 Newton's Bucket

Isaac Newton put forth extremely strong views in favor of "absolute space."
His "bucket experiment" (1687), shown schematically in Fig. 5.1, was for him *the* compelling example.

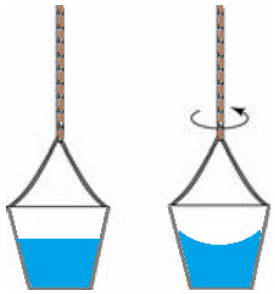

Figure 5.1: Newtons Bucket experiment. There is only one state of rotation in which the surface of water in the bucket is flat. No differential theory can predict *which state of rotation that will be* without assuming it *a priori*. G4v, along with Sciama's theory[62], predict that state to be the frame of reference of the Universe. Figure from Marett[42].

Newton describes the experiment in own words:[48]

> If a vessel, hung by a long cord, is so often turned about that the cord is strongly twisted, then filled with water, and held at rest together with the water; after, by the sudden action of another force, it is whirled about in the contrary way, and while the cord is untwisting itself, the vessel continues for some time this motion; the surface of the water will at first be plain, as before the vessel began to move; but the vessel by gradually communicating its motion to the water, will make it begin sensibly to revolve, and recede by little and little, and ascend to the sides of the vessel, forming itself into a concave figure (as I have experienced), and the swifter the motion becomes the higher will the water rise, till at last, performing its revolutions in the same time with the vessel, it becomes relatively at rest with it. This ascent of the water shows its endeavor to recede from the axis of its motion; and the true and absolute circular motion of the water, which is here directly contrary to the relative, discovers itself, and may be measured by this endeavor. At first, when when the relative motion of the water in the vessel was the greatest, it produced no endeavor to recede from the axis; the water showed no tendency to the circumference, nor any ascent towards the sides of the vessel, but remained of a plain surface, and its true circular motion had not yet begun. But afterwards, when the relative motion of the water had decreased, the ascent thereof towards the sides of the vessel proved its endeavor to recede from the axis; and this endeavor showed the real circular motion of the water perpetually increasing, till it had acquired its greatest quantity, when the water rested relatively in the vessel. And therefore, this endeavor does not depend upon any translation of the water in respect to ambient bodies, nor can true circular motion be defined by such translation. . . . but relative motions. . . are altogether destitute of any real effect. . . . It is indeed a matter of great difficulty to discover, and effectually to distinguish, the true motions of particular bodies from the apparent; because the parts of that immovable space in which these motions are performed, do by no means come under the observations of our senses.

5.2 G4v Treatment

Modern discussions go to great lengths to show the compatibility of both special and general relativistic treatments with the outcome of this experiment and its more modern counterparts. Still, it remains the case that there is one and only one rotational state in which the surface of the water is flat, and no differential theory can tell us which rotation state that is. But Mach's Principle, being an integral theory, provides us a deep and compelling answer: It is the state not rotating with respect to all the matter in the Universe, suitably weighted. From Eq. 3.14, in the weak-gravity limit

$$\vec{k} \approx k_0 \frac{\vec{v}}{c} \qquad \text{and} \qquad \omega \approx k_0 \left(c + \frac{v^2}{2c} + \frac{gh}{c} \right) \tag{5.1}$$

where we have taken c to be the value at the surface of the water, and have approximated the gravitational potential of the Earth by the local acceleration g.

We must emphasize here that v is the velocity *in the frame of the universe*, not just any arbitrary frame. Eq. 2.6 determines the phase Φ around a path of radius r on the water surface, where the velocity $v = \Omega r$ and the height is $h(r)$.

$$\begin{aligned} \Phi &= \int (k ds - \omega dt) = \int \left(k - \omega \frac{\partial t}{\partial s} \right) ds = \int \left(k - \frac{\omega}{v} \right) ds \\ &= k_0 \int \left(\frac{v}{c} - \frac{c}{v} - \frac{v}{2c} - \frac{gh}{c\,v} \right) ds = k_0 \int \left(\frac{v}{2c} - \frac{c}{v} - \frac{gh}{c\,v} \right) ds \\ &= 2\pi r k_0 \left(\frac{\Omega r}{2c} - \frac{c}{\Omega r} - \frac{gh}{c\,\Omega r} \right) = 2\pi k_0 \left(\frac{\Omega r^2}{2c} - \frac{c}{\Omega} - \frac{gh}{c\,\Omega} \right) \end{aligned} \tag{5.2}$$

For the correct path, the phase must be stationary with respect to changes in r:

$$\frac{\partial \Phi}{\partial r} = 2\pi k_0 \left(\frac{\Omega r}{c} - \frac{g}{c\,\Omega} \frac{\partial h}{\partial r} \right) = 0 \quad \Rightarrow \quad \frac{\partial h}{\partial r} = \frac{\Omega^2 r}{g} \quad \Rightarrow \quad h = \frac{\Omega^2 r^2}{2g} \tag{5.3}$$

So, for the water surface to be flat ($\partial h / \partial r = 0$)
the rotation rate Ω of the water must be zero *in the frame of reference of the Universe!*
So one fundamental difference between G4v and differential theories is that *it knows where zero is!*

5.3 Sagnac Effect with Light

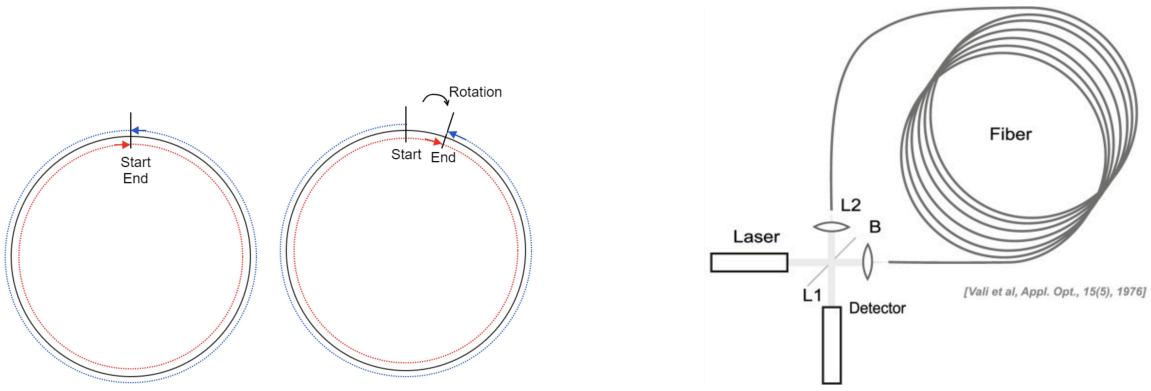

Figure 5.2: Sagnac Effect[60] with Light

The modern version of Newton's Bucket is the Fiber-Optic Gyroscope. The principle of its operation is shown on the left in Fig. 5.3. In the frame of the Universe, light going both directions has the same distance to travel, and there is no phase shift when they meet after their trip. If the path is rotating, the path in the direction of rotation will be longer than the opposite one, and they will develop a phase shift at their point of meeting. The effect can be magnified by a factor of N by making the light go around N turns, as shown in the sketch on the right. Commercial devices of this sort are now universally used for inertial navigation. Once again, the effect is

consistent with Special Relativity, once an inertial frame of reference is defined as not rotating with respect to the distant galaxies, but provides no causal connection between the Universe and inertia. Mach was enraged that no connection had been found.

So strongly did Einstein believe at that time in the relativity of inertia that in 1918 he stated as being on an equal footing three principles upon which a satisfactory theory of gravitation should rest:

1. The principle of relativity as expressed by general covariance.
2. The principle of equivalence.
3. Mach's principle: That the $g_{\mu\nu}$ are completely determined by the mass of bodies, more generally by $T_{\mu\nu}$.

In 1922, Einstein noted that others were satisfied to proceed without this third criterion and added, "This contentedness will appear incomprehensible to a later generation..." See Wikipedia "Mach's Principle."

As expressed earlier in this document, I believe that differential theories, by their very nature, cannot make the Mach-Principle connection—it is only by working directly with the gravitational four-potential (or 4×4 tensor potential) that a seamless connection can be made.

5.4 Sagnac Effect with Wave Functions

The Neutron interferometer described at the beginning of Chapter 4 was continually improved and adapted specifically to observing the vector coupling of the Universe on the propagation vector $\vec{k}$ of neutrons, as shown in Fig. 5.3.

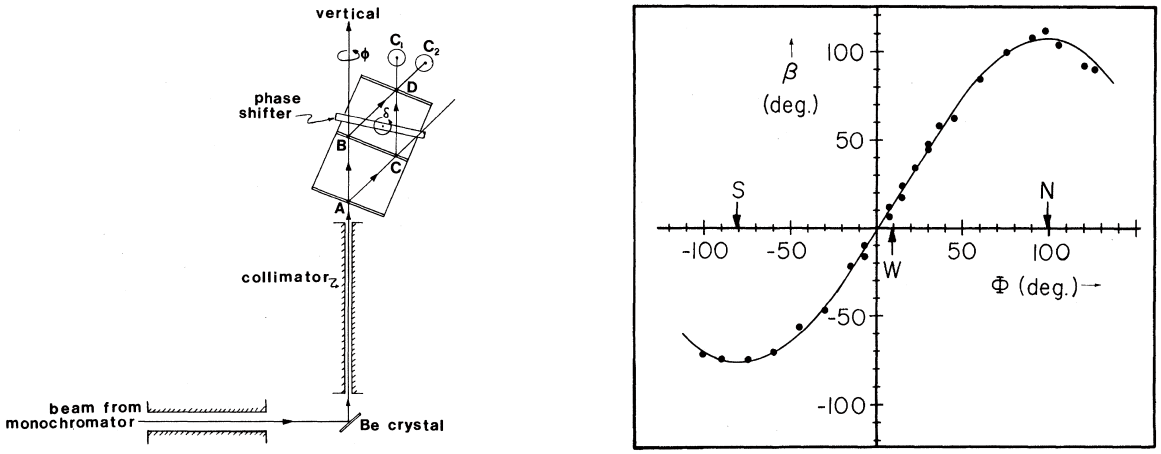

Figure 5.3: Sagnac Effect with Neutron wave function

The colatitude angle at Columbia, Missouri, where the experiment was performed, is 51.37 degrees, so the "vertical" axis is pointing into the northern sky. The orientation ϕ is that of a vector perpendicular to the ABDC plane, and is zero when that vector points west, parallel to the Earth's surface. At 90 deg, that vector points up into the northern sky, and, in that position it has a maximum projection onto the Earth's rotation vector. At -90 deg, that vector points down into the Earth, and, in that position it has a maximum negative projection onto the Earth's rotation vector. So the Sagnac effect can be exposed by varying ϕ and recording the phase shift β as a function of ϕ. The plot is shown on the right panel of Fig. 5.3. This is the first direct observation of the gravitational vector coupling of matter in the distant Universe to the wave vector $\vec{k}$ of a single element of matter. Together with the scalar coupling exhibited by an earlier version of the same interferometer,
It made the four-vector gravitational potential at the fundamental level Evident.

Chapter 6

London Moment

The huge density of electrons in a superconductor join into pairs of opposite spin, which allows them to form a collective "Bose Condensate", which is a Quantum state of macroscopic proportions. This condensate has a collective wave function, whose frequency and propagation vector have a dispersion relation just like the one discussed in Section 2.4. H. K. Onnes found already in 1911 that once started, the current in a superconducting ring will keep flowing undiminished as long as the material is kept in its superconducting state[50][49][51].

In 1961 two independent groups[14][16] found that the reason such a "persistent current" can persist is because its wave function phase must stay continuous, and so must have an integer number of cycles around the ring.
So the collective wave function in a superconducting ring is
a perfect, lossless, free-floating macroscopic Quantum state!
It is by far the most accessible of all quantum states—a fantastic place to introduce students to matter waves.

In *Collective Electrodynamics* 1.9 and 1.10 [44] we saw that the total momentum $\vec{p} = \hbar\vec{k}$ of each electron was the sum of the ordinary mechanical momentum $m\vec{v}$ and the electrodynamic momentum $q\vec{A}$:

$$\vec{p} = \hbar\vec{k} = m\vec{v} + q_0\vec{A} \tag{6.1}$$

The velocity $\vec{v}$ of the electron is thus

$$\vec{v} = \frac{\hbar\vec{k} - q_0\vec{A}}{m} \tag{6.2}$$

and thus each electron will carry a current $\vec{I}_e = q_0\vec{v}$. If there are $\mathcal{N}$ electrons per unit volume moving together, then there will be a current density $\vec{J}$ given by

$$\vec{J} = \mathcal{N}I_e = \mathcal{N}q_0\vec{v} = \mathcal{N}q_0\frac{\hbar\vec{k} - q_0\vec{A}}{m} \tag{6.3}$$

6.1 Null Phase Experiments

It was shown in CE [44] that, when a superconductor in which $\vec{k}$ is initially zero is subjected to an external vector potential, that vector potential dies out with distance into the superconductor with space constant λ, called the **superconducting penetration depth**. For typical superconductors like Niobium, λ is a few tens of nanometers. So the vector potential and all of its derivatives approach zero in the bulk of the superconductor, and only penetrate the material in this very thin "skin" layer. Of course the magnetic field $\vec{B} = \nabla \times \vec{A}$ also approaches zero, and the superconductor is said to "expel the magnetic field."' This phenomenon was discovered in 1933 by W. Meissner and R. Ochsenfeld, and is called the **Meissner effect**. It was explained by Fritz London [39] as a natural consequence of the superconducting condensate being a macroscopic quantum system with a well-defined phase. The electrical current density is the difference between the propagation vector and the vector potential. When the propagation vector is constrained by the coherence of the wave function and the boundary conditions of the geometry, current flows to reduce the "mismatch" between these two vectors. Deep within the superconductor, the two quantities approach each other $q_0\vec{A} \to \hbar\vec{k}$ and the current approaches zero.

Let us consider a loop of radius r made of superconducting wire at rest with respect to the universe, and initialized with the electron wave function in phase at every point around the loop ($\vec{k} = 0$). If the loop is located in an environment free of magnetic flux, for example by carefully shielding it from the influence of outside currents, $\vec{A} = 0$ and thus $\vec{J} = 0$ as well. With this initial condition we now perform two experiments:

1. We locate another loop of wire, coaxial with the first loop, and carrying a current. Because the loops are coaxial, the symmetry of the arrangement dictates that the vector potential at the surface of the first loop due to the current in the second loop will be parallel to the center line of the first loop. We do not know the magnitude of the vector potential at the surface of the first loop, but let's call it A_s. If all dimensions of the loop are large compared with λ, we can apply the analysis of CE Section 1.11 and discover that the vector potential approaches zero deep inside the superconducting wire of the first loop. The magnetic flux is the integral of the vector potential around the loop, which we can take in the center of the wire, and therefore the flux in the loop is zero in this state, independent of the current in the second loop. This is just the Meissner effect for the loop as a whole.

2. We remove the second loop, so no external current is present, and therefore no external vector potential. We then spin the first loop around its axis with angular rotation rate Ω. We know from persistent current experiments that the electron wave function behaves like a perfect, frictionless object: totally uncoupled from the crystal lattice in which it resides. The $\mathcal{N}$ positive charges per unit volume responsible for keeping the entire wire charge neutral are, however, part of the lattice, and are forced to move when the loop is mechanically rotated about its axis. The current density is therefore the difference between the positive charges moving with velocity Ωr and the superconducting condensate moving with velocity v as given by Eq. 6.2. The current density J of Eq. 6.3 then becomes

$$J = -\frac{\mathcal{N}q_0}{m}\left(\hbar\vec{k} - m\Omega r - q_0 A\right) \tag{6.4}$$

Our initial conditions on this experiment constrained the total phase around the loop to be zero, so $\vec{k} = 0$ and the current density is

$$J = \mathcal{N}q_0\left(\Omega r + \frac{q_0}{m}A\right) \tag{6.5}$$

As detailed in CE Section 1.11 the current density represented by the total of all $\mathcal{N}$ positive charges per unit volume moving with velocity Ωr is huge compared with the currents actually observed in these experiments, so we assume that $J \ll \mathcal{N}q_0\Omega r$ and check our result later. Under this assumption

$$A \approx -\frac{m\Omega r}{q_0} \qquad \Rightarrow \qquad \Phi = 2\pi r A \approx -\frac{m\Omega\, 2\pi r^2}{q_0} = \frac{m\Omega}{q_0} \times \text{loop area} \tag{6.6}$$

The rotation has induced a magnetic flux equal to the line integral of $\vec{A}$ around the loop. The negative sign indicates that the flux is in the opposite direction from that induced by electronic charges moving with velocity Ωr. The flux is proportional to the loop area, and hence is the equivalent of a uniform magnetic field of magnitude B_{rot}. If we take $q_0 = -q$ as the electronic charge and m the electronic mass, the field per unit angular velocity is

$$\begin{aligned}\frac{B_{\text{rot}}}{\Omega} = \frac{\Phi}{\Omega \times \text{Area}} = \frac{2m}{q} &= 1.137 \times 10^{-11} \text{ Tessla sec} \\ &= 1.137 \times 10^{-7} \text{ Gauss sec}\end{aligned} \tag{6.7}$$

We can understand the effect as follows: When we initiate the rotation, the motion of the positive charges in the lattice creates a change in vector potential that acts on the electron wave function. The sign of the interaction is that required to accelerate the electrons in the direction of rotation, to match the motion of the positive charges. The inertia of the electrons opposes this acceleration. If the electrons were extremely massive, they would accelerate only a small amount, and the "slip" between their motion and that of the positive charges would be large, implying a large current density, and therefore a large magnetic flux. If the electrons had no inertia, their motion would exactly match that of the positive charges, and there would be no magnetic flux. In any case, the net result is that, in the interior of the wire, the propagation vector of the wave function is matched to the vector potential, and the current is therefore zero. As we approach the surface, the positive charges slightly outpace the electrons, $\vec{A}$ decreases slightly, and the difference between $\vec{k}$ and $\vec{A}q_0/\hbar$ is manifest as a "skin" current. At the surface, the value and radial slope of $\vec{A}$ inside and outside the wire match, and the value of $\vec{A}$ is still within one part in 10^4 of that in the center of the wire, exactly as in the case of a persistent current

The flux produced by a rotating superconducting loop was predicted by London [39], and is called the **London Moment**. It was first measured in 1964 by Hildebrandt[29], and found to be within about 5% of the predicted value. The experimental data from that experiment is shown in Fig. 6.1.

Notice that we have taken the value of q_0 as that of a single electron, not that of two electrons as in the case of the quantized flux. The doubling of the effective charge is usually attributed to pairing of electrons. If that were the case in the present circumstance, the doubling of charge for a pair would be accompanied by a doubling of the mass as well, and the magnitude of the effect would be the same. If, as suggested by Berry[4], the doubling in the effective charge per unit wave vector is a result of the fact that the spin–$\frac{1}{2}$ electron wave function can match up with itself with a π phase twist, that fact would have no effect in the present experiment, since there is no phase accumulation around the loop. Thus the present experiment cannot shed any light on the origin of the value of q_0 in quantized flux experiments.

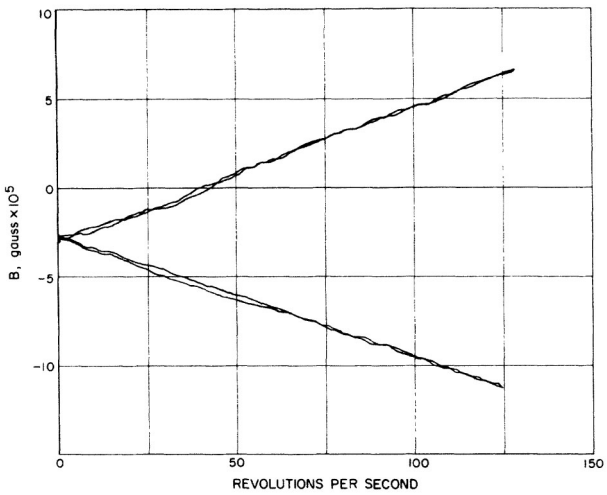

Figure 6.1: Magnetic field in rotating loop as a function of rotation rate from Hildebrandt[29].
The upper curve is for clockwise and the lower curve is for counterclockwise rotation.

The important lesson this experiment teaches us is that, in the interior of the loop, the inertial effect from the electrons' coupling to the rest of the universe is, to very high accuracy, cancelled by the motion of the positive charges, each contributing equally in opposite directions to the reference frame of the electrons.
Thus this was a null-phase measurement—the wave function phase around the loop was fixed at zero while the magnetic flux was measured as a function of rotation rate. The result was a measurement of the ratio of gravitational to electromagnetic vector coupling, represented by the mass–to–charge ratio in Eq. 6.7.

6.2 Null Flux Measurement

Although limited by the precision of the magnetic flux measurement, Hildebrandt's 1964 paper was the first demonstration of the London moment, and determined the mass–to–charge ratio to be that predicted by Fritz London. It could not, for the reasons mentioned above, discriminate between a condensate composed of single electrons and one composed of electron pairs.

In 1990 a Stanford group[68], leveraging the technology developed for the Gravity Probe B satellite, extended Hildebrandt's technique and achieved a direct determination of the inertial properties of the condensate in a Niobium superconductor. The insight that led to this innovation was that the magnetic flux *vs* rotation rate could be measured for a large number of discrete values of $\hbar k = mv - qA$, each of which was assumed to correspond to an integral number n of cycles of the wave function phase around the loop. The data obtained in this manner is shown in Fig. 6.2.

The $\mathcal{N}$ positive charges per unit volume in the loop of radius r are moving with velocity Ωr because they are fixed in the Niobium lattice. The superconducting condensate is composed of $\mathcal{N}$ negative charges per unit volume, and is "free-floating" with respect to the lattice. Its frame of reference is determined by the mass of the Universe, vector-coupled gravitationally, and the positive charges, vector-coupled magnetically.

Eq. 6.6 becomes

$$q_0\vec{A} + m\vec{v}_c = \hbar\vec{k} = \hbar\frac{2\pi n}{2\pi r} = \frac{\hbar n}{r} \qquad \Rightarrow \qquad q_0 Ar = \hbar n - mrv_c \tag{6.8}$$

The flux $\Phi = 0$ in the loop, and the frequency of the zero crossings in Fig. 6.2 is then a linear function of condensate velocity v_c.

$$\Phi = \oint \vec{A}\cdot d\vec{l} = 2\pi rA = \frac{\hbar}{q_0}n - \frac{mrv_c}{q_0} = 0 \qquad \Rightarrow \qquad m = \frac{\hbar n}{rv_c} \tag{6.9}$$

Because the data actually used in the analysis are the points of zero flux, they are also the points of zero current, at which the condensate moves exactly with the positive charges, which allows Eq. 6.9 to be written as a function

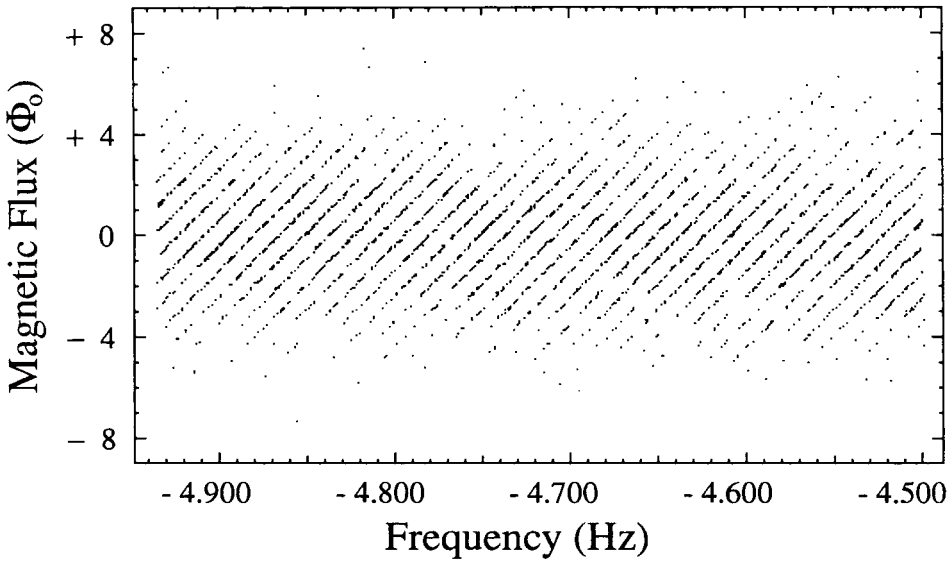

Figure 6.2: Magnetic flux enclosed by rotating loop as a function of rotation frequency (revolutions/sec.). Each sloping line of data points, corresponding to an integer number of wave function phase cycles around the loop, is equivalent to the upper plot in Fig. 6.1. The lines are separated vertically by one flux-quantum Φ_0 and horizontally by the incremental rotation rate such that the additional velocity adds one cycle to the phase of the wave function. The spacing of the zero crossings in this data is a measurement of the wave vector k as a function of condensate velocity at zero current.

of rotational frequency Ω:

$$m = \frac{\hbar n}{r^2\Omega} = \frac{hn}{2S\Omega} = \frac{h}{4\pi S}\frac{\Delta n}{\Delta \nu} \tag{6.10}$$

which is Eq. 3 in the Stanford paper[68], in which S is the area of the loop, and $\Delta n/\Delta\nu$ is the slope of the plot of n *vs* rotational frequency. The Stanford experiment obtained $\Delta n/\Delta\nu = 69.922$, from which they inferred the mass of the condensate pair $m' = 2m_e \times 1.000084(21)$. The experiment was afflicted with a systematic error due to charging of the quartz rotor which supported the Niobium loop. Rotation of this charge created a current that was indistinguishable from current in the loop. To correct for this effect. the loop was heated until it became normal and the flux measurement from this "zero point" was used to construct a model of the charge contribution. The corrections to the final result were around 2000 ppm. So the accuracy quoted for the final result (84 ppm) depended critically on the accuracy of the model used for the corrections. After careful examination of the data, it is our opinion that the result may be interpreted as consistent with $m' = 2m_e$ within experimental uncertainty.

6.3 Discussion

The Stanford experiment was the first measurement to determine the inertial properties of the superconducting condensate without relying on any electromagnetic contributions to the wave function phase. It was thus a new landmark in our knowledge about the condensate itself. However, like the quantized–flux experiments and the original London moment experiment, it cannot discriminate between a condensate composed of spin–$\frac{1}{2}$ electrons with $m' \approx m_e$ and one composed of spin–zero pairs of mass $m' \approx 2m_e$, as assumed in the literature. In the former case, the Berry phase around the loop would be πn instead of $2\pi n$ in Eq. 6.8, and the mass in Eq. 6.10 would become $m' = m_e \times 1.000084(21)$. Thus, once again, we are unable to determine the most fundamental properties of the elements of a superconducting condensate. All experiments are *consistent with* either interpretation. We are led to ask the question "is a condensate formed of spin–$\frac{1}{2}$ electrons *really different in any measurable way* from one formed of spin–zero electron pairs?"

A second question raised by the Stanford experiment is, apart from issues about spin, what mass would we expect? Electrons moving in solids have a well-characterized **effective mass** that is usually very different from the "bare" electron mass. This effective mass is the result of electron current interacting with the positive charges of the

lattice. Niobium has 5 conduction electrons per atom and a complicated Fermi surface. As such the effective mass depends wildly on the position of the electron wave function in k-space. Magnetic measurements used to characterize the effective mass at the Fermi energy as a function of the position of the electron wave function in k-space[10] give values between $-1.5 \times m_e$ and $-4.8 \times m_e$ (the negative sign indicating hole-like conduction), all assuming that the charge of the conduction elements is $1 \times q_e$. The sign of the effective mass (inverse of $\partial v_c/\partial k$) is opposite of that obtained from the Stanford experiment! Thus, independent of possible very small deviations from $m' = 2m_e$, the Stanford result result is certainly sufficient to rule out any significant contribution of the normal-state effective mass to the inertia of the condensate.

Given this complexity of conduction electron behavior, how can the experimental value of the condensate mass lie so close to the bare electron value? One hint is that the conduction electrons in the magnetic experiments are moving with respect to the positive charges in the lattice, while those in the Stanford experiment are not. Another hint is that the superconducting condensate is a much more collective state than the normal electrons in Nb, and a superconducting gap has been created at the Fermi level that has completely different symmetry than that of the normal Fermi surface. Whatever our theoretical speculations, this landmark experiment is telling us that the inertial properties of the condensate, when freed from electromagnetic interference and allowed to interact *via* its vector gravitational coupling with the matter in the universe at large, is extremely close to the inertial properties of its isolated constituent elements. Both of these questions lead us deep into the fundamental nature of the collective state of a condensate—a discussion well beyond the scope of this section.

Chapter 7

Gravitation and Light Propagation

7.1 Introduction

The effect of gravity on the propagation of light was taken up by Einstein in 1907, and in a more complete manner in his 1911 paper specifically on the subject[23]. One is struck by the clarity of reasoning in this paper, and the power of its conclusions. Reasoning strictly from the *equivalence principle*, he reached the conclusion:

> If we call the velocity of light at the origin of co-ordinates c_0, then the velocity of light c at a place with the gravitation potential Φ will be given by the relation
>
> $$c = c_0 \left(1 + \frac{\Phi}{c_0^2}\right) \tag{7.1}$$

In 1911 there was no direct way to test the variation in the speed of light as the path of propagation passed near a massive body. In 1964, Irwin Shapiro published a visionary paper *Fourth Test of General Relativity*[63] which opened with the statement:

> Recent advances in radar astronomy have made possible a fourth test of Einstein's theory of general relativity. The test involves measuring the time delays between transmission of radar pulses towards either of the inner planets (Venus or Mercury) and detection of the echoes. Because, according to the general theory, the speed of a light wave depends on the strength of the gravitational potential along its path, these time delays should thereby be increased by almost 2×10^{-4} sec when the radar pulses pass near the sun.

Shapiro's first (1966) measurements of the delay were made by upgrading the MIT Haystack radar with a high-power transmitter and sensitive receiver so it could determine the time delay of the faint returns from radar pulses sent from Earth to Venus and Mercury. When the orbits were such that the line of sight came close to the Sun, a large "excess delay" was detected due to the reduction of the speed of light along the path, as shown in Fig. 7.1.

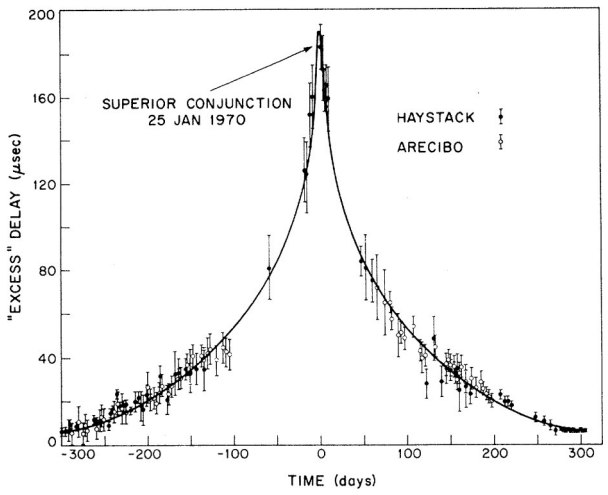

Figure 7.1: Excess delay in propagation of a radar signal from Earth to Venus and back, as the path of propagation passed near the Sun. The zero of time denotes the time when the line of sight between the two planets passed closest to the Sun. Tests such as this one provide us with direct evidence that the speed of light varies with gravitational potential. Plot from Shapiro *et al.* (1971)[65]

7.2 Speed of Light in G4v

We have seen that the energy and momentum of any propagating wave interacts gravitationally with nearby matter. We consider a large massive body of Compton wave number k_0 and energy ω_0. According to Mach's Principle, embodied in Eq. 3.10, the frame of reference for the momentum of M is the resultant of all other momentum vectors in the universe. For simplicity, let us consider the case where M is at rest with respect to the universe as a whole. We now add a ray of light of frequency ω and wave vector $\vec{k}$ propagating at a distance r from M. According to Eq. 3.2, that light ray will result in a gravitational vector potential at M of

$$\vec{A} = -\chi \frac{\vec{k}}{r} \tag{7.2}$$

From Eq. 3.7, that vector potential will result in M acquiring a propagation vector $\vec{k}_M$

$$\vec{k}_M = -k_0 \vec{A} = -k_0 \chi \frac{\vec{k}}{r} \tag{7.3}$$

In other words, the light ray has become part of the frame of reference for M, and M acquires a momentum, however slight, by virtue of the light ray's motion with respect to it.

The total momentum, light ray plus M, is conserved, exactly as was the case for two matter waves, as highlighted in Eq. 3.14. The light ray thus acquires an equal and opposite additional momentum by its interaction with M.

$$k = \frac{\omega}{c} - k_M = \frac{\omega}{c} + k_0 \chi \frac{k}{r} \qquad \Rightarrow \qquad k = \frac{\omega}{c} \frac{1}{1 - \frac{k_0 \chi}{r}} \tag{7.4}$$

We note here that the foregoing calculation has a self-referential character, of which we spoke earlier:
We don't know k, but know it will have a contribution from M. We don't have a closed-form way to determine the contribution of M to k in the light ray's reference frame because the light ray is moving with the velocity of light. But the light ray will have a finite and well-defined k, so we calculate its contribution to the momentum of M, and invoke the conservation of momentum to determine the "back reaction" from M to the light ray. Thus the problem has the character of a feedback loop, and the solution is the self-consistency condition. The form of the solution will recur many times as the vector contribution to the momentum. It is not limited to a light ray, but applies to any matter wave, whatever its ω/c is from scalar interactions. It is the source of essentially all the measured deviations of observed phenomena from their Newtonian form, which are normally attributed to GR.

Returning now to the path of propagation of the light wave, Eq. 7.4 gives the vector-gravity contribution to the light propagation vector k. We also need to take into account the scalar contribution due to the Eq. 3.2 dependence of the speed of light c on the gravitational potential c:

$$c = c_0 - \frac{\omega_0 \chi}{r} \tag{7.5}$$

where c_0 includes the interaction with the entire universe, not including M.
Substituting this value of c in Eq. 7.4, we obtain an expression for k valid for arbitrary potentials:

$$k = \frac{\omega}{c_0} \frac{1}{\left(1 - \frac{k_0 \chi}{r}\right)\left(1 - \frac{\omega_0 \chi}{c_0 r}\right)} \tag{7.6}$$

We can compare our value with that predicted by GR by noting that both k_0 and χ are independent of the gravitational potential c.

$$k_0 = \frac{M c_0}{\hbar} \qquad \text{and} \qquad \chi = \frac{\hbar G}{c_0^3} \qquad \text{and} \qquad \omega_0 = k_0 c_M = \frac{M c_0 c_M}{\hbar} \tag{7.7}$$

where M and G are the values in potential c_0, and c_M is the potential at the massive body.
So, in terms of these conventional variables, Eq. 7.6 becomes

$$k = \frac{\omega}{c_0} \frac{1}{\left(1 - \frac{MG}{r c_0^2}\right)\left(1 - \frac{MG\, c_M}{c_0^3 r}\right)} \tag{7.8}$$

in the weak-gravity limit $c_M \approx c_0$, and Eq. 7.6 becomes

$$k \approx \frac{\omega}{c_0}\frac{1}{\left(1-\frac{MG}{rc_0^2}\right)^2} \approx \frac{\omega}{c_0}\left(1+\frac{2MG}{c_0^2 r}\right) = \frac{\omega}{c_0}\left(1+\frac{\delta}{r}\right) \tag{7.9}$$

In this and the following expressions

$$\delta \approx \frac{2MG}{c_0^2} \tag{7.10}$$

7.3 Shapiro Delay in G4v

Armed with a value of k as a function of r (Eq. 7.9) we can evaluate the phase along the path x traversed by the light ray from a source at $x = x_p$ to an observatory on earth at $x = x_e$. For the moment we approximate the path as a straight line, and check later to see what errors are introduced. The mass M is located at $x = 0$ and spaced from the path of propagation by the distance d, as shown in Fig. 7.2.

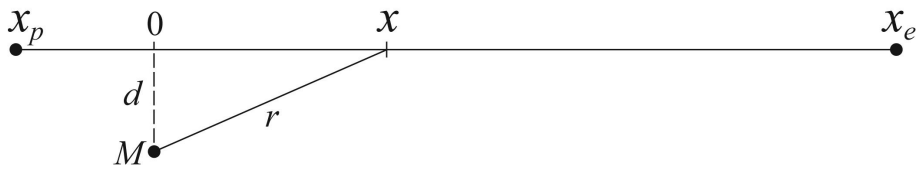

Figure 7.2: Massive object M separated a distance d from the path of propagation from source at x_p to the Earth at x_e. At any given x, the path element is spaced from M by a distance $r = \sqrt{d^2+x^2}$.

The phase ϕ along the light path will, from Eq. 7.9 be

$$\begin{aligned}\phi = \int_{x_p}^{x_e} k\,dx \;&\approx\; \frac{\omega}{c_0}\int_{x_p}^{x_e}\left(1+\frac{\delta}{r}\right)dx = \frac{\omega}{c_0}\int_{x_p}^{x_e}\left(1+\frac{\delta}{\sqrt{d^2+x^2}}\right)dx \\ &= \frac{\omega}{c_0}\left(x_e - x_p + \delta\log\left(\frac{x_e+\sqrt{d^2+x_e^2}}{x_p+\sqrt{d^2+x_p^2}}\right)\right)\end{aligned} \tag{7.11}$$

The propagation time τ is just the phase divided by the frequency ω:

$$\tau = \frac{1}{c_0}\left(x_e - x_p + \delta\log\left(\frac{x_e+\sqrt{d^2+x_e^2}}{x_p+\sqrt{d^2+x_p^2}}\right)\right) \tag{7.12}$$

Because $x_e - x_p = R_{ep}$ is the total distance the signal has propagated, those terms give the time required for propagation from the source to earth in vacuum without the contribution of M to the reduction of the speed of light. That contribution of the $\delta\log()$ term is the additional **Shapiro delay**$\Delta\tau$:

$$\Delta\tau = \frac{1}{c_0}\left(\delta\log\left(\frac{x_e+\sqrt{d^2+x_e^2}}{x_p+\sqrt{d^2+x_p^2}}\right)\right) = \frac{2MG}{c_0^3}\log\left(\frac{x_e+R_e}{x_p+R_p}\right) \tag{7.13}$$

where R_e and R_p are the magnitudes of the distances from M to Earth and from M to the planet, respectively. This result is in agreement with Shapiro's original GR expression[63], valid for weak gravity, and so evident in Fig. 7.1. This expression is not convenient for comparison with observation because the coordinates x_e and x_p are not directly measurable. A more convenient form[69][30], which contains only the distances between the three objects, can be obtained by noticing that, if the correction due to the rotation of M is negligible, the Shapiro delay is the same if the direction of propagation is reversed, *i.e.*, R_e and R_p are interchanged, x_e is replaced by $-x_p$, and x_p is replaced by $-x_e$ in the argument of the logarithm:

$$\begin{aligned}\frac{x_e+R_e}{x_p+R_p} = \frac{-x_p+R_p}{-x_e+R_e} = \frac{x_e-x_p+R_p+R_e}{x_p-x_e+R_e+R_p} = \frac{R_p+R_e+R_{ep}}{R_e+R_p-R_{ep}} \\ \Delta\tau = \frac{2MG}{c_0^3}\log\left(\frac{R_e+R_p+R_{ep}}{R_e+R_p-R_{ep}}\right)\end{aligned} \tag{7.14}$$

This form uses all positive distances, which, in G4v, are independent of the inertial coordinate system chosen for the analysis.

In general G4v is much less sensitive to coordinate system issues than GR. The Shapiro delay is given in the time unit determined by the location of the radar clock. For this and many other experiments, the objects involved are all in free-fall.

This gravitational effect of local matter on the speed of light has been measured with increasingly high precision as time has progressed: The effect was first detected by Shapiro and his collaborators during the superior conjunction of Venus on Nov. 9, 1966, and during 3 such conjunctions of Mercury in early 1967[64]. The excess delays measured on these occasions agreed with Eq. 7.13 to well within the experimental uncertainty of ±20%. By 1971, numerous improvements had been made in the experiment, which resulted in the plot in Fig. 7.1, the excess delay agreeing with Eq. 7.14 to within about 2%[65]. Also in 1971, the JPL team tracked the Mariner spacecraft as the line of sight to it came close to the Sun[1], with results that agreed with Shapiro's Venus/Mercury experiments. Once the JPL Viking landers were firmly planted on Mars[56], the range could be established much more precisely, and the agreement between the observed excess delay and that predicted by Eq. 7.14 and by GR was good to 0.1%. More recently, the Cassini spacecraft was equipped with a high precision multiple-frequency two-way radio link when it passed by the Sun in 2002. Observations and analysis by the Cassini team[5] resulted in an excess delay within less than $\pm 10^{-4}$ of Eq. 7.14. The calculations involved in comparing these observations with GR involve ever more parameters as the precision becomes higher, so the calculations are carried out, with the parameterized (beta, gamma, ...) form of general relativity, to about two orders of magnitude higher accuracy than the standard deviations of the measurements. Thus, for example, they consider the motions—orbital and spin—of the earth between transmission and reception of the echoes of the radar signals, the precise orbits of the planets and spacecraft, etc. Consult the original papers for details.

A spectacular example involving many fewer parameters is the Shapiro delay of a one-way transmission from the recently discovered pulsar J1614-2230[15] in a close orbit with a white dwarf companion, as shown in Fig. 7.3.

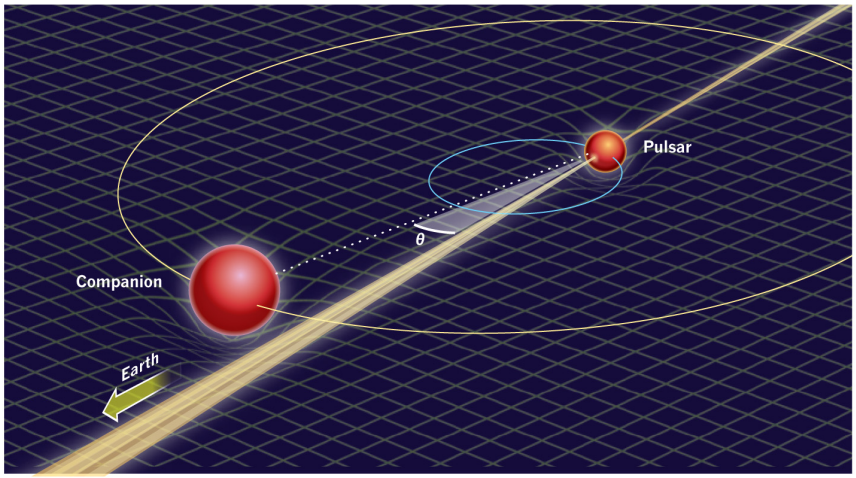

Figure 7.3: Artist's conception of pulsar and white-dwarf companion. As viewed from Earth, the orbit is nearly edge-on, so the pulsar radio beam comes very close to the companion, resulting in a large Shapiro delay as shown in Fig. 7.4. The shaded grid in the background shows the gravitational potential. The drawing is not to scale: The pulsar is only .002 the diameter and 4 times the mass of the companion, so its gravitational potential well is 2000 times deeper. The Shapiro delay is only the contribution of the companion potential, which changes with orbital phase angle θ. The inclination ι (the angle from the axis of the orbit to the line of sight) is nearly 90° in this configuration. From Miller[46].

After applying a little geometry to the orbit (see [45], Fig. 1). Eq. 7.14 gives the standard expression[11] for the Shapiro delay of this configuration.

$$\Delta\tau = -(2MG/c^3)\ln(1 - \sin\iota\,\cos\theta) \tag{7.15}$$

The observed delay is compared with this expression in Fig. 7.4.

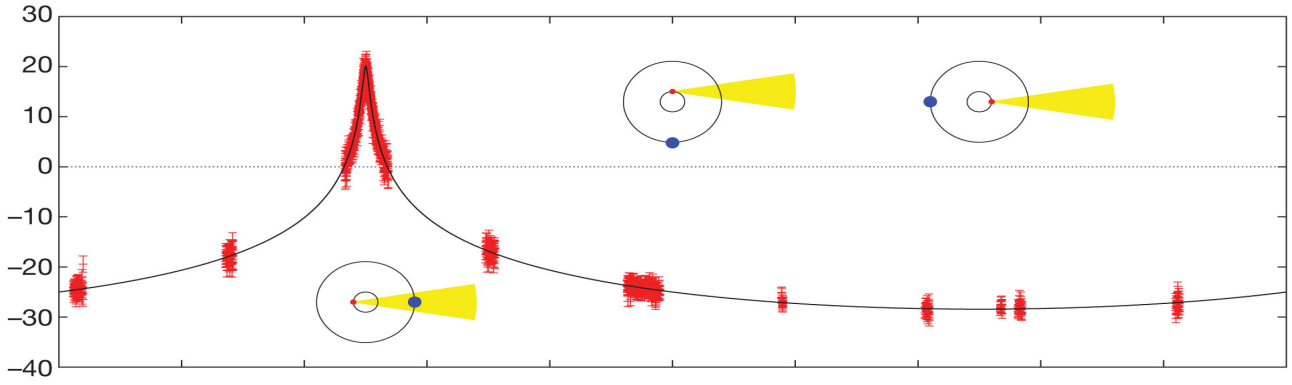

Figure 7.4: Delay $\Delta\tau$ of pulsar J1614-2230 radio signal (in μsec) as a function of orbital phase θ. Red error bars are the observed delay after the signal-travel-time across the Keplerian orbit has been subtracted. The solid black line is the Shapiro delay calculated from Eq. 7.15. The insets are cartoons of the orbit as seen from the top at three particular phases. The direction of propagation to the Earth is indicated by the yellow fans. The pulsar is colored red and the companion blue. Although the ultimate precision of this example is not as high as that of the solar-system observations described above, it seems to be the most direct illustration to date of the gravitational influence on the speed of a one-way signal from an independent astronomical source. From Demorest *et al.*[15]. Reprinted by permission from Macmillan Publishers Ltd: Nature, ©2010.

7.4 Gravitational Deflection of Light

Usual treatments of this subject make a great deal of the fact that Einstein's result for the delay and the concomitant deflection of a light ray by a massive object gave only half the value given by GR, and observed experimentally. In fact, this "failure" of Einstein's early formulations of gravitation theories is often cited as the justification for Metric (curved space-time) formulations, of which GR is the best known. Einstein formulated his gravito-magnetic theory in 1912[19]. He seems to have never returned to the light-deflection problem and asked the question: "What result is obtained if the 'magnetic analog' effect is taken into account?"

We can see immediately from Eq. 7.9 that, in this weak-gravity limit, the scalar and vector gravitational interactions make equal contributions to the propagation vector k. Thus the total effect will be twice that calculated by Einstein in 1911, in agreement with GR. Einstein's "failure" was simply that he included the scalar part, and overlooked the vector part of the relativistic 4-vector interaction. Very odd: Einstein knew perfectly well the four-vector construction of his old teacher Hermann Minkowski, but seemed ignorant of the brilliant 1910 electromagnetism synthesis of G. N. Lewis—published in an obscure journal[36]

Because the Shapiro delay is larger when the light ray is closer to the massive object, the light path will, in keeping with the principle of stationary phase, bend or "refract" to minimize the phase of its path around the massive object. The deflection of the path depends on the spatial derivative of the gravitational potential, rather than on the potential itself.

For the situations considered in the "standard tests," it will, in terms of the precision of the measurement, be a much smaller effect than the Shapiro delay. However the gravitational deflection of light was first observed during the 1919 solar eclipse, long before precision radar observations were feasible. Sir Arthur Eddington organized an expedition to northern Brazil, and also to the island of Principé off the west coast of Africa, specifically to measure the effect. The final results of the expedition are shown in Fig. 7.5.

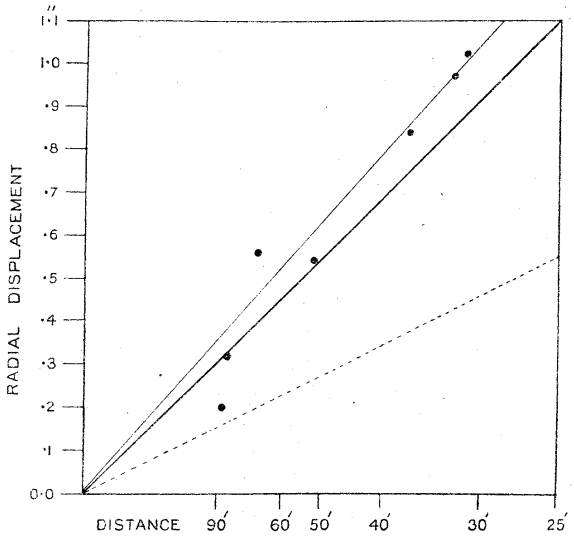

Figure 7.5: Final results of the 1919 solar eclipse expedition, taken from the report of Sir Arthur Eddington and colleagues[17]. During each exposure the telescope tracked the Sun, the direct image of which was blocked by the Moon, so background stars were visible. The best data were obtained from Sobral, Brazil by comparing each exposure with a reference image of the same star field taken with the same instrument two months later when the sun was not present. The deflection (in arc seconds) is plotted *vs* the reciprocal angular distance from the center of the Sun (in arc minutes). The maximum deflection observed was only 1 part in 1800 of the Sun's diameter. The GR prediction is the dark solid line, and the dotted line is half the GR prediction.

Despite the large scatter in the data, the results of this expedition were sufficient to rule out the earlier "half-GR" prediction, and were taken by the investigators as confirmation of the GR prediction. The announcement was considered spectacular news and made headlines in major newspapers around the world. It made Einstein and his theory of general relativity world-famous.

The measurement has been repeated a number of times since, but never with the accuracy obtainable with direct observation of the Shapiro delay. See The Wikipedia entry "Deflection of Light by the Sun"[74] for additional discussion, references and photo.

7.5 Light Deflection in G4v

To obtain the angle of deflection, we once again evaluate the phase along the path traversed by the light ray. We take the mass M as the origin and consider propagation along the path Γ between two points P_1 at $x = R_1$ and P_2 at $x = -R_2$, such that M is located exactly on the line between P_1 and P_2.

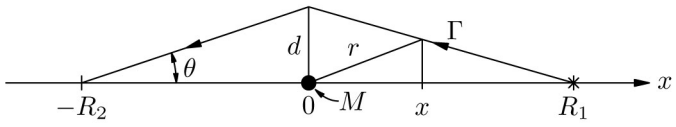

Figure 7.6: Gravitational focusing of light.

We ask if there are paths of stationary phase ϕ at a distance $d > 0$ from M. If there are such paths, a star at P_1 will appear to an observer at P_2 as a bright "Einstein ring" surrounding M. The total light flux from P_1 can thus be greatly enhanced, as Einstein showed in a short 1936 note.[22] Many examples of this kind of gravitational focusing have been documented in recent years, for example
https://www.livescience.com/james-webb-perfect-einstein-ring.

The presence of this effect has profound consequences for certain classes of astronomical observation, and is of great current interest[67]. Anticipating that the deflection will be very small, we consider paths whose distance of closest approach to M is $d \ll R_1$ and $d \ll R_2$, and apply the condition of stationary phase:

$$\frac{\partial \phi}{\partial d} = 0 \qquad \text{where} \qquad \phi = \int \vec{k} \cdot ds \;\approx\; \frac{\omega}{c_0} \int \left(1 + \frac{\delta}{r}\right) ds \tag{7.16}$$

In the following derivation, we use R generically for either R_1 or R_2. At any given x, the distance r from M will be

$$r = \sqrt{x^2 + d^2 \left(1 - \frac{x}{R}\right)^2} \tag{7.17}$$

The distance element ds along which we integrate is

$$ds = dx \sqrt{1 + \frac{d^2}{R^2}} \tag{7.18}$$

The integral of Eq. 7.16 thus becomes

$$\begin{aligned} \phi = \int \vec{k} \cdot ds &= \frac{\omega}{c_0} \left[R\sqrt{1 + \frac{d^2}{R^2}} + \delta \log \left(\frac{\left(\sqrt{1 + \frac{d^2}{R^2}} + 1\right)\left(R\sqrt{1 + \frac{d^2}{R^2}} + d\right)}{d} \right) \right] \\ &\approx \frac{\omega}{c_0} \left(R + \frac{d^2}{2R} + \delta \log \left(\frac{2\,(R+d)}{d} \right) \right) \approx \frac{\omega}{c_0} \left(R + \frac{d^2}{2R} - \delta \log \left(\frac{d}{2R} \right) \right) \end{aligned} \tag{7.19}$$

where the approximations follow because $d/R \ll 1$.

The total phase is the sum of two such terms, one in which $R = R_1$ and one in which $R = R_2$.

$$\begin{aligned} \phi_{\text{tot}} &\approx \frac{\omega}{c_0} \left(R_1 + \frac{d^2}{2R_1} - \delta \log \left(\frac{d}{2R_1} \right) + R_2 + \frac{d^2}{2R_2} - \delta \log \left(\frac{d}{2R_2} \right) \right) \\ &\approx \frac{\omega}{c_0} \left(R_1 + \frac{d^2}{2R_1} + R_2 + \frac{d^2}{2R_2} - \delta \log \left(\frac{d^2}{4R_1 R_2} \right) \right) \end{aligned} \tag{7.20}$$

For stationary phase, we require that the derivative of this expression with respect to d^2 vanish:

$$\frac{1}{2R_1} + \frac{1}{2R_2} - \frac{\delta}{d^2} = 0 \qquad \Rightarrow \qquad \frac{\delta}{d^2} = \frac{1}{2R_1} + \frac{1}{2R_2} \tag{7.21}$$

Eq. 7.21 is reminiscent of the equation of a lens with focal length f:

$$\frac{1}{R_1} + \frac{1}{R_2} = \frac{1}{f} \qquad \Rightarrow \qquad f = \frac{d^2}{2\delta} = \frac{c_0^2 d^2}{4MG} \tag{7.22}$$

However, in the gravitational case, the focal length f depends on the distance d of the light path from the center of a mass concentration, and hence a single "point-like" mass cannot form an image the way a lens does. Instead of an image of the object at R_2, an observer at R_1 will see an "Einstein ring" of angular diameter d/R_1. In practice, an observed object is never precisely aligned with M, and what is observed is a crescent-shaped image. It is possible, under special circumstances, for a special mass profiles to imitate a lens in forming an image, but we are not aware of a case where this has been observed.

Einstein (1936) treated the special case where $R_1 \gg R_2$. In this special case, Eq. 7.21 becomes

$$d = \sqrt{2\delta R_2} \qquad \Rightarrow \qquad \theta \approx \frac{d}{R_2} = \sqrt{\frac{2\delta}{R_2}} = \sqrt{\frac{4MG}{c_0^2 R_2}} \tag{7.23}$$

which is precisely the result Einstein obtained with GR[20].

In the symmetrical case where $R_1 = R_2 = R$, Eq. 7.21 becomes

$$\frac{\delta}{d^2} = \frac{1}{R} \qquad \Rightarrow \qquad \theta \approx \frac{d}{R} = \sqrt{\frac{\delta}{R}} = \sqrt{\frac{2MG}{c_0^2 R}} \tag{7.24}$$

The Eq. 7.23 deflection angle is extremely small in any of the Shapiro delay observations described in the previous section. The effect of that deflection on the Shapiro delay is second-order in the already small angle, and hence can be ignored in those experiments.
Of course, when the deflection is the quantity being measured, we must pay attention to it, however small it may be. In that case GR and G4v predict the same deflection to first order beyond Newton.

$$k = \frac{\omega}{c_0}\left(1 - \frac{k_0\chi}{r}\right)\left(1 - \frac{\omega_0\chi}{c_0 r}\right) \tag{7.25}$$

The vector effect is not, to first order, directional, since it simply modifies the existing propagation vector by a very small factor proportional to the inverse distance to the local mass concentration. However, once the effect from the galaxy has been detected, it may possible to observe second-order directional dependencies. Only time and careful experiments will tell.

It is notable that we use the one-way speed of light in the Shapiro delay analysis, and simply add the outgoing delay to the return delay. We must be careful not to associate such a round-trip radar signal with a standing wave, because it would take many coherent round trips to build up a standing-wave, and a radar experiment consists of one outward-going signal followed by a later return signal. Each of these one-way signals experiences a Shapiro delay according to Eq. 7.13.

Direct evidence for light propagating at different velocities in different directions is the Sagnac effect, widely used for optical gyroscopes. This effect has often been cited as evidence for Mach's Principle: See Sections 5.35.4.

7.6 Local Experiments Suggested by G4v

A curious consequence of the vector coupling can be seen in Eq. 7.6 and Eq. 7.9. Because light propagation is non-dispersive, its propagation velocity $v_c = \omega/k$ at all frequencies, and, near a massive body, is not equal to either c or c_0. In general and in the limit of weak gravity:

$$v_c = c_0\left(1 - \frac{k_0\chi}{r}\right)\left(1 - \frac{\omega_0\chi}{c_0 r}\right) \approx c_0\left(1 - \frac{2MG}{c_0^2 r}\right) \tag{7.26}$$

Said more simply, the vector coupling causes the one-way speed of light propagation v_c to be different from the velocity c inferred from a standing wave. A standing wave has no net momentum and therefore has no net vector interaction with a nearby massive body.

Let us compare the properties of a local measurement done in a gravitational potential c due to a local massive body with the same experiment done in space where $c = v_c = c_0$. The frequency $\omega_{\rm loc}$ of local atomic transitions scales as c, as observed.

$$\omega_{\rm loc} \approx \omega_0\left(1 - \frac{MG}{c_0^2 r}\right) \qquad v_c \approx c_0\left(1 - \frac{2MG}{c_0^2 r}\right) \tag{7.27}$$

The wave vector k of the radiation propagating one-way from a local atomic clock therefore scales as

$$k_{\rm loc} = \frac{\omega_{\rm loc}}{v_c} \approx \frac{\omega_0}{c_0}\left(1 + \frac{MG}{c_0^2 r}\right) \tag{7.28}$$

In G4v the length scale of local matter does not depend on the local gravitational potential. It follows that the local wavelength $\lambda_{\rm loc} = 2\pi/k_{\rm loc}$ will depend on gravitational potential when measured relative to local measuring rods. The reason for the disparity between wavelength of propagating light and length scale of matter is that stationary matter, or standing-wave light, has no net momentum and therefore is not affected by the vector coupling, whereas one-way propagating light has a net propagation vector and therefore has both a scalar and vector interaction with the massive body in the same manner as a conductor carrying net current has a magnetic interaction with other charges and currents whereas electron standing-waves in the conductor carry no current and thus have no such interaction.

The difference in speed of light between standing waves and propagating waves is widely observed in precision measurements of optical cavities. When a high-Q cavity is excited by an optical-frequency comb, it supports pulses propagating at the group velocity and, at the same time, standing waves at the carrier frequency determined by

the phase velocity. In a vacuum, without gravitational vector interaction, the phase velocity and group velocity should be the same. When these two velocities are not the same, a beat note is generated between the frequency at which pulses are bouncing back and forth between the cavity mirrors and the resonant modes of steady-state standing waves supported between the same mirrors. This beat note is called the **carrier-envelope offset frequency** f_{CEO} of the optical cavity. This widely observed offset is usually attributed to dispersion in mirrors and optical material in the cavity, all of which mask the gravitational effect.

Using the techniques described by Ref.[28], a vacuum cavity stabilized laser showed a frequency instability below $\sim 10^{-14}$ for averaging times between 1 ms and 1 s, and a cavity drift of a few Hz over hour-long time periods. An extension of this design would be to lock a frequency comb instead of the continuous-wave laser, to the cavity. The frequency of the circulating optical pulses in the cavity f_{rep} would then the inverse of the round-trip group delay, which is directly monitored at one end of the cavity. If not stabilized, the CEO frequency f_{CEO} of the comb will be that of the cavity, equal to the inverse difference between the round-trip phase delay and the round-trip group delay. A waveform at that frequency is conventionally derived by heterodyning the fundamental and second harmonic optical output frequencies of the comb[35]. The phase of this waveform is equal to the phase difference *at the optical frequency*, so f_{CEO} can be resolved to the optical frequency instability limit by simply counting enough cycles. The f_{CEO} of the cavity described in [28] is $\sim 10^{10}$ Hz, so it can be counted to $\sim 10^{-13}$ in a few minutes. The system can count one frequency using the other as a reference, thereby rendering the cavity and mirror drift common mode, contributing to the result in only second order. This is a strong prediction of the G4v theory, and is testable with presently available technology[61]. I *Really* want to do this experiment!

7.7 Future Work

By Far the most important work ahead of us is to perform the f_{CEO} experiment just described. If it fails to show a gravitational effect on the CEO frequency of a vacuum cavity, G4v will need to be either revised in a major way, or totally abandoned!

In the real universe, virtually all bodies are rotating, often at relativistic speeds. The vector contribution to light propagating near rotating bodies will depend on the direction of light propagation relative to the direction of rotation. This asymmetry will almost certainly be discernible in the Shapiro delay of eclipsing or near-eclipsing binary pulsars.

It is clear that the present discussion is limited to lower energies where "particle physics" reactions are not involved. It thus provides a simple and straightforward approach to "low energy" phenomena.

Eq. 7.8 gives a propagation vector for light as a function of the gravitational effective mass M as follows:

$$k = \frac{\omega}{c_0} \frac{1}{\left(1 - \frac{MG}{rc_0^2}\right)\left(1 - \frac{MG\,c_M}{c_0^3 r}\right)} \tag{7.29}$$

where c_M is the gravitational potential at the surface of the massive body. As long as the light path remains in the weak-gravity limit, $c_M \approx c_0$, the Shapiro delay and light deflection are given by the above treatment, and the agreement with GR and astronomical observation are satisfactory. In strong gravity, however, c_M can be much less than c_0, and quite different results are obtained. One example is the diameter of a light-ring and horizon around "gravistars" and "black holes" which we analyze in Sections 12.6 and 12.7.

Gravitational waves from merging ultra-dense objects are giving us a new window through which to observe the properties of such objects. There will, no doubt, be numerous observations in the future where G4v may make different predictions from GR in this regard.

Chapter 8

Gravitational Red Shift

8.1 Introduction

We now analyze the most fundamental phenomenon predicted by Einstein in 1911, and later by GR: Clocks at different gravitational potentials c tick at different rates.

Consider a specific experiment where one clock is stationed at the bottom of a building of height h and a second nominally identical clock is stationed next to it. Clock 1 generates a frequency ω_1 and Clock 2 generates a frequency ω_2. Clock 2 is connected by a coaxial cable of length h to a frequency comparator that is also stationed next to Clock 1. In this configuration, the clocks are adjusted so that $\omega_1 = \omega_2$. Clock 2 is now carefully carried to the top of the building of height h without damaging the coaxial cable. The frequency comparator now registers a difference frequency

$$\omega_2 = \omega_1 \left(1 + \frac{gh}{c^2}\right) \tag{8.1}$$

where g is the gravitational field $\partial c/\partial h$ at the location of the clocks.

This simple experiment brings us to an extremely fundamental question:
What changed between the two configurations that caused the frequencies to become different?

Einstein based his 1911 conclusion strictly on the *equivalence principle*, and thus provided no hint as to a mechanism. The standard GR answer is that "time flows differently at different gravitational potentials." But GR has purposely constructed its curved spacetime such that this result will occur. There is, therefore, no physics in the statement. The result was assumed in the construction of spacetime itself.

So our question can be rephrased: How does the clock know about the curved spacetime GR has constructed?
We conclude that GR is good at describing what the clock does,
but provides no understanding of the underlying mechanism.

We understand how coaxial cables work, and we know that, in spite of many errant textbook arguments that "the photons get tired going uphill," the frequency difference cannot be due to propagation up the coaxial cable. Whatever the gravitational potential does to the propagation vector of radiation in the cable, once it has reached steady state, there are a given number of cycles in the cable. This implies that every time a cycle enters one end of the cable, a cycle must come out the other end. So *it is the clock itself that runs at a rate that depends on gravitational potential*. Einstein reached this conclusion from the same reasoning in 1911. Something in the physics of the clock causes it to behave that way—*What Is It?*

The scaling law that allows us to construct a theory in which the speed of light changes with gravitational potential was discovered by Max Abraham in 1913[57]. It was re-discovered independently nearly a hundred years later in the course of the present investigation. We have thus adopted *Abraham Scaling* in which lengths, and therefore wave vectors (including k_0), are independent of the gravitational scalar potential, which is equal to the speed of light c. Frequencies, and therefore energies, scale directly with c, and thus times scale inversely with c.

8.2 Physics of Clocks

Einstein commented that the conceptually simplest clock is made with two parallel mirrors separated by a meter bar. Light bounces back and forth between the mirrors, making a tick every time it reaches one end. A modern realization of such a clock is a laser,where light traveling with velocity c forms a standing wave between two mirrors separated by a length l, and a gain medium is present to make up for the light that is taken out of the cavity to preform measurements. The frequency of the standing wave is proportional to c/l. So for the frequency to change with gravitational potential, either the speed of light c, or the length l, (or both) must be a function of gravitational potential. As discussed in Section 7, we have direct and incontrovertible evidence that the speed of light depends on the gravitational potential, so in G4v, it is c that changes with gravitational potential, and l does not. So the frequency of a laser scales directly with the speed of light c, as observed.

8.3 Atomic Energies

Another form of clock relies on the frequency of an atomic transition. Each atomic transition energy is some constant of proportionality times the Rydberg constant Ry.

$$\mathrm{Ry} = \frac{\alpha^2}{2} m_e c^2 \tag{8.2}$$

In G4v, the quantity $k_0 = mc$ is independent of gravitational potential. The fine-structure constant α has been studied closely for any sign of variation with location in the universe or cosmological epoch, placing an upper bound on any potential variation of a few parts per million. From Eq. 8.2 we can see that, to the extent that α is truly constant, the Rydberg energy scales in exactly the same way as the laser frequency with gravitational potential. So the frequency of an atomic clock is proportional to c just like that of an optical clock.

From our point of view, $\alpha^2/2$ is the scale factor between the electron rest energy and the energy of atomic orbits. From the accepted value of α

$$\frac{1}{\alpha} = 137.035\,999\,68 \tag{8.3}$$

the factor between these two energy scales indicated by Eq. 8.2 is $\approx 3.75 \times 10^4$. We encountered α in CE Section 3.12 [44] as the ratio of the impedance of free space to the quantized Hall resistance.

8.4 Atomic Dimensions

Atomic dimensions, and hence dimensions of material bodies, all scale with the **Bohr Radius** a_0.

$$a_0 = \frac{4\pi\epsilon_0\hbar^2}{m_e e^2} = \frac{\hbar}{m_e\, c\, \alpha} \tag{8.4}$$

We have seen in Eq. 2.3 that the quantity of matter, given by the Compton wave number $k_0 = mc/\hbar$ is constant, independent of gravitational potential. Therefore, to the extent that α is truly constant, atomic dimensions, and thus measuring rods, retain their length and can be used to construct a coordinate system in which massive bodies reside.

Thus we have concluded that Abraham scaling does indeed allow us to construct a self-consistent theory in which the speed of light scales directly with gravitational potential.

There is a deep principle here, hiding in the guise of the dimensionless fine-structure constant α. Matter wave functions develop their character from interacting with other matter in the universe.

Most of the macroscopic phenomena we observe, like the force between permanent magnets, atomic spectral lines, etc., come about because energy is transferred between local electromagnetic interaction and cosmological gravitational interaction, as indicated by the presence of the mass m in the equations. At some distance scale, the change in local electromagnetic energy is just comparable to the change in gravitational vector interaction energy, manifested as inertia and kinetic energy. This is the distance scale at which matter, chemistry, and the building-blocks of life reside.

8.5 Nuclear Energies

At even smaller distance scales, other interactions come into play. The vast majority of the rest energy of matter resides in the nuclei of atoms, where the nuclear interaction fixes the Compton scale for k_0. The behavior of the nuclear interaction at short distances constrains the wave functions much more tightly than is possible with electromagnetic interaction. That confinement of the wave function gives very high k_0 to the aggregate, which is why the nuclear "mass" is so dominant. To the extent that the Compton scale for protons and neutrons is truly constant, nuclear energies scale directly with the speed of light c. From studies on the nuclei of atoms, it is clear that the k_0 of an aggregate nucleus is only approximately the sum of the k_0 of its constituent protons and neutrons. The non-linear interaction of matter at densities even higher than those of an atomic nucleus becomes important in neutron stars and black holes, and is poorly understood at present. Nonetheless, the total inertia of complex aggregations of matter are still precisely proportional to their rest energies, and hence to the gravitational potential, and thus to the local velocity of light c. This precise proportionality, is a natural consequence of Mach's Principle as embodied in G4v.

8.6 Effect of Coordinate Systems

The discussion throughout this section has been in the context of a coordinate system fixed with respect to the universe as a whole. In that situation, energies and frequencies scale directly with the gravitational potential c as discussed above. When a clock is moving with respect to the universe as a whole, its frequency is proportional to the *total energy* of matter in its state of motion, as given by, *e.g.,* Eq. 2.12. This result is a direct result of the *equivalence principle*: The energy of any object is equivalent to a frequency, and all frequencies scale in the same way.

Real measurements are most often made from a platform, such as the Earth or a spacecraft, which is in free-fall: *e.g.,* in orbit around the Earth or Sun. The local coordinate system takes the platform as its origin, and the angular orientation fixed with respect to the distant universe—an excellent example is the GPB satellite described in Chapter 11. The simplest free-fall system was shown as the black arrow in Fig. 2.1.

Any object that is stationary within that coordinate system will have constant total energy as the system traverses its trajectory. This principle, although obvious, is invaluable when reasoning about experiments involving a number of objects of interest (planets, spacecraft, etc.) which are communicating.

This dependence of clock rate on total energy per unit matter predicts a curious outcome for the well-known and highly overworked **twin paradox**: Any twin embarking on space travel must, of necessity, reach a higher energy due to her motion in the free-fall coordinate system of her brother who is left behind. It is thus inevitable that her clock will run faster than his, and (sadly) she will age faster than he. This conclusion is opposite of that reached from special-relativistic arguments for a totally obvious reason: It is simply not a special-relativity problem!

8.7 Future Work

The way nuclear and other short-range interactions contribute to the Compton wave number k_0 of a composite object, and how the resulting object behaves in extreme gravitational potential wells such as those encountered in neutron stars and black holes, is a whole field of study in its own right. These extremely dense bodies are certainly huge nearly-coherent states, the nearest earthbound counterpart being superconductors. It is known that the superconducting ground state cannot be arrived at by a perturbation expansion, even with an infinite number of terms. For that reason the equation of state for ultra-dense matter will most likely not be arrived at using "particle" basis states and interactions. It remains an open question whether the CE-G4v line of reasoning can enable progress on this front. More on neutron stars in Chapter 12.

Chapter 9

Cosmology

Any cosmology is built on a few central tenets. The central tenet of G4v is Mach's Principle, which states that matter derives its inertia through interaction with other matter in the universe. Because virtually all modern formulations of physics are differential in nature, there is a widespread misconception that integral formulations such as Mach's cannot add anything substantive to our understanding of physical law. In order to help dispell this myth we give a brief review of this deep and compelling principle.

9.1 Mach's Principle

The recent (2004) successful launch of the historic Gravity Probe B (GPB) satellite has been widely heralded as a test of GR. In a larger context, it can be viewed as an investigation into the origin of inertia. In Newtonian physics, inertia was viewed as an intrinsic local property of a massive body, moving with respect to absolute space. Gravitation was a quite separate phenomenon, evidenced by the attraction of nearby massive bodies. Elegant experiments by Eötvös showed that the inertial mass and the gravitational mass were equal, to extremely high precision. Ernst Mach[40] was an outspoken critic of Newton's notion of "absolute space." He believed that the motion of an object had no meaning except with reference to other objects in the universe. In his view, a mass would have no inertia if the rest of the mass in the universe were not interacting with it. The idea that matter derives its inertia through interaction with other matter in the universe is known as "Mach's Principle".

A number of workers have attempted to realize a mathematically precise formulation of Mach's Principle: An excellent account with many references can be found in Barbour and Pfister[2]. A wonderfully well-reasoned and historically important exposition was given by Sciama[62]. In a fully Machian universe, Gravitation becomes the universal interaction of all matter. There is no longer such a thing as an isolated experiment. Local physics cannot be separated from cosmology, and the identity of inertial and gravitational mass is automatic.

If gravitation is to serve as the mechanism for establishing a frame of reference, the gravitational interaction of an element of matter with all other matter in the visible universe must be responsible for the inertia of that element of matter. Inertia is the property that allows matter moving with a velocity $\vec{v}$ to exhibit a momentum $\vec{p}$. For gravitation to be the origin of inertia, it must have a momentum effect as well as the usual energy effect associated with the gravitational potential energy of nearby massive bodies. In the same way that magnetism is the vector aspect of electrical interaction, "gravitomagnetism" must be responsible for inertia.

In the title of his 1912 paper, Einstein[19] asks the question:
Is There a Gravitational Effect which is Analogous to Electrodynamic Induction?
This paper contains the first concrete proposal for how distant matter in the universe could serve as an inertial frame of reference:

> This suggests that the *entire* inertia of a point mass is an effect of the presence of all other masses, which is based on a kind of interaction with the latter.

At this point, Einstein inserts a footnote

> This is exactly the same point of view that E. Mach advanced in his astute investigations on the subject. (E. Mach, *The Evolution of the Principles of Dynamics*, Chapter 2. Newton's Views on Time, Space and Motion.).

He then remarks

> The degree to which this conception is justified will become known when we will be fortunate enough to have come into possession of a serviceable dynamics of gravitation.

In a number of his other writings, Einstein indicates that Mach's Principle had been one of his guiding principles in the evolution of his theories of gravitation. In his later years he became uncomfortable with what he saw as the failure of GR to incorporate Mach's principle in any deep way. It is thus unfortunate that the coming of GR cut short what, in retrospect, might have been a very productive co-development of cosmology and gravitation theories based on Special Relativity and Mach's Principle. The present approach is a return to this line of thought in the light of recent experimental findings.

9.2 Basic Cosmological Assumptions

It is not obvious at the outset that G4v is compatible with a universe having the properties we observe. Here we analyze the simplest and most basic properties of a G4v universe. In accord with our goal of obtaining the maximum physical insight with the minimum of mathematical complexity, we introduce what we see as the minimal assumptions which could underlie any form of cosmology whatsoever. The assumptions upon which this formulation is based are:

1. The universe is homogeneous, isotropic, expanding.
2. Energy density ρ_E is the source of gravitational scalar potential.
3. The gravitational scalar potential is the speed of light c.
4. Energy density is subject to a continuity equation.

9.3 Gravitational Potential

In G4v, the gravitational vector potential takes the same place in the matter wave equation as the electromagnetic vector potential. For that reason, the source of the gravitational four-potential is the energy-momentum four-vector. The coupling constant χ is equal to the square of the Planck length, and the scalar potential Z is equal to the local speed of light c.

Whatever the makeup of matter in the universe, it will have some energy density ρ_E Joules/m^3, and that energy density is the source for gravitational scalar potential Z, governed by the Abraham Equation[1]:

$$\Box^2 Z = \nabla^2 Z - \frac{1}{c}\frac{\partial}{\partial t}\left(\frac{1}{c}\frac{\partial Z}{\partial t}\right) = 4\pi\chi\rho_E \tag{9.1}$$

where $\chi = {\ell_P}^2$ is the coupling constant. Because the potential is equal to the speed of light c, the equation is highly non-linear due to the $1/c = 1/Z$ terms, so it has no scalable solutions. We are accustomed to solving it in the limit of nearly-constant gravitational potential, in which case it becomes nearly linear, and ordinary methods apply. In the case of cosmology, we must look for a particular solution.

Assuming a uniform solution throughout space, consistent with the cosmological principle, both Z and ρ_E are functions of t alone and Eq. 9.1 becomes

$$-\frac{1}{Z}\frac{\partial}{\partial t}\left(\frac{1}{Z}\frac{\partial Z}{\partial t}\right) = 4\pi\chi\rho_E \tag{9.2}$$

which has solution

$$\begin{aligned} Z &= c_\infty \tanh\left(nH_0 t\right) \\ \rho_E &= \frac{\rho_0 \cosh\left(2nH_0 t\right)}{\cosh\left(nH_0 t\right)\sinh^3\left(nH_0 t\right)} \\ \rho_0 &= \frac{n^2 H_0^2}{4\pi\chi c_\infty} \end{aligned} \tag{9.3}$$

where n is a parameter of the theory that is chosen for the self-consistency condition as described in Section 9.8.3. So the speed of light is uniquely determined by the Hubble Constant, H_0, and the energy density.

[1] Abraham, in his 1913 paper (page 356 in [57]), saw that this form of the equation must be used when the speed of light $c = Z$ is changing with time. Unfortunately he applied it to a theory in which the variable was $\sqrt{Z}$ instead of Z. Nonetheless we have chosen to name this form of the equation, when used for gravitational potential calculations, after Abraham.

9.4 Continuity Condition

A necessary constraint on the solution is the continuity of energy density ρ_E. We express the expansion in a spherical coordinate system, in which the expansion velocity v is in the r direction:
For a universe whose density is uniform at any given cosmic time, ρ_E is a function of t alone:

$$\begin{aligned} -\frac{\partial(\rho_E)}{\partial t} &= \nabla\cdot(v\,\rho_E) = \rho_E\,\nabla\cdot v \\ -\frac{1}{\rho_E}\frac{\partial\rho_E}{\partial t} &= \frac{\partial\, v}{\partial r} + 2\frac{v}{r} \end{aligned} \tag{9.4}$$

We assume a separable solution for the velocity $v = v_t\,H_0 r$, where v_t is a function of t alone:

$$\frac{1}{\rho_E}\frac{\partial\rho_E}{\partial t} = -3H_0 v_t \tag{9.5}$$

So the full solution for the expansion velocity is

$$v = \frac{nH_0 r}{3}\Big(3\coth(nH_0 t) + \tanh(nH_0 t) - 2\tanh(2nH_0 t)\Big) \tag{9.6}$$

Henceforth we shall express the relations of Eq. 9.3 and Eq. 9.6 in terms of dimensionless variables as follows:

$$\begin{aligned} c(H_0 t) &= \frac{c}{c_\infty} = \tanh(nH_0 t) \\ \rho(H_0 t) &= \frac{\rho_E}{\rho_0} = \frac{\cosh(2nH_0 t)}{\cosh(nH_0 t)\,\sinh^3(nH_0 t)} \\ v(H_0 t, R) &= \frac{v}{c_\infty} = \frac{R}{3}\Big(3\coth(nH_0 t) + \tanh(nH_0 t) - 2\tanh(2nH_0 t)\Big) \\ \text{where}\quad R &= \frac{r}{r_H} \qquad r_H = \frac{c_\infty}{nH_0} \end{aligned} \tag{9.7}$$

The evolution of those quantities with cosmic time is shown in Fig. 9.1.

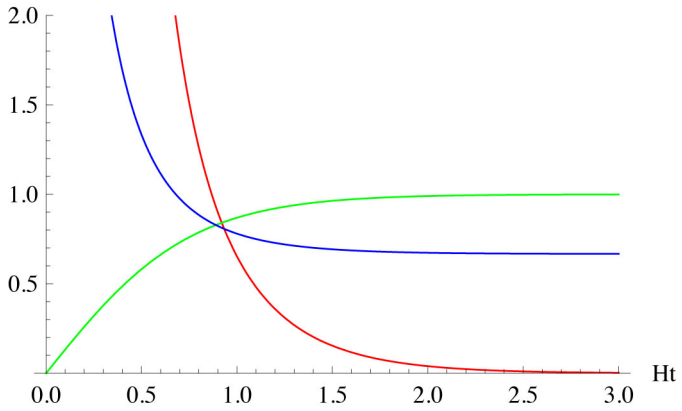

Figure 9.1: The three dimensionless functions of cosmic time in Eq. 9.7 for the self-consistent value $n = 1.33$. The green curve is the normalized speed of light c, equal to the gravitational potential Z. It is determined by the energy density and expansion rate, and is nearly constant after about two Hubble times. The blue curve of the normalized expansion velocity can be thought of as the effective Hubble constant, which also becomes constant after about two Hubble times. The red curve is the normalized energy density.

9.5 Light Cone Distance

A light signal leaving a source at time t_1 will reach an observer at distance d at $t = t_2$, where

$$\begin{aligned} \frac{\partial d}{\partial t} = c(t) = \tanh\left(nH_0 t\right) \quad \Rightarrow \quad d = \int_{t_1}^{t_2} c(t)\, dt \\ d = r_H \, \log\left(\frac{\cosh\left(nH_0 t_2\right)}{\cosh\left(nH_0 t_1\right)}\right) \quad \text{where} \quad r_H = \frac{c_\infty}{nH_0} \end{aligned} \tag{9.8}$$

We note that d is not the distance at one particular cosmic time, but *the distance along the light cone.* For a well-evolved universe, older than about two Hubble times, Eq. 9.8 reduces to the usual expression where the speed of light is constant. In dimensional units:

$$d \approx r_H(H_0 t_2 - H_0 t_1) = c_\infty(t_2 - t_1) \quad \text{for} \quad H_0 t \gg 1 \tag{9.9}$$

9.6 Co-Moving Distance

We wish to follow the evolution of a small volume *as it moves with the Hubble flow* (called a co-moving volume in the cosmology literature). The dimensionless radius R_c reached by a co-moving volume at cosmic time t will be the solution to

$$\begin{aligned} v = \frac{\partial R}{\partial t} = \frac{R}{3}\Big(3\coth\left(nH_0 t\right) + \tanh\left(nH_0 t\right) - 2\tanh\left(2nH_0 t\right)\Big) \\ R_c(t) = R_s\big(\cosh\left(nH_0 t\right)\big)^{\frac{-1}{3n}} \cdot \big(\cosh\left(2nH_0 t\right)\big)^{\frac{-1}{2n}} \cdot \big(\sinh\left(nH_0 t\right)\big)^{\frac{1}{3n}} \\ \cdot \big(\sinh\left(2nH_0 t\right)\big)^{\frac{1}{2n}} \cdot \big(\sinh\left(4nH_0 t\right)\big)^{\frac{1}{6n}} \end{aligned} \tag{9.10}$$

The co-moving radius has an arbitrary scale constant R_s which, when viewed as a vector, is unique to each element in the universe. It identifies that element's position, relative to our chosen origin, at any given cosmic time.

9.7 Horizon

From Eq. 9.8 we have a "lookback radius"—the distance from which light can reach us. The maximum such distance occurs at the normalized **horizon radius** R_0, where $v = c$ in the chosen frame of reference. From Eq. 9.7

$$R_0 = \frac{3\,\tanh\left(nH_0 t\right)}{3\coth\left(nH_0 t\right) + \tanh\left(nH_0 t\right) - 2\tanh\left(2nH_0 t\right)} \tag{9.11}$$

The Light-Cone Distance, Co-Moving Distance, and Horizon Radius, normalized to the Hubble Radius, are shown in Fig. 9.2. This plot would look the same, independent of which element in the visible universe is chosen as the origin. We have chosen the frame of reference to be the co-moving frame of the observer.

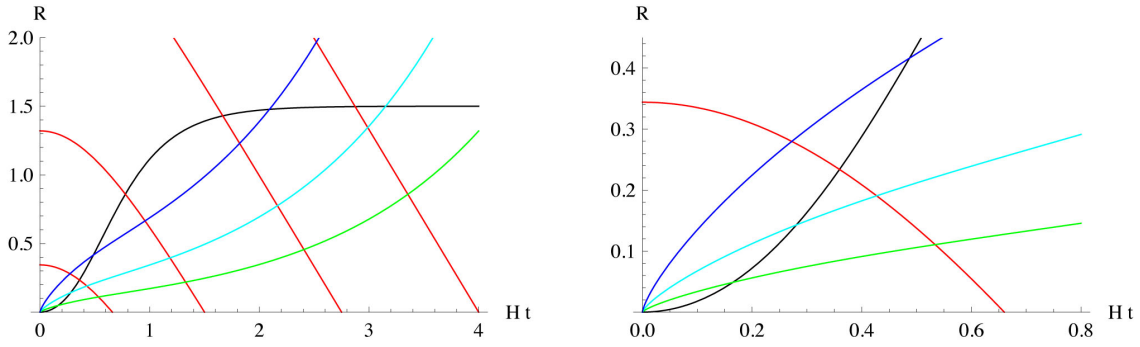

Figure 9.2: Cosmic distances for $n = 1.33$, in units of the Hubble Radius r_H, relative to an arbitrarily chosen origin, plotted as a function of cosmic time in units of the Hubble time. The Horizon Radius is shown in black.

The green, cyan, and blue curves are co-moving distances R_c for objects with $R_s = 0.1$, $R_s = 0.2$ and $R_s = 0.4$. The expansion decelerates in the early stages of cosmic evolution, and accelerates during the later stages. It is clear that, at late cosmic time, more and more volume elements disappear beyond the horizon. The right plot is an enlargement of the lower-left corner of the left plot. The red curves are the light paths emitted by the green, cyan, and blue sources at earlier times $H_0 t_1$, and received by observers at $H_0 t_2 = 0.66$, 1.5 and 2.75 and 4.0. The $n = 1.33$, $H_0 t_2 = 0.66$ curve will turn out to be internally consistent, and to give the best fit to recently observed SN1a Hubble data. The early universe is beyond the horizon in this model.

9.8 Comparison with Astrophysical Observations

9.8.1 Redshift

Let the rest-frame frequency of an atomic transition at r_1, t_1 be ω_1 where the speed of light is c_1 and the corresponding quantities at r_2, t_2 be ω_2 and c_2. The rest-frame frequencies will be proportional to the corresponding gravitational potentials:

$$\frac{\omega_2}{\omega_1} = \frac{c_2}{c_1} \tag{9.12}$$

The frequency $\omega_{\rm obs}$ we observe at r_2, t_2 where the speed of light is c_2, is further reduced by the Doppler effect at the source:

$$\frac{\omega_2}{\omega_{\rm obs}} = 1 + z = \frac{c_2}{c_1}\sqrt{\frac{1 + v/c_1}{1 - v/c_1}} \tag{9.13}$$

9.8.2 Magnitude

A certain number of excited atoms in the supernova we are observing radiate energy at a frequency given by Eq. 9.13. All time scales change inversely with gravitational potential, and are affected the same way by the Doppler effect, so both the energy per photon and the rate at which photons are received will be inversely proportional to the factor given by Eq. 9.13. It follows that the received energy per second f will be inversely proportional to the square of that factor, and of the distance R:

$$f \propto \left(\frac{c_1}{c_2}\sqrt{\frac{1 - v/c_1}{1 + v/c_1}} \cdot \frac{1}{R}\right)^2 \tag{9.14}$$

The Eq. 9.14 relation is valid in the frame of reference of the source, where R is the radius of a sphere upon whose surface the energy flux f is constant. However, in the frame of reference of the observer, the spheres of constant flux are lengthened in the direction of source motion and flattened in the direction opposite to the source motion. This problem is known as **relativistic beaming**, and is well known in particle-physics circles. It has has been carefully worked out by K. T. McDonald[43]. The result is that, for an isotropically radiating source moving away from the observer, the received energy flux $f_{\rm obs}$ is reduced from that of a stationary source $f_{\rm sta}$ by the factor[2]

$$\frac{f_{\rm obs}}{f_{\rm sta}} = \left(\frac{1 - v/c_2}{1 + v/c_2}\right)^2 \tag{9.15}$$

so the total received flux becomes

$$f \propto \left(\frac{c_1}{c_2}\sqrt{\frac{1 - v/c_1}{1 + v/c_1}} \cdot \frac{1 - v/c_2}{1 + v/c_2} \cdot \frac{1}{R}\right)^2 = \left(\frac{1}{1+z} \cdot \frac{1 - v/c_2}{1 + v/c_2} \cdot \frac{1}{R}\right)^2 \tag{9.16}$$

$$m = -2.5 \log_{10}(f) + \text{constant}$$

The predictions of this model, plotted along with recent observations in Fig. 9.3, were arrived at by the iterative process described in the following section.

[2] In a theory like G4v, where the speed of light changes over the path, this relationship will probably be more complicated. The analysis should actually be done with an integral along the light path.

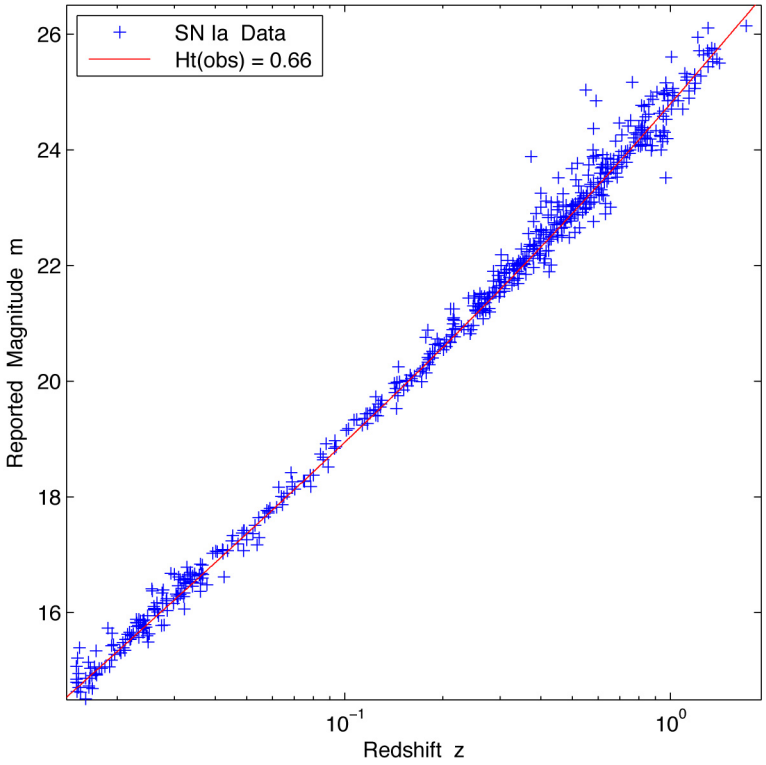

Figure 9.3: Hubble plot showing the results predicted by the G4v cosmological model using $n = 1.33$ from Fig. 9.4. The blue points are the Union2.1 data set, augmented with the 2013 $z = 1.71$ observation. The red curve shows the magnitude-redshift relation predicted for an observer at $H_0 t_2 = 0.66$ in Fig. 9.2, which is the self-consistent value. The upturn of the curves at high redshift is predominantly due to the moving-source factor (Eq. 9.15).

9.8.3 Internal Consistency

It is a principle of G4v that the speed of light is equal to the gravitational potential, and thus determined by Mach's Principle *i.e.* by the gravitational interaction with every other element of matter on both our future and past light cones within our horizon. Thus far we have used only differential relations, and $Z = c$ is determined by Eq. 9.3. Experimentally we have found that equally good Hubble plot fits can be obtained for a wide range of the parameter n, each of which has a different value for the present age of the universe $H_0 t_2$ that gives the best fit. By doing a number of best fits with different n values, we can find the dependence of $H_0 t_2$ on n as shown in the left plot Fig. 9.4.

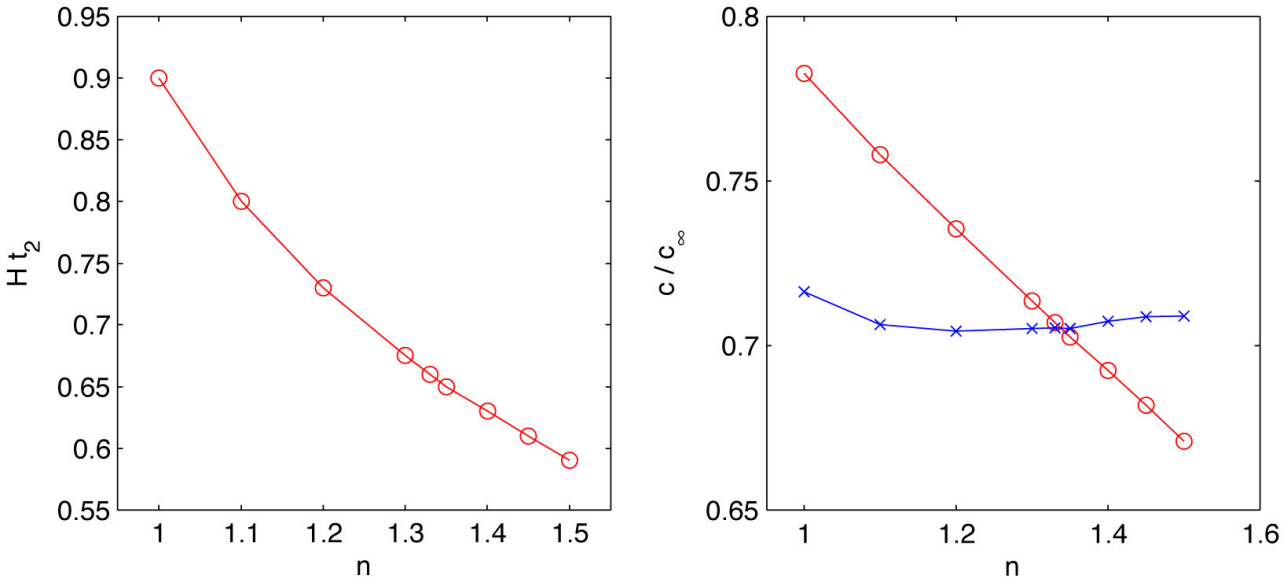

Figure 9.4: Left: Present age of the universe giving the best Hubble plot fit, as a function of $1/n$. The red line merely connects the points. The best fit values entailed considerable judgement, but with care could be reproduced within $\pm 1\%$. Right: Velocity of light determined from Eq. 9.7 (blue crosses) and from the full Mach integral (red circles), both plotted as functions of the parameter n. The intersection at $n \approx 1.33$, $H_0 t_2 \approx 0.66$, $c/c_\infty \approx 0.706$ is taken as our best estimate of a self-consistent solution.

For each $H_0 t_2$, n pair, we can determine the value of every variable, including the speed of light, at every point in space-time from Eq. 9.7.

Because we have the density at every point on the light cone of our present point of observation, we can carry out the Mach integral and thereby determine the gravitational potential, and hence the speed of light. When our theory is internally consistent, these two values must agree.

9.8.4 Mach Integral

According to the G4v interpretation of Mach's Principle, the gravitational potential, and therefore the rest energy and hence the inertia of matter, is determined by the energy density of matter, weighted inversely with distance, and corrected for the Doppler effect. Because of the non-linear nature of the equations involved, we are not guaranteed that an integral determination of the potential will yield the same result as that assumed in the differential formulation. So we must carry out the integration to the point where the two values can be compared to evaluate the internal consistency of the entire approach.

From the definitions of the dimensionless variables in Eq. 9.6 and Eq. 9.7 we obtain

$$
\begin{aligned}
c &= c_\infty - \chi \int_0^{r_0} \frac{\rho_E(r)}{r} \sqrt{\frac{1 - v(r)/c(r)}{1 + v(r)/c(r)}}\ 4\pi r^2\, dr \\
1 - \frac{c}{c_\infty} &= \frac{4\pi\chi}{c_\infty} \int_0^{r_0} \rho_E(r) \sqrt{\frac{1 - v(r)/c(r)}{1 + v(r)/c(r)}}\ r\, dr \\
&= \frac{4\pi\chi\rho_0}{c_\infty} \int_{t_2}^{t_1} \frac{\rho_E}{\rho_0}(t) \sqrt{\frac{1 - v(t)/c(t)}{1 + v(t)/c(t)}}\ r(t)\, c(t) dt \\
&= 4\pi\chi\rho_0 \cdot \frac{r_H}{H_0} \int_{H_0 t_2}^{H_0 t_1} \frac{\rho_E}{\rho_0}(t) \sqrt{\frac{1 - v(t)/c(t)}{1 + v(t)/c(t)}}\ \frac{r}{r_H}(H_0 t)\, \frac{c}{c_\infty}(H_0 t)\, d(H_0 t) \\
&= 4\pi\chi\rho_0 \cdot \frac{c_\infty}{H_0^2} \int_{H_0 t_2}^{H_0 t_1} \rho(t) \sqrt{\frac{1 - v(t)/c(t)}{1 + v(t)/c(t)}}\ R(H_0 t)\, c(H_0 t)\, d(H_0 t) \\
&= n^2 \int_{H_0 t_2}^{H_0 t_1} \rho(t) \sqrt{\frac{1 - v(t)/c(t)}{1 + v(t)/c(t)}}\ R(H_0 t)\, c(H_0 t)\, d(H_0 t)
\end{aligned}
\tag{9.17}
$$

As with any Mach's Principle based theory, the integration must be carried out over both the past and future light cones. The integrand is shown as a function of R in Fig. 9.5.

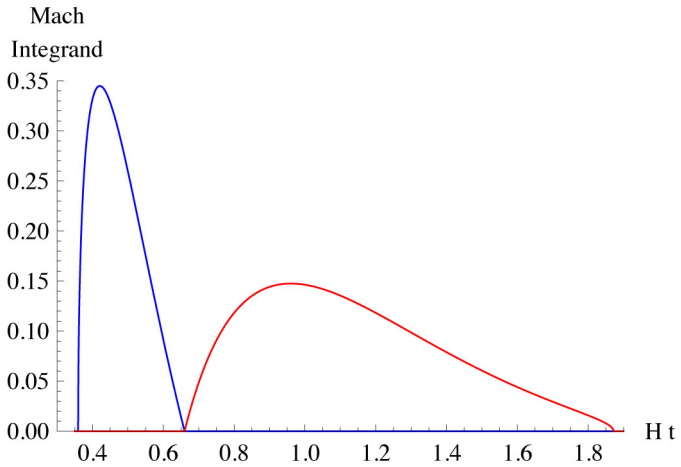

Figure 9.5: Integrand of Eq. 9.17 as a function of cosmic time at the radius on the light cone where the source matter is located. The blue curve is the contribution of the past light cone and the red curve is that of the future light cone. Both curves cut off where the light cone encounters the horizon. The value of $H_0 t_2 = 0.66$ used for this plot is that which gives a self-consistent solution.

The determination of the self-consistent values of the parameters proceeds as follows:

1. Choose a value for n.
2. Compute ρ and c from Eq. 9.7, R from Eq. 9.8, and v/c from Eq. 9.11 as functions of H_0t_1 and H_0t_2.
3. Choose a value for H_0t_2 and make a Hubble plot. Iterate H_0t_2 until a best fit is obtained.
4. Using these values, calculate $c(H_0t_2)/c_\infty$ from Eq. 9.17.
5. Iterate with a new value of n

In this way a plot can be made of the two values of $c(H_0t_2)$ as functions of n, as shown in the right plot in Fig. 9.4. The best fit self-consistent values obtained are $n = 1.33$, $H_0t_2 = 0.66$ and $c(H_0t_2) = 0.706$.

9.8.5 Absolute Distance and The Hubble Constant

To establish the $z \ll 1$ absolute distance scale, we need a single measurement of both z and distance.
In 1999, the water masers in NGC4258 were observed with VLBI parallax, and the distance to that galaxy has been followed and updated regularly. The most recent (2013) distance was reported by Humphreys *et al.*[32] as 7.6 ± 0.23 Mpc[3]. This distance is too close to obtain a reliable Hubble flow velocity, so Riess *et al.*[58] used Cephide variable star magnitudes in NGC4258 and more distant galaxies to infer the magnitude of a hypothetical SN Ia in NGC4258 of $m_{4298} = 10.25$. In a more recent study Riess *et al.*[59] inferred a magnitude of $m_{4258} = 10.18$. These two values of m_{4258} and the $\pm$ Humphreys distance estimates give us four values for the conversion factor from redshift to distance. For each combination we follow our model Hubble plot back to m_{4258} and read off the redshift inferred for NGC4258 if it were in the Hubble flow. The mean value so obtained is $z_{4258} = .00192$. Then, using the Humphreys distance, we can determine the absolute conversion factor between the redshift z and the distance r:

$$r = z\, r_0 \qquad \text{where} \qquad r_0 = (3.96 \pm 0.16) \times 10^3\,\text{Mpc} \tag{9.18}$$

Although it is not an object of this analysis to derive an independent estimate of the Hubble Constant H_0, the Eq. 9.18 relation between the redshift z and the distance r is equivalent to one. All theories, even the most naive Doppler interpretation, predict $z = v/c$ for small redshift, where v is the recession velocity. The $z = .00192$ redshift inferred for NGC4258 (if it were in the Hubble flow) certainly meets the $z \ll 1$ criterion. The Hubble constant H_0 thus determined is

$$H_0 = \frac{v}{r} = \frac{z\,c}{r} = \frac{z\,c}{z\,r_0} = \frac{c}{r_0} = 75.9 \pm 5\ \frac{\text{km/sec}}{\text{Mpc}} \tag{9.19}$$

Of the ± 5 estimated uncertainty in the result, ± 3 is attributable to the uncertainty in the distance to NGC4258 and the uncertainty in m_{4258}. The balance is directly attributable to the value for H_0t_2 chosen as best fit, and the particular fit adopted to the data set. To use this class of G4v models for a serious determination of H_0 would require a much more exacting analysis. Nevertheless, the value obtained here is only a bit higher than that of Riess *et al.*[59], Freedman *et al.*[26], and Humphreys[32] *et al.*, and very close to Suyu *et al.*[67], and midway between the uppermost recent values, all of which are considerably higher than the Planck value[55], as shown in Fig. 9.6.

[3] One megaparsec (Mpc) = 3.09×10^{22} m

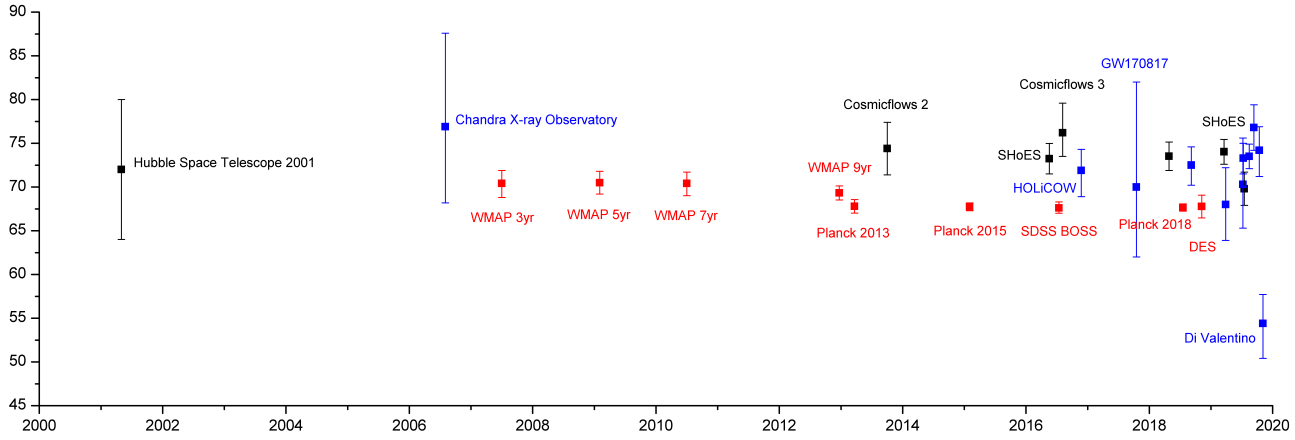

Figure 9.6: Reported values of the Hubble Constant. Our value is between the upper rightmost two data points.

9.8.6 Energy Density

Using the values quoted above, we can, with Eq. 9.3, determine the value of ρ_0 and thus the present energy density rho_E in the universe[4]:

$$\begin{aligned}\rho_0 &= \frac{n^2H^2}{4\pi\chi c_\infty} = \frac{n^2H^2\,\cosh(2nHt)}{4\pi\chi\, c(Ht_2)\cosh(nHt)\,\sinh^3(nHt)} \\ &= 11.5 \;\text{ H atoms equivalent per } m^3\end{aligned} \tag{9.20}$$

This value is about twice the recently quoted value of 5.9 equivalent protons/cubic meter, arrived at with GR-based theory. Our approach has the advantage that it does not place any restrictions on the particular form of energy making up the universe. Thus the simple G4v model does away with the need for some mysterious "dark energy" while, in many other respects, agreeing with the main conclusions of GR-based models. We have thus demonstrated that an internally consistent G4v model cosmology based on Mach's Principle gives results that are within the bounds of reason. This approach places no restrictions on the makeup of the universe, and has a minimum of other assumptions.

[4] An $\hbar$ is needed to convert from our standard G4v frequency units to ordinary energy units.

Chapter 10

Orbits around Massive Objects

10.1 Introduction

One of the celebrated predictions of GR was the precession of an elliptical orbit around a massive body. This prediction resolved a long-standing anomaly in the observed orbit of the planet Mercury. More recently such precession has been observed with exquisite precision in the orbits of double pulsars, and therefore promises to be an important test of the limits of gravitational theories. Here we show that the G4v result without vector interaction corresponds to the classical "Newtonian" result, and that adding the vector coupling gives precisely the same result as GR, to the first post-Newtonian order.

10.2 Classical Solution

The Kepler problem is most simply posed as:
Determine the orbit of an object of mass m around a much heavier object of mass M fixed at the origin.

Assuming there exists a closed orbit, Kepler's second law:

The radius vector from the sun to a planet sweeps out equal areas in equal time.

follows directly from the conservation of angular momentum L:

$$L = mrv_\theta = mr\left(\frac{r\partial\theta}{\partial t}\right) = \frac{m}{2}\cdot\frac{\partial\text{Area}}{\partial\,\text{Time}} = \text{Constant} \tag{10.1}$$

To obtain the orbit we start with conservation of energy E:

$$\begin{aligned}\frac{2E}{m} &= v^2 - \frac{2MG}{r} = v_r^2 + v_\theta^2 - \frac{2MG}{r} = \left(\frac{\partial r}{\partial t}\right)^2 + \left(r\frac{\partial\theta}{\partial t}\right)^2 - \frac{2MG}{r} \\ &= \left(\frac{\partial r}{\partial\theta}\right)^2\left(\frac{\partial\theta}{\partial t}\right)^2 + \left(r\frac{\partial\theta}{\partial t}\right)^2 - \frac{2MG}{r} = \left[\left(\frac{\partial r}{\partial\theta}\right)^2 + r^2\right]\left(\frac{\partial\theta}{\partial t}\right)^2 - \frac{2MG}{r}\end{aligned} \tag{10.2}$$

In terms of the conserved quantities, Eq.10.2 becomes

$$\frac{2E}{m} = \left[\left(\frac{\partial r}{\partial\theta}\right)^2 + r^2\right]\frac{L^2}{m^2r^4} - \frac{2MG}{r} \qquad \Rightarrow \qquad 2E = \left[\left(\frac{\partial r}{\partial\theta}\right)^2 + r^2\right]\frac{L^2}{mr^4} - \frac{2mMG}{r} \tag{10.3}$$

which may be written

$$\left(\frac{\partial r}{\partial\theta}\right)^2 = \frac{2Em}{L^2}\,r^4 + \frac{2MGm^2}{L^2}\,r^3 - r^2 \tag{10.4}$$

Substituting the variable $u = 1/r$, we first work out the derivative:

$$\frac{\partial r}{\partial\theta} = \frac{\partial r}{\partial u}\frac{\partial u}{\partial\theta} = -\frac{1}{u^2}\frac{\partial u}{\partial\theta} \tag{10.5}$$

after which Eq. 10.3 becomes

$$2E = \frac{L^2}{m}\left[\left(\frac{\partial u}{\partial\theta}\right)^2 + u^2\right] - 2MmGu \tag{10.6}$$

$$\left(\frac{\partial u}{\partial\theta}\right)^2 + u^2 = 2\big(E + MmGu\big)\frac{m}{L^2} \tag{10.7}$$

Differentiating with respect to θ

$$2\frac{\partial u}{\partial\theta}\frac{\partial^2 u}{\partial\theta^2} + 2u\frac{\partial u}{\partial\theta} - \frac{2Mm^2G}{L^2}\frac{\partial u}{\partial\theta} = 0 \tag{10.8}$$

we obtain the final form, which, by some miracle, turns out to be linear.

$$\frac{\partial^2 u}{\partial \theta^2} + u = \frac{Mm^2G}{L^2} \tag{10.9}$$

The solution is

$$u = \frac{Mm^2G}{L^2}\Big(1 + \epsilon\cos(\theta)\Big) \quad \Rightarrow \quad r = \frac{r_0}{1+\epsilon\cos(\theta)} \quad \text{where} \quad r_0 = \frac{L^2}{Mm^2G} \tag{10.10}$$

which is the standard polar form of an ellipse relative to its focus. The distance r_0 is called the **semi-lattice rectum** of the ellipse. We have thus demonstrated Kepler's first law:

Each planet moves in an ellipse with the sun at one focus.

Direct substitution into Eq. 10.7 gives the value for the eccentricity ϵ

$$\epsilon = \sqrt{1 + \frac{2EL^2}{m^3M^2G^2}} \tag{10.11}$$

The geometry of the orbit is completely determined by r_0, which gives the *size* scale and ϵ, which gives the *shape* of the orbit.

From Eq. 10.1 we can integrate the angular momentum L around the orbit, requiring time equal to the period T:

$$\int_0^T L\,dt = \int_0^{2\pi} mr^2\frac{\partial\theta}{\partial t}\,dt = m\int_0^{2\pi}\left(\frac{r_0}{1+\epsilon\cos(\theta)}\right)^2 d\theta = \frac{2\pi r_0^2\, m}{\left(1-\epsilon^2\right)^{3/2}} = LT \tag{10.12}$$

$$T = \frac{m}{L}\frac{2\pi r_0^2}{\left(1-\epsilon^2\right)^{3/2}} = \frac{2\pi}{\sqrt{MG}}\left(\frac{r_0}{1-\epsilon^2}\right)^{3/2} = 2\pi\sqrt{\frac{a^3}{MG}} \tag{10.13}$$

where the final form follows from Eq. 10.10 and the fact that the **semi-major axis** $a = r_0/(1-\epsilon^2)$.
We have thus demonstrated Kepler's third law:

The square of the orbital period of a planet is proportional to the cube of the semi-major axis of its orbit.

We notice that we have not needed Newton's law of force to solve this problem. The only assumptions were the mutual conservation of energy and angular momentum.

10.3 Matter-Wave Treatment

We now view the orbit as a path of stationary phase around the massive body. Any element of the path is stationary only if the propagation vector $\vec{k}$ is in the direction $\vec{ds}$ of the path. The differential element in the r direction is dr, and the differential element in the θ direction is $r\,d\theta$

$$\frac{\partial r}{r\partial\theta} = \frac{k_r}{k_\theta} \qquad \Rightarrow \qquad \frac{\partial r}{\partial\theta} = \frac{rk_r}{k_\theta} \tag{10.14}$$

It is a deep principle of nature that, in a system of this kind, the phase shift $d\phi$ allocated to each increment $d\theta$ of the angle θ does not depend on θ.
This principle is called the **conservation of angular momentum**.

$$L \equiv \frac{\partial\phi}{\partial\theta} = rk_\theta = \text{constant} \tag{10.15}$$

Eq.10.14 can thus be expressed

$$k_r = \frac{L}{r^2}\frac{\partial r}{\partial\theta} \tag{10.16}$$

We recall from our treatment of the deflection of light that the dependence of the speed of light c on the gravitational potential was responsible for only half of the deflection of light by a massive body. The additional deflection, equal in magnitude and of the same sign, was contributed by vector coupling to the massive body. The fact that the two contributions were equal was a unique property of the dispersion relation of light: $\omega = kc$. The dispersion relation of a matter wave $\omega^2 = \omega_0^2 + k^2c^2$ contains the rest energy in addition to the kinetic energy. When we include the vector interaction, we find that the orbital equation is affected at the very next order beyond Newtonian. What emerges is a much clearer view of gravitation than that accessible through the quasi-Newtonian view. We are considering the case where the central body of Compton wavenumber K_0 is much more massive than the orbiting body $K_0 \gg k_0$, and hence its velocity can be neglected. From Eq. 3.10, in the weak-gravity approximation, the gravitational potential c at radius r from the central body is:

$$\frac{c}{c_0} = 1 - \chi\frac{K_0}{r} \tag{10.17}$$

The corresponding approximation for the momentum of our orbiting object then becomes

$$\vec{k} \approx k_0 \frac{\vec{v}}{c_0}\frac{c_0}{c} \tag{10.18}$$

The c_0/c term captures the "back reaction" of the vector coupling on the momentum of the orbiting object, as we saw in Eq. 3.14. In the present context, we can interpret the vector interaction as follows:
For any given radius and energy, the wave vector is larger than we would expect without the vector interaction by a factor of c_0/c. That factor first appears in the relationship between $\partial r/\partial\theta$ and wave vector in Eq. 10.16. We must therefore supplement that expression to take the vector interaction into account:

$$k_r = \frac{L}{r^2}\frac{\partial r}{\partial\theta}\left(\frac{c_0}{c}\right) \qquad \Rightarrow \qquad k_r^2 = \frac{L^2}{r^4}\left(\frac{c_0}{c}\right)^2\left(\frac{\partial r}{\partial\theta}\right)^2 \tag{10.19}$$

Of course k_θ is affected by the same factor, but that dependence is absorbed into the angular momentum L, which is a constant of the motion.

The dispersion relation for an element of matter is

$$\omega^2 = \left(k_0^2 + k^2\right)c^2 = \left(k_0^2 + k_r^2 + k_\theta^2\right)c^2 = \left(k_0^2 + k_r^2 + \frac{L^2}{r^2}\right)c^2 \tag{10.20}$$

which, using Eq. 10.19, becomes

$$\frac{\omega^2}{c^2} - k_0^2 - \frac{L^2}{r^2} = k_r^2 = \left(\frac{\partial r}{\partial\theta}\right)^2\left(\frac{c_0}{c}\right)^2\frac{L^2}{r^4} \tag{10.21}$$

which simplifies to

$$\left(\frac{\partial r}{\partial\theta}\right)^2 = \left(\frac{\omega^2}{L^2c_0^2} - \frac{k_0^2c^2}{L^2c_0^2}\right)r^4 - \frac{c^2}{c_0^2}r^2 \tag{10.22}$$

Eq. 10.22 describes the orbit of a matter wave propagating around a stationary (non-spinning) mass concentration.

10.4 Weak-Field Limit

The gravitational potential appears as the speed of light c in Eq. 10.22. For a body that is not too massive, we can approximate

$$c \approx c_0\left(1 - \frac{GM}{rc_0^2}\right) \qquad \Rightarrow \qquad c^2 \approx c_0^2\left(1 - \frac{2GM}{rc_0^2}\right) \tag{10.23}$$

Using this approximation, Eq.10.22 becomes

$$\left(\frac{\partial r}{\partial\theta}\right)^2 \approx \left(\frac{\omega^2 - k_0^2c_0^2}{L^2c_0^2}\right)r^4 + \frac{2GMk_0^2}{L^2c_0^2}\,r^3 - r^2 + \frac{2GM}{c_0^2}\,r \tag{10.24}$$

When we substitute $k_0 = mc_0$ and $E = \omega$ we obtain

$$\left(\frac{\partial r}{\partial \theta}\right)^2 \approx \frac{E^2 - m^2c_0^4}{L^2c_0^2}\, r^4 + \frac{2GMm^2}{L^2}\, r^3 - r^2 + \frac{2GM}{c_0^2}\, r \tag{10.25}$$

Which is to be compared with the GR result:[20]

$$\left(\frac{\partial r}{\partial \theta}\right)^2 \approx \frac{E^2 - m^2c^4}{L^2c^2}\, r^4 + \frac{2GMm^2}{L^2}\, r^3 - r^2 + \frac{2GM}{c^2}\, r \tag{10.26}$$

The two results are in agreement to this order. To compare with the classical treatment, we assume the energy is only slightly different from the rest energy

$$E = mc_0^2 + \epsilon \qquad \Rightarrow \qquad E^2 \approx m^2c_0^4 + 2mc_0^2\epsilon \tag{10.27}$$

to this order Eq. 10.25 becomes

$$\left(\frac{\partial r}{\partial \theta}\right)^2 \approx \frac{2m\epsilon}{L^2}\, r^4 + \frac{2GMm^2}{L^2}\, r^3 - r^2 + \frac{2GM}{c_0^2}\, r \tag{10.28}$$

When ϵ is identified as the classical energy E, Eq. 10.28 is identically Eq. 10.4, with the addition of the last term. Tracing back through the derivation, we see that the last term was obtained only by including the vector interaction.

10.5 Apsidal Precession

To assess the effect of the last term on the orbit, we substitute the variable $u = 1/r$, for which we first work out the derivative:

$$\frac{\partial r}{\partial \theta} = \frac{\partial r}{\partial u}\frac{\partial u}{\partial \theta} = -\frac{1}{u^2}\frac{\partial u}{\partial \theta} = -r^2\frac{\partial u}{\partial \theta} \tag{10.29}$$

upon which Eq. 10.24 becomes

$$\begin{aligned} \frac{1}{r^4}\left(\frac{\partial r}{\partial \theta}\right)^2 &\approx \left(\frac{\omega^2 - k_0^2c_0^2}{L^2c_0^2}\right) + \frac{2GMk_0^2}{L^2c_0^2}\,\frac{1}{r} - \frac{1}{r^2} + \frac{2GM}{c_0^2}\,\frac{1}{r^3} \\ \left(\frac{\partial u}{\partial \theta}\right)^2 &\approx \left(\frac{\omega^2 - k_0^2c_0^2}{L^2c_0^2}\right) + \frac{2GMk_0^2}{L^2c_0^2}\, u - u^2 + \frac{2GM}{c_0^2}\, u^3 \end{aligned} \tag{10.30}$$

Differentiating with respect to θ

$$2\left(\frac{\partial u}{\partial \theta}\right)\left(\frac{\partial^2 u}{\partial \theta^2}\right) \approx \frac{2GMk_0^2}{L^2c_0^2}\frac{\partial u}{\partial \theta} - 2u\frac{\partial u}{\partial \theta} + \frac{6GM}{c_0^2}u^2\frac{\partial u}{\partial \theta} \tag{10.31}$$

Dividing by $2\ \partial u/\partial\theta$ we obtain

$$\frac{\partial^2 u}{\partial \theta^2} \approx \frac{GMk_0^2}{L^2c_0^2} - u + \frac{3GM}{c_0^2}u^2 \tag{10.32}$$

which, in the limit where $GMu/c_0^2 \ll 1$, reduces to the classical Kepler standard form.

Following Bergman[3] pp. 215-216 we use a trial solution with parameter ρ, of the form

$$u = u_0 + u_0\epsilon\cos(\rho\theta) \tag{10.33}$$

Substituting into Eq. 10.32, expanding the result into a Fourier cosine series in $\rho\theta$, ignoring terms of order higher than 1 in GM/c_0^2, and setting the coefficient of the residual $\cos(\rho\theta)$ to zero we find

$$\begin{aligned} &1 - \rho^2 \approx 6u_0\delta \quad \Rightarrow \quad \rho \approx \sqrt{1 - 6u_0\delta} \approx 1 - 3u_0\delta \\ &\rho \approx 1 - 3u_0\delta \approx 1 - 3\frac{MGm^2}{L^2}\frac{MG}{c_0^2} = 1 - 3\frac{M^2G^2m^2}{L^2c_0^2} \end{aligned} \tag{10.34}$$

which is Bergman's Eq. 14.24.

To the level of approximation required we can use the Newtonian Kepler relations for the period T from Eq. 10.13:

$$T = 2\pi\sqrt{\frac{a^3}{(m_1+m_2)G}} \quad \Rightarrow \quad T^2 = 4\pi^2\frac{a^3}{2MG} \quad \Rightarrow \quad MG = 2\pi^2\frac{a^3}{T^2} \tag{10.35}$$

where the semi-major axis a is given by

$$\begin{aligned} a &= \frac{2r_0}{(1-\epsilon^2)} = \frac{2}{u_0\,(1-\epsilon^2)} \\ \mu_0\delta &= \frac{2}{a\,(1-\epsilon^2)}\cdot\frac{MG}{c_0^2} = \frac{2}{a\,(1-\epsilon^2)}\cdot\frac{2\pi^2a^3}{c_0^2T^2} = \frac{4\pi^2a^2}{T^2c_0^2\,(1-\epsilon^2)} \end{aligned} \tag{10.36}$$

From Eq. 10.34, the angular increment $\Delta\theta$ for a full rotation is $2\pi \times\ 3\mu_0\delta$:

$$\Delta\theta = \frac{24\pi^3a^2}{T^2c_0^2\,(1-\epsilon^2)} \tag{10.37}$$

which is the expression Einstein arrived at in his original paper.

Once again we have demonstrated that the gravitational 4-potential in flat space-time gives results in agreement with observation at the first order beyond Newton. Even to first order, the apsidal precession required both the relativistic dispersion relation and the vector coupling. These results hold only in the context of Mach's Principle, whereby the entire rest energy of a massive body is the result of its gravitational interaction with the rest of the universe.

10.6 Future Work

The relativistic and vector-coupling terms that give rise to the apsidal precession have only been included here to first order. For ultra-massive objects with small orbits, such as those involved in black hole mergers, a full relativistic treatment must be used. A great deal of work has been done with the corresponding GR analysis, but virtually none with G4v.

The relativistic and vector-coupling terms that give rise to the apsidal precession also affect the orbit at the same order. These effects will modify the gravitational radiation to this order as well. The required modifications remain to be worked out for G4v, and compared with the GR working expressions for gravitational radiation used by astronomers.

As noted in Section 7.7, Virtually all bodies in the real universe are rotating, often at relativistic speeds. The vector contribution to orbital precession due to the rotation of such bodies in binary systems goes under the rubric of **spin-orbit coupling,** and has been analyzed in detail in a GR context. Modern high-precision observations of the double pulsar J0737-3039A/B agree with the GR predictions to first order beyond Newton [6]. In Chapter 11 We analyze the spin-orbit coupling of a more local system and show that, to first order, G4v predicts the same result as GR. It remains to be analyzed whether the two theories agree to higher order. Any difference might be experimentally discernible as the pulsar observations are continued.

Chapter 11

Gravity Probe B

11.1 Introduction

The Gravity Probe B (GPB) experiment[27] launched in 2004, is, from the viewpoint of G4v, the first direct measurement of vector coupling in its pure form, free from scalar effects, and not obscured by other interactions. It is important, in part because its magnitude, relative to the scalar magnitude, gives the propagation speed of a gravitational wave. Both GR and G4v predict gravitational waves traveling at c, but before GPB we had no independent experimental corroboration of that expectation. Of course, our direct knowledge of the speed of gravitational waves became good to 10^{-15} with the LIGO sighting of 2017[38][37].

The GPB spacecraft is orbiting the earth, following the trajectory of a carefully shielded "proof mass" which we will identify with m_1. The proof mass sphere is in free-fall, and therefore experiences no acceleration whatsoever. From the point of view of the proof mass, there is a massive universe at large distance, and a local mass called the Earth which is revolving around it with angular velocity $\Omega = 1$ revolution every 1hr 37min 34sec, and the Earth rotating on its own axis every 24 hours. as illustrated in Fig. 11.1.

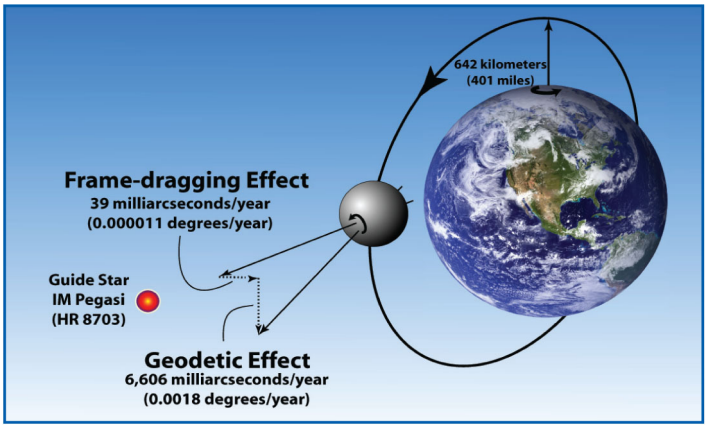

Figure 11.1: Configuration of the gyroscope sphere in orbit aboard the GPB satellite. This Earth-centered view somewhat obscures the basic physics of the experiment: Because the sphere is in free-fall, it can be taken as the origin of the coordinate system, and the Earth visualized as being in orbit around it. When looked at this way, the sphere is stationary in its coordinate system, which consists of the mass of the universe, the mass of the Earth orbiting around it, contributing the "Geodetic Effect", and the Earth rotating on its own axis, contributing the "Frame-dragging Effect." From the GPB web site[27].

11.2 Frame of Reference

The rotation rate of the proof mass' frame of reference with respect to the universe due to the Earth's vector potential will be the rotation rate of the earth around the proof mass multiplied by the fraction of the frame of reference contributed by the earth's mass.

$$\left.\frac{\partial\Phi}{\partial t}\right|_{\rm A} = \Omega \cdot \frac{\text{Earth contribution}}{\text{Universe contribution}} = \Omega\frac{Gm_{\rm earth}}{r_{\rm orbit}c^2} \tag{11.1}$$

where the Earth contribution is from Eq. 3.14. By the Virial theorem, an orbiting object of mass m_1 has kinetic energy equal to half of its (negative) potential energy:

$$m_1\ G(m_{\rm earth}/r_{\rm orbit}) \ = \ m_1\ v^2_{\rm orbit} \tag{11.2}$$

Substituting Eq. 11.2 into Eq. 11.1 we obtain

$$\frac{\text{Earth contribution}}{\text{Universe contribution}} \ = \ \frac{v^2_{\rm orbit}}{c^2} \tag{11.3}$$

Therefore the Earth's vector coupling induces a rotation in the proof mass' frame of reference of

$$\left.\frac{\partial \Phi}{\partial t}\right|_{\mathrm{A}} = \frac{v^2}{c^2}\,\Omega \tag{11.4}$$

The rotation given by Eq. 11.4 does not depend in any way on the nature of the proof mass. In particular, the effect will be the same whether the proof mass is stationary or spinning. It is the contribution to the geodetic effect explained in GR in terms of the curvature of space[70].

11.3 Gyroscope precession

There is, in addition to Eq. 11.4, an effect due to the vector coupling of the orbit of the earth with the spin of the gyroscope. The relationships involved are illustrated in Fig. 11.2.

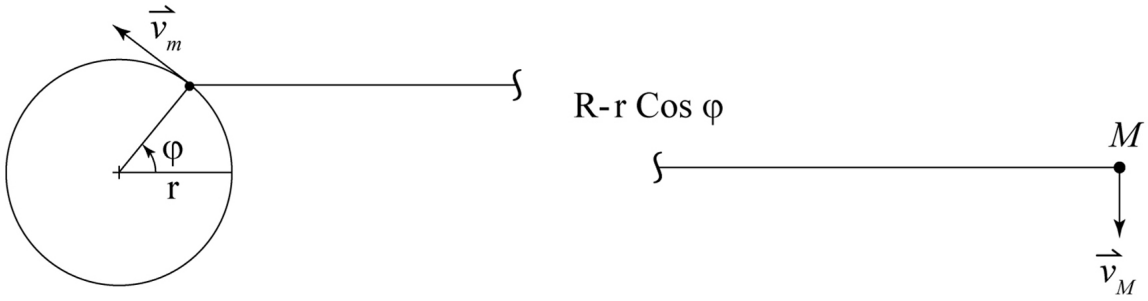

Figure 11.2: Vector coupling of Earth with mass M to gyroscope, which we represent as a ring of matter of mass m and radius r, rotating with angular velocity ω and therefore velocity $v_m = \omega r$.

The Earth has mass M at radius R from the satellite, moving with velocity v_M. Anticipating that the detailed structure of the gyroscope will not affect the result, we represent it as a ring of matter of mass m and radius r, rotating with angular velocity ω.

From Eq. 3.14 we can write the **kinetic energy** $K.E.$ of the arrangement:

$$K.E. \approx \frac{p^2}{2m} = \frac{m}{2}v_m^2 + \frac{m}{2}\left(\frac{MG}{rc^2}\right)^2 v_M^2 - \frac{mMG}{rc^2}\;(\vec{v}_m \cdot \vec{v}_M) \tag{11.5}$$

The last term is the gravitational equivalent of the magnetic coupling energy $\vec{A} \cdot \vec{J}$. We use Eq. 11.5 to compute the coupling energy. The v_m^2 and v_M^2 terms do not depend on the angle between Earth's orbit and the spin axis of the gyroscope. The last term gives the vector part of the coupling energy of the Earth to an element of the gyroscope of length dl at angle ϕ around the ring. The gyroscope has mass per unit length $m/2\pi r$ moving at velocity ωr. When the gyroscope ring and Earth's orbit are concentric and lie in the same plane, the vector coupling energy E_{mM} is

$$
\begin{aligned}
E_{mM} &\approx -\frac{mMG}{2\pi rc^2}\int_0^{2\pi}\frac{1}{R-r\cos\phi}\ (\vec{v}_m\cdot\vec{v}_M)\ rd\phi \\
&= \frac{mMG}{2\pi c^2}\int_0^{2\pi}\frac{v_M\ \omega r\cos\phi}{R-r\cos\phi}\ d\phi = \frac{m\omega Mv_MG}{2\pi c^2}\int_0^{2\pi}\frac{r\cos\phi}{R-r\cos\phi}\ d\phi \\
&= \frac{m\omega Mv_MG}{2\pi c^2}\int_0^{2\pi}\frac{\frac{r}{R}\cos\phi}{1-\frac{r}{R}\cos\phi}\ d\phi \\
&\approx \frac{m\omega Mv_MG}{2\pi c^2}\int_0^{2\pi}\frac{r}{R}\cos\phi\left(1+\frac{r}{R}\cos\phi\right)d\phi \\
&= \frac{m\omega Mv_MG}{2\pi c^2}\int_0^{2\pi}\frac{r^2}{R^2}\cos^2\phi\ d\phi = \frac{m\omega r^2Mv_MG}{2\pi R^2c^2}\ \pi = \frac{m\omega r^2Mv_MG}{2R^2c^2}
\end{aligned}
\tag{11.6}
$$

When the gyroscope ring and Earth's orbit are concentric but not in the same plane, this expression must be multiplied by $\cos\theta$, where θ is the angle between Earth's orbit and the gyroscope ring. In Fig. 11.1, $\theta = \pi/2$, while in Fig. 11.2, $\theta = 0$.

$$
E_{mM} = \frac{MG}{Rc^2}\ \frac{mv_M\omega r}{2}\ \frac{r}{R}\ \cos\theta\ =\ \frac{MG}{2Rc^2}\ L\ \frac{v_M}{R}\ \cos\theta \tag{11.7}
$$

where the gyroscope angular momentum $L = m\omega r^2$.
The first form makes the dimensional correctness more explicit.

The torque τ on the gyroscope is

$$
\tau = -\frac{\partial E_{mM}}{\partial\theta}\ =\ \frac{MG}{2Rc^2}\ L\ \frac{v_M}{R}\ \sin\theta \tag{11.8}
$$

For the GPB configuration (Fig. 11.1) the spin axis of the gyroscope is orthonogal to the orbit, so $\sin\theta = 1$. Two superconducting loops carrying persistent current are at lowest energy when the currents are aligned (See Sect. 1.7 [44]) Gravitational vector interaction is of the opposite sign, so is of lowest energy when the the angular momenta are anti-aligned. The torque thus produces a precession of the spin axis in the direction of orbital rotation:

$$
\tau\ =\ \frac{\partial L}{\partial t}\ =\ L\ \frac{\partial\Phi}{\partial t}\ =\ \frac{MG}{2Rc^2}\ L\ \frac{v_M}{R} \tag{11.9}
$$

As we anticipated, all the parameters of the gyroscope cancel out. Remembering that $v_M = MG/R$ from Eq. 11.2, and taking $v = -v_M = -\Omega R$, the precession is

$$
\left.\frac{\partial\Phi}{\partial t}\right|_{\text{gyro}}\ =\ \frac{MG}{2Rc^2}\ \frac{v_M}{R}\ =\frac{v^2}{2c^2}\ \Omega \tag{11.10}
$$

This rate is just half that due to Mach's principle (Eq. 11.4), and of the same sign. The total rotation is the sum of the two separate effects:

$$
\left.\frac{\partial\Phi}{\partial t}\right|_{\text{total}} = \left.\frac{\partial\Phi}{\partial t}\right|_{\text{A}} + \left.\frac{\partial\Phi}{\partial t}\right|_{\text{gyro}}\ =\ \frac{3}{2}\ \frac{v^2}{c^2}\ \Omega \tag{11.11}
$$

This extremely simple result can be misleading. The additional rotation given by Eq. 11.10 is entirely due to the fact that the proof mass is spinning at a rate that is very large compared with the orbital rotation rate, and would be zero for a non-spinning proof mass. The result obtained from our four-vector theory of gravitation, with parameters forced upon us by Mach's principle, gives a value for the result of the GPB experiment that is identical to that predicted by GR. Here, then, is Einstein's "analog of electrodynamic induction" in its purest form: All traces of any scalar effect have been removed because the proof mass is in free-fall.

GR-based discussions of the GPB experiment make a distinction between the geodetic effect and the additional precession due to Earth's rotation on its axis, which is called **frame dragging**. In G4v, both effects are analyzed in the free-fall frame of the test mass, and both are due to the vector "dragging" of the local frame of reference due to Earth's motion. The geodetic effect is easier to evaluate because the satellite orbital period and the Virial theorem give its magnitude without further knowledge of the mass distribution in the Earth. However the E-W "Lense-Thirring" effect does require this detailed knowledge, and hence is not included in our analysis.

11.4 Future Work

In the preceding analysis of the gyroscope precession, we have resorted to a force-law approach.
A much simpler approach should be possible using direct momentum coupling.

A detailed G4v analysis of the E-W frame-dragging using a good Earth model should be performed to see if the vector coupling is sufficient, or if tensor terms are required.

The spin-orbit coupling calculation for the gyroscope precession should be applied to the double pulsar J0737-3039A/B [6]. `http://www.sciencemag.org/content/321/5885/104.full.html`

Since the influence of gravitational waves on the LIGO mirror spacing is second-order in the vector coupling, it is of the same order in v/c as the diagonal tensor coupling, and 1/4 the value. It is not obvious how the GPB spin-orbit coupling comes out the same while the GW coupling differs. This question should be investigated.

Chapter 12

Static Spherical Distribution

12.1 Introduction

We first consider a sphere of matter of constant density n elements of matter per unit volume, each element having intrinsic Compton wave vector k_1. The energy of each element will be $k_1 c(r)$, where r is the radial distance to the element from the center of the massive object, and $c(r)$ is the gravitational potential at r. Thus the energy density $\rho_E(r) = n\, k_1 c(r)$. We might think of this idealization as being some approximation to the potential within and outside a Neutron Star or Black Hole of matter radius R. Inside the matter, the potential satisfies the Abraham Equation (Eq. 9.1) for the scalar potential $c(r)$ in the special case where the time derivative is zero:

$$\nabla^2 c(r) = 4\pi\chi\, \rho_E(r) = 4\pi\chi\, n\, k_1 c(r) \tag{12.1}$$

It is convenient to define a dimensionless scalar potential $Z = c/c_0$, whereby Eq. 12.1 becomes:

$$\nabla^2 Z(r) = 4\pi\chi\, n\, k_1 Z(r) = \rho Z(r) \tag{12.2}$$

Using the **wave number density** ρ is given by

$$\rho = 4\pi\chi n k_1 \tag{12.3}$$

Eq. 12.2 can be written:

$$\frac{2}{r}\left(\frac{\partial Z}{\partial r}\right) + \left(\frac{\partial^2 Z}{\partial r^2}\right) = \rho\, Z \tag{12.4}$$

Which has solution

$$Z(r < R) = \frac{Z_c\ \sinh(R_n)}{R_n} \tag{12.5}$$

where Z_c is the dimensionless potential at the center of the object and $R_n = R\sqrt{\rho}$.
We emphasize that ρ has the units of length^{-2}.

Outside the object, $\rho = 0$ and the potential decays as the inverse of r:

$$Z(r > R) = 1 - \frac{A}{r} \tag{12.6}$$

where A is some constant to be determined.

The constant unity is fixed by the requirement that the potential $c \to c_0$ ($Z \to 1$) as $r \to \infty$.

Equating Z and $\partial Z/\partial r$ of the two solutions, Eq. 12.5 and Eq. 12.6, at $r = R$, we obtain the value of the minimum potential Z_c at the center of our massive object and the constant A:

$$Z_c = \mathrm{sech}\Big(R_n\Big) \qquad A = R - \frac{\tanh(R_n)}{\sqrt{\rho}} \tag{12.7}$$

The dimensionless potential inside and outside the object is thus:

$$\begin{aligned} Z(r < R) &= \frac{\mathrm{sech}\Big(R_n\Big)\ \sinh(R_n)}{R_n} \\ Z(r > R) &= 1 - \frac{R_n - \tanh R_n}{R_n} \\ Z(R) &= \frac{\tanh R_n}{R_n} \end{aligned} \tag{12.8}$$

The dimensionless gravitational potential Z given by Eq. 12.8 is shown as a function of the dimensionless radius $r_n = R_n$ in Fig. 12.1 for several values of the dimensionless matter radius $R_n = R_n$.

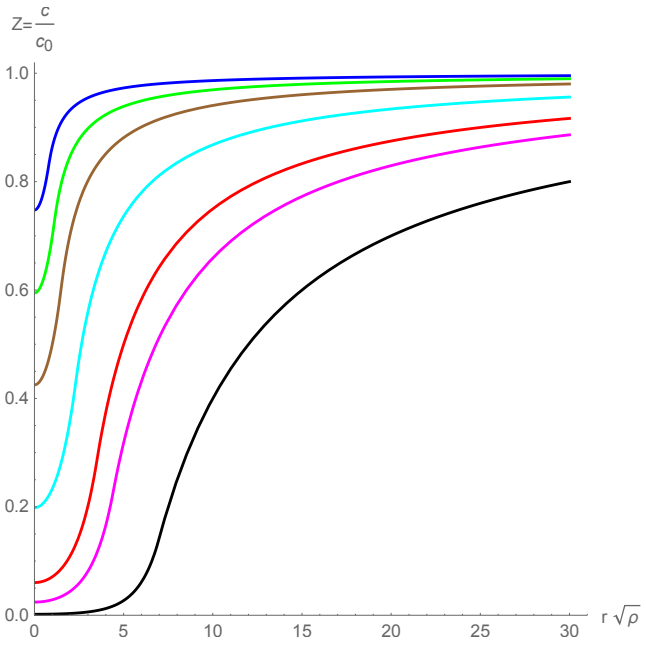

Figure 12.1: Dimensionless gravitational potential as a function of dimensionless radius for spherical objects of dimensionless matter radius $R_n = 0.8, 1.11, 1.5, 2.3, 3.5, 3.5\times1.9^{1/3}, 7$.
All curves are for the same value of uniform matter density ρ.
The self-limiting nature of the source term is apparent, especially for very large objects.
The maximum gravitational field occurs at the boundary of the matter sphere ($r = R$).
The super-massive object derived from this theory of gravitation has no singularity.
The blue curve represents a typical neutron star. The red curve is for a black hole of the general size of those involved in the GW150914 merger. The magenta curve below it represents the final merged object, of 1.9 times the original individual masses.

The dimensionless potential Z_{surf} at the matter surface given by Eq. 12.8, and the maximum dimensionless gravitational field given by Eq. 12.9, are plotted in Fig. 12.2.

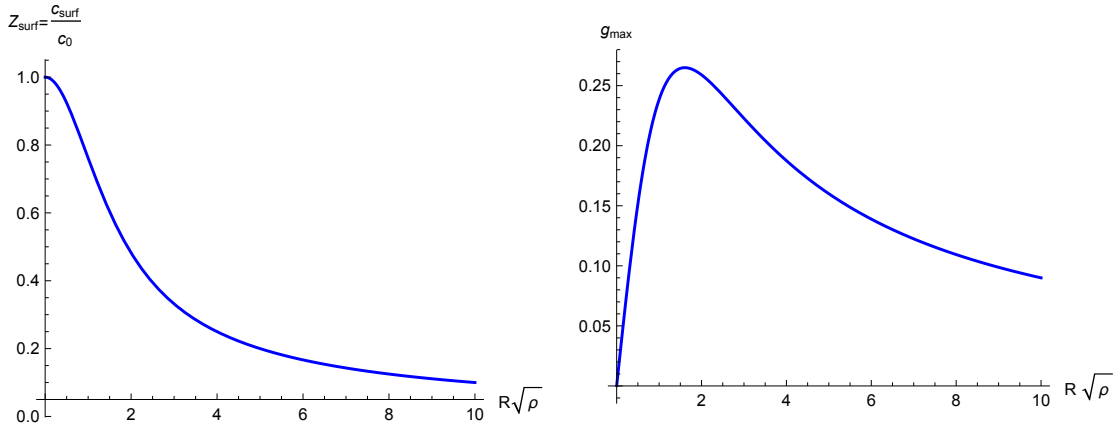

Figure 12.2: (Left): Dimensionless gravitational potential at the surface of a massive object, (Right): Dimensionless maximum gravitational field, both *vs* dimensionless matter radius.

As the total accumulated matter increases, the gravitational potential within the sphere becomes lower, thereby reducing the effectiveness of the central matter as a gravitational source. Even unlimited accumulations of matter are not able to drive the potential Z, and therefore the speed of light c, negative.

The reduction in source value at the center of large matter accumulations also occurs in GR, but not quickly enough to save it from forming a singularity.
The predictions of the two theories are thus strikingly different:

The super-massive object of G4v has no singularity

Nonetheless, extremely strong gravitational fields can develop at the boundaries of high density objects.
The maximum gravitational field, which occurs at $r = R$, is

$$g_{\max} = \left.\frac{\partial Z}{\partial\left(R_n\right)}\right|_R = \frac{R_n - \tanh\left(R_n\right)}{\left(R_n\right)^2} \tag{12.9}$$

12.2 Scaling of the Results

To proceed farther we need a realistic value for the density ρ, for which real units are required:

Speed of light $c = 299{,}792{,}458$ m/s.
Gravitational Constant $G = 6.674 \times 10^{-11}\ \frac{\mathrm{m}^3}{\mathrm{kg\ sec}^2}$
Mass of Sun $M_\odot = 1.9 \times 10^{30}$ kg
Planck constant $\hbar = 6.5821191 \times 10^{-16}$ eV s=1.0545717 $\times 10^{-34}$ J s.
Planck Length $\ell_P = \sqrt{\hbar G/c_0^3} \approx 1.6162 \times 10^{-35}$m
Coupling Constant $\chi = \ell_P^2 = 2.61 \times 10^{-70}\mathrm{m}^2$
Neutron mass = $1.6749273 \times 10^{-27}$ kg.
Neutron rest energy $\hbar\omega_0 = 939.56536$ MeV.
Neutron intrinsic wave vector $k_1 = \omega_N/c_0 = 4.76 \times 10^{15}\,\mathrm{m}^{-1}$.
Neutron Star average density n is thought to be between 0.3 and 1.2 neutrons/fm^3 [52].
This density corresponds to $\rho = 4\pi\chi n k_1$ between 4.7×10^{-9} and 1.9×10^{-8} m^{-2}, corresponding to a length scale of 14.5 to 7.2 km, respectively. The same study[52] reviews extensive observational evidence and concludes that neutron stars have radii between 6 and 14 km, with an average of ≈ 10 km.

In the spirit of our engineering approximation, we will assume a fixed density of $\rho = 10^{-8}$, corresponding to a length scale of $1/\sqrt{\rho} = 10$ km, thereby adopting a very "stiff equation of state" for our coherent neutron-star matter at the core of our super-massive objects.

The gravitational potential at the surface of a few neutron stars has been estimated to be $\approx 0.75\,c_0$.
The surface gravitational potential of our objects is plotted in Fig. 12.2, from which we see that an object having $Z_{\mathrm{surf}} \approx 0.75$ has $R_n \approx 1 \rightarrow R \approx 10$km, consistent with our order-of-magnitude analysis.

There is a great deal of ongoing discussion of the density and compressibility of the matter that comprises neutron stars. This discussion has all been in the context of GR, which predicts a singularity for matter accumulations above a certain threshold. However, we can see from Fig. 12.2 that, in G4v, the maximum gravitational field never gets more than $\approx 11\%$ larger than it is at the surface of a neutron star, and actually decreases for objects of $R_n > 2$.

So the horrible "gravitational collapse," so vividly portrayed by GR, does not come to pass in G4v.

In addition, we can have confidence that what we learn from neutron stars is a reliable guide to the physics of the matter cores inside objects much more massive than neutron stars—in particular those that are presently called "Black Holes." More about those in the upcoming sections.

12.3 Weak Gravity Limit

At small values of the argument R_n, we may expand $\tanh x \approx x - x^3/3$ in Eq. 12.8:

$$Z(r > R) \approx 1 - \frac{R_n - R_n + \frac{1}{3}R^3\rho^{3/2}}{R_n} = 1 - \frac{R^3\rho}{3r} = 1 - \frac{R_n^3}{3r_n} \tag{12.10}$$

where $r_n = r\sqrt{\rho}$. Using $\rho = 4\pi\chi\, n\, k_1$ from Eq. 12.3

$$Z(r > R) \approx 1 - \frac{R^3 4\pi\chi\, n\, k_1}{3r} = 1 - \frac{\chi\, k_0\sqrt{\rho}}{r_n} \tag{12.11}$$

where, in the weak-gravity limit, the total quantity of matter in the star k_0 is just the volume of the star times nk_1, given by

$$k_0 = \frac{4}{3}\pi R^3 n\, k_1 \tag{12.12}$$

Because $\chi = \frac{\hbar G}{c_0^3}$ from $Z = c/c_0$ and $\hbar k_0 = Mc \approx Mc_0$, Eq. 12.11 can be compared with the standard Newtonian expression for gravitational potential:

$$c(r > R) \approx c_0 \left(1 - \frac{\chi\, M c_0}{\hbar\, r}\right) = c_0 \left(1 - \frac{MG}{r c_0^2}\right) \tag{12.13}$$

Again our weak-gravity limit reduces to the well-known relations of classical Newtonian mechanics.

12.4 Total Energy

Even when the matter accumulation is far greater than the weak-gravity limit, the potential outside the matter still has a well-defined $1/r$ dependence. Hence every massive object has a total energy $\omega_{\rm tot}$ that defines how it interacts gravitationally with other objects at a distance. Eq. 12.8 gives the potential at the boundary $r = R$, from which we can obtain the total energy $\omega_{\rm tot}$ of the body by Eq. 3.6:

$$\begin{aligned} Z(R) &= \frac{c(R)}{c_0} = \frac{\tanh(R_n)}{R_n} \\ c(R) &= c_0 - \frac{\chi\, \omega_{\rm tot}}{R} \\ \omega_{\rm tot} &= c_0 \frac{R_n - \tanh(R_n)}{\chi\sqrt{\rho}} \end{aligned} \tag{12.14}$$

We can check this result by direct integration of the energy in spherical shells from $r = 0$ to $r = R$. Recalling from Eq. 12.3 that $\rho = 4\pi\chi\, n\, k_1$,

$$\omega_{\rm tot} = \int_0^R 4\pi r^2 n k_1 c(r)\; dr = \int_0^R 4\pi r^2 \frac{\rho}{4\pi\chi} c_0 Z(r)\; dr \tag{12.15}$$

Using $c(r) = c_0 Z(r < R)$ from Eq. 12.8, this integral gives the same result as Eq. 12.14.

In strong gravity, the effective Compton wave-number k_0 is not the total of that of all neutrons in the star for the same reason that the total energy is not the sum of that of its isolated components. The matter that is active as a source of gravitational interaction forms a "shell" of thickness $1/\sqrt{\rho}$ on the surface of extremely massive bodies. It is still true that $k_0 c_0 Z(R) = \omega_{\rm tot}$, thus from Eq. 12.14 we obtain the dimensionless form of the Compton wave-number for the entire body:

$$\begin{aligned} k_0\, c_0 \left(\frac{\tanh(R_n)}{R_n}\right) &= \omega_{\rm tot} = c_0 \frac{R_n - \tanh(R_n)}{\chi\sqrt{\rho}} \\ k_0 &= \frac{R\,(R_n \coth(R_n) - 1)}{\chi} = \frac{R_n\,(R_n \coth(R_n) - 1)}{\chi\sqrt{\rho}} \end{aligned} \tag{12.16}$$

A convenient dimensionless form of the Compton wave-number follows from Eq. 12.16:

$$\begin{aligned} k_0 \chi\sqrt{\rho} &= R_n^2 \coth(R_n) - R_n \\ &\to \frac{R_n^3}{3} \quad \text{as} \quad R_n \to 0 \quad \text{Weak Gravity} \\ &\to R_n^2 - R_n \quad \text{when} \quad R_n \gtrsim 3 \quad \text{"Black Hole"} \end{aligned} \tag{12.17}$$

Using $\rho = 4\pi\chi\, n\, k_1$ from Eq. 12.2, the last line of this equation reduces to Eq. 12.12 in the limit of weak gravity. In the strong-gravity "Black Hole" limit, $R_n \gg 1$, the coth approaches unity, giving $k_0 \to \frac{1}{\sqrt{\rho}} 4\pi R^2 n k_1$, so the "active" matter is effectively a shell of thickness $1/\sqrt{\rho}$.

12.5 Effective Mass

Eq. 12.14 and Eq. 12.16 give directly the total energy $\omega_0 = \omega_{\rm tot}$ and Compton wave number k_0 of the massive body analyzed earlier in this section:

$$k_0 = \frac{(R_n)^2 \coth(R_n) - R_n}{\chi\sqrt{\rho}} \quad \text{and} \quad \omega_0 = k_0 Z(R) = c_0 \frac{R_n - \tanh(R_n)}{\chi\sqrt{\rho}} \tag{12.18}$$

We see here a graphic example of how the reduced potential at the surface of the mass concentration lowers ω_0, which mediates the scalar interaction, but does not affect k_0, which mediates the vector interaction. The vector interaction can, for this reason, be much larger than the scalar interaction for objects in the "Black Hole" limit. However the "shielding effect," which decreases the coupling of an external vector potential to interior matter, is governed by the vector equivalent of Eq. 12.1, which guarantees that the equivalence principle is satisfied. The physics involved is the gravitational parallel of the electromagnetic **skin effect** discussed in CE [44] 1.10. The simultaneous solution of both scalar and vector equations is required, *e.g.*, for a spinning matter distribution.

Following, Eq. 2.12, we can define a **gravitational effective mass** $M_{\rm eff}$:

$$\omega = \frac{k_0 c}{\sqrt{1 - v^2/c^2}} = \frac{M_{\rm eff} c^2}{\hbar\sqrt{1 - v^2/c^2}} \qquad \text{and} \qquad \vec{k} = \frac{k_0\, \vec{v}/c}{\sqrt{1 - v^2/c^2}} = \frac{M_{\rm eff}\vec{v}}{\hbar\sqrt{1 - v^2/c^2}} \tag{12.19}$$

from which we might conclude that $\hbar k_0 = M_{\rm eff}\, c$. However, the entire reason for defining an effective mass is to compare our results with those of conventional Newtonian and GR treatments, which all use the term "Mass" to represent the invariant quantity of matter. If we wish our $M_{\rm eff}$ to have this meaning, we cannot have it changing with the gravitational potential c. We therefore adopt the following definition:

$$M_{\rm eff} = \frac{\hbar k_0}{c_0} = \frac{\hbar}{c_0\chi\sqrt{\rho}}\left(R_n^2 \coth(R_n) - R_n\right) \tag{12.20}$$

The **energy** E and **momentum** $\vec{p}$ of the body form the energy-momentum four-vector $\mathbf{P} = \hbar\mathbf{k}$:

$$\mathbf{P} = \left\{\frac{E}{c}, \vec{p}\right\} = M_{\rm eff}\mathbf{U} = M_{\rm eff}\frac{\{c, \vec{v}\}}{\sqrt{1 - v^2/c^2}} = \hbar\mathbf{k} = \hbar\left\{\frac{\omega}{c}, \vec{k}\right\}$$
$$E_0 = \hbar\omega_0 = M_{\rm eff} c_0 c \qquad \textbf{rest energy} \tag{12.21}$$

From Eq. 12.20, we see that there is a universal dimensionless form for the effective mass:

$$\frac{M_{\rm eff} c_0 \chi\sqrt{\rho}}{\hbar} = \frac{M_{\rm eff} G\sqrt{\rho}}{c_0^2} = R_n^2 \coth(R_n) - R_n \tag{12.22}$$

This dimensionless effective mass is plotted *vs* the dimensionless matter radius in Fig. 12.3:

Expanding Eq. 12.22 for $R_n \ll 1$, the weak-gravity effective mass becomes

$$\frac{M_{\rm eff} G\sqrt{\rho}}{c_0^2} \approx \frac{(R_n)^3}{3} \propto \text{volume of star for } R_n \ll 1 \tag{12.23}$$

However, for a sufficiently massive body, we can no longer add up the properties of all its constituent elements in this manner to obtain its total energy $\omega_{\rm tot}$ or total Compton wave number k_0. As more matter is accumulated, the effective gravitational source, as seen outside the massive body, becomes ever less than the sum of the individual source values of the elements matter accumulated.
In the "Black Hole" limit, Eq. 12.22 becomes:

$$\frac{M_{\rm eff} G\sqrt{\rho}}{c_0^2} \approx R_n^2 - R_n \qquad \text{for } R_n \gg 1 \tag{12.24}$$

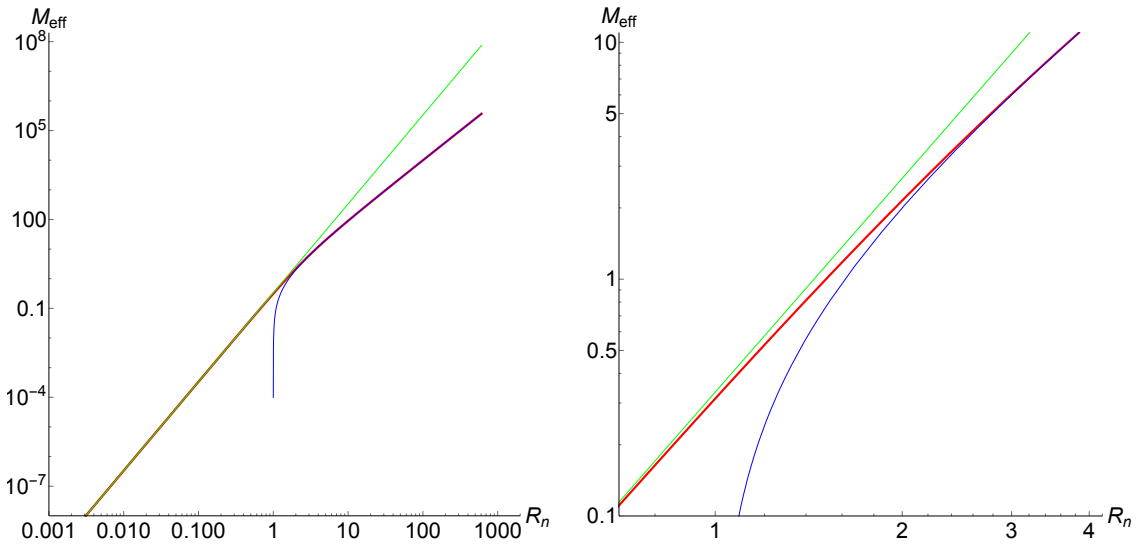

Figure 12.3: Dimensionless gravitational effective mass as a function of dimensionless matter radius for non-spinning spherical ultra-dense bodies of fixed density.
The blue curve is the "black-hole" approximation of Eq. 12.24.
The straight green line is the weak-gravity approximation of Eq. 12.23.

12.5.1 Effective Mass in Real Units

Astronomers use $M_\odot$, the mass of the Sun, as the unit of matter, rather than the neutron-star units we have adopted. We have already seen in Section 12.2 that our natural unit of length $\frac{1}{\sqrt{\rho}} \approx 10$ km.
Since $M_\odot = 1.9 \times 10^{30}$kg, our natural unit of matter $c_0^2/G\sqrt{\rho} \approx 1.35 \times 10^{31}$kg corresponds to $\approx 7M_\odot$.
Substituting these units for our natural units, Eq. 12.22 is, in easy-to-use form:

$$M_{\text{eff}} = \frac{c_0^2}{G\sqrt{\rho}}\Big(R_n^2 \coth(R_n) - R_n\Big) \approx 7M_\odot \times \left(\left(\frac{R}{10\text{km}}\right)^2 \coth\left(\frac{R}{10\text{km}}\right) - \frac{R}{10\text{km}}\right) \tag{12.25}$$

This expression is plotted in Fig. 12.4:

12.5.2 Pulsars

Until 2015, the vast majority of our knowledge of extreme-density massive objects has come from astronomical observation of pulsars. Fortunately an excellent recent review by Özel & Freire [53] nicely summarizes these findings through late 2016. The field is evolving very rapidly, with interesting new discoveries appearing on a weekly basis. Because the pulse period of many pulsars is extremely stable, the timing of arriving pulses (integrated Doppler shift) gives an astoundingly accurate measure of the motion of the pulsar along the line of sight. When, as often happens, the pulsar is part of a binary system, the knowledge of its motion can translate into a detailed description of several parameters of the orbit of the binary. Occasionally one of these systems will appear "edge-on," and the signal from the pulsar will pass very close to its binary companion. In this configuration the Shapiro delay described in Section7.3 pins down additional parameters. When the companion can be seen optically, its motion can be extracted from the Doppler shift of spectroscopic lines. In one case (the only case to date), both objects in the binary were pulsars, and an even more detailed and precise determination of the orbit was possible. When a near-complete determination of the orbit is possible, the individual masses of the two objects can be found. Relatively precise values have been obtained for quite a number of pulsars, and are summarized (with error bars) in Figure 2 of [53].

A fascinating aspect of these findings is that there appears to be a maximum pulsar mass somewhat larger than $2\,M_\odot$. In G4v, this maximum can represent the appearance of a **light-ring**, where light or other signals can propagate in circular orbits around the object (the subject of Section 12.5.3).

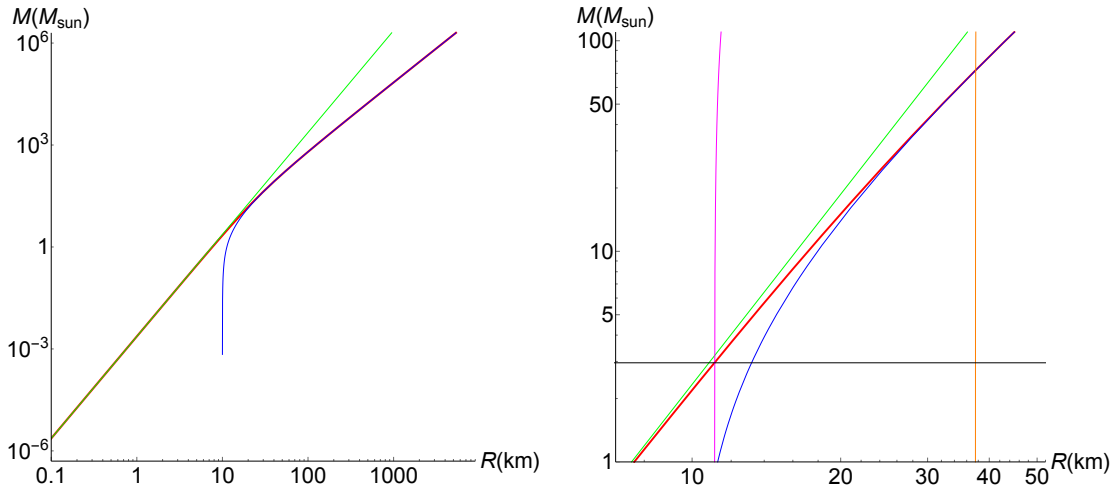

Figure 12.4: Gravitational effective mass as a function of matter radius for non-spinning spherical ultra-dense bodies of fixed density. The blue curve is the "black-hole" approximation of Eq. 12.24. The straight green line is the weak-gravity approximation of Eq. 12.23.
Vertical magenta and orange lines show the inner and outer light ring radii of Section 12.5.3.

Once a light-ring is formed, the nature of emitted signals changes in fundamental ways, and the resulting object develops many of the external appearances associated with the Black Hole of GR.

While it is possible in many cases to make quite precise determination of the pulsar mass, the determination of the pulsar radius is not nearly as advanced, as shown in Fig. 4 of [53]. The best values are good to $\approx 30\%$, and an uncertainty of a factor of 2 is normal. Taken as a group, the average radius seems to be near 10 km, which is the value we have used to determine our density ρ.

The reader is cautioned that the Özel-Freire review [53], and virtually all of the related literature, assume that GR is the correct theory of gravitation. As we have seen, in many cases G4v gives the same results as GR to the first order beyond Newton. However, the gravitational potential at the surface of a pulsar is already below c_0 by a substantial fraction, and first-order corrections may or may not give the same results. For slightly more massive objects, G4v gives well-behaved continuous solutions where GR may give singular ones. In light of these deep fundamental differences, it is somewhat surprising that the two theories predict quite similar observed behavior for a wide range of binary systems. In what follows we will attempt to highlight both the similarities and differences as they arise.

12.5.3 Circular Propagation of Light

Because light is deflected toward a massive body, there must be a radius at which a stable circular propagating solution around a sufficiently dense accumulation of matter is possible. We assume the body is sufficiently dense that r_c, the radius of the "light orbit," is outside the matter making up the body, and hence the interaction is of the form $1/r$. We can find that radius using the principle of stationary phase given in Eq. 7.16. The light propagation vector as a function of radius is given by Eq. 7.6:

$$k(r) = \frac{\omega}{c_0}\,\frac{1}{\left(1-\frac{k_0\chi}{r}\right)\left(1-\frac{\omega_0\chi}{c_0 r}\right)} \quad\Rightarrow\quad k(r_n) = \frac{\omega}{c_0}\,\frac{1}{\left(1-\frac{k_0\chi\sqrt{\rho}}{r_n}\right)\left(1-\frac{\omega_0\chi\sqrt{\rho}}{c_0 r_n}\right)} \tag{12.26}$$

To obtain the total phase ϕ around the orbit, we integrate around a circle of radius r centered on the object with Compton wave number k_0.

$$\phi = \int \vec{k}\cdot\vec{ds} \;=\; \frac{\omega}{c_0}\,\frac{2\pi r}{\left(1-\frac{k_0\chi}{r}\right)\left(1-\frac{\omega_0\chi}{c_0 r}\right)} = \frac{\omega}{c_0\sqrt{\rho}}\,\frac{2\pi r_n}{\left(1-\frac{k_0\chi\sqrt{\rho}}{r_n}\right)\left(1-\frac{\omega_0\chi\sqrt{\rho}}{c_0 r_n}\right)} \tag{12.27}$$

Using the values of ω_0 and k_0 from Eq. 12.18, we obtain

$$\phi_n = \phi \frac{c_0\sqrt{\rho}}{2\pi\omega} = \frac{r_n^3 \coth(R_n)}{((r_n - R_n)\coth(R_n) + 1)\,(r_n + R_n - R_n^2(\coth(R_n)))} \tag{12.28}$$

This equation has solutions for both positive and negative ϕ, corresponding to light propagating in opposite directions. The normalized phase ϕ_n is plotted as a function of normalized radius r_n in Fig. 12.5.

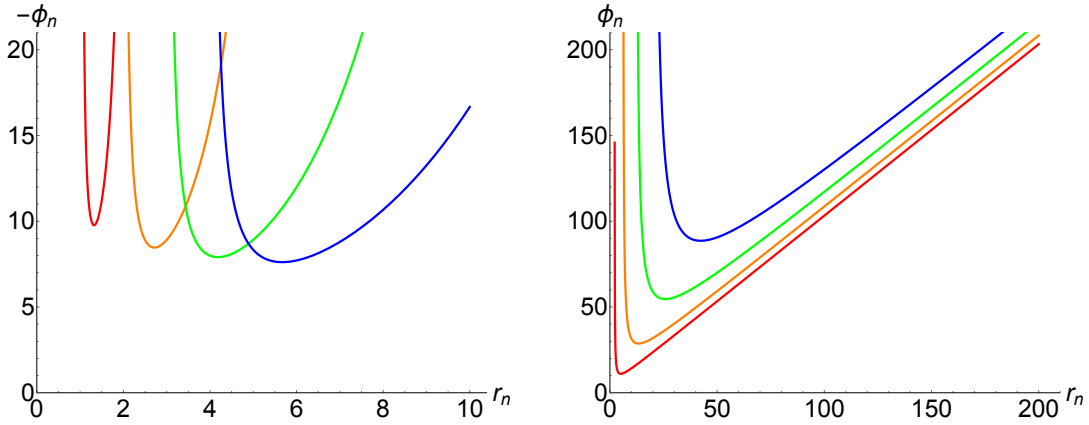

Figure 12.5: Normalized phase of circular paths from Eq. 12.28 for objects of R_n=2(red), 3(orange), 4(green), and 5(blue). The left curves are the negative branch and the right curves are the positive branch of ϕ. For both branches the minima indicate light rings.

This phase is stationary at the normalized **light-ring radius** r_{cn} where $\frac{\partial\phi_n}{\partial r_n} = 0$:

$$r_{cn} = \Big(R_n - \tanh(R_n)\Big)\left(R_n \coth(R_n) + 1 \pm \sqrt{R_n^2 \coth^2(R_n) - R_n \coth(R_n) + 1}\right) \tag{12.29}$$

where the $\pm\sqrt{\ }$ gives r_{cn} for both positive and negative branches of ϕ. An excellent approximation is available for the negative solution of large objects:

$$\text{“Black Hole”} \qquad R_n \gg 1 \qquad r_{cn} \to \frac{3R_n}{2} - \frac{15}{8} \tag{12.30}$$

The full expression is plotted for both negative and positive branches in Fig. 12.6.

12.6 Neutron Stars and Light-Rings

In Fig. 12.6 we have determined the conditions under which an accumulation of matter can result in a **light-ring**, where light can propagate in a circle around the object and not escape. We have seen that such a light-ring can form when $R_n > 1.11$ or $R \gtrsim 11$ km. We can express this result in terms of the minimum effective gravitational mass $M_{\rm min}$ of a massive body required to form a light-ring. From Eq. 12.25:

$$M_{\rm min} \approx 7M_\odot \times \Big(1.11^2\ \coth(1.11) - 1.11\Big) \approx 2.97M_\odot \tag{12.31}$$

As noted above, the most decisive information we have about neutron stars comes from observations of binary pulsars. Most observed pulsars have gravitational effective masses near $1.5M_\odot$, but individual pulsars have been observed with effective masses near $2M_\odot$. For $M_{\rm eff} < 2.97M_\odot$ the matter radius is larger than the light-ring radius, and the object acts like a normal neutron star. Although there are hints of neutron stars with masses edging up toward $3M_\odot$, so far the well-measured pulsars all fall in the normal neutron-star range, as highlighted in Fig. 12.7.

This figure should be compared with Fig. 4 (right) of Özel & Freire [53].

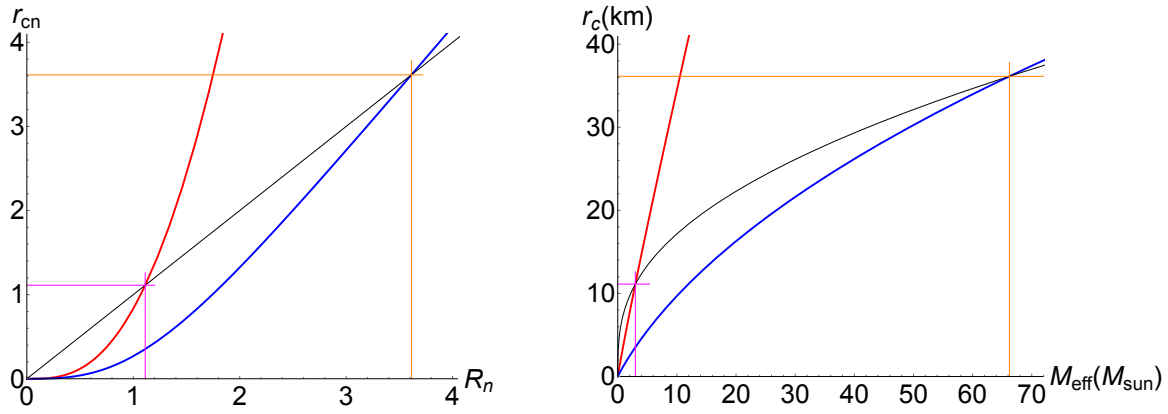

Figure 12.6: Light-ring radii r_c for negative (blue) and positive (red) branches of ϕ.
Left: r_{cn} *vs* R_n. Right: r_c *vs* effective mass M_{eff}. The black line is the matter radius R.
A light-ring can form when $r_c > R$, which corresponds to $R_n > 1.11$, $M_{\text{eff}} > 2.97$ (magenta) for the positive branch and $R_n > 3.613$, $M_{\text{eff}} > 66.2$ (orange) for the negative branch.

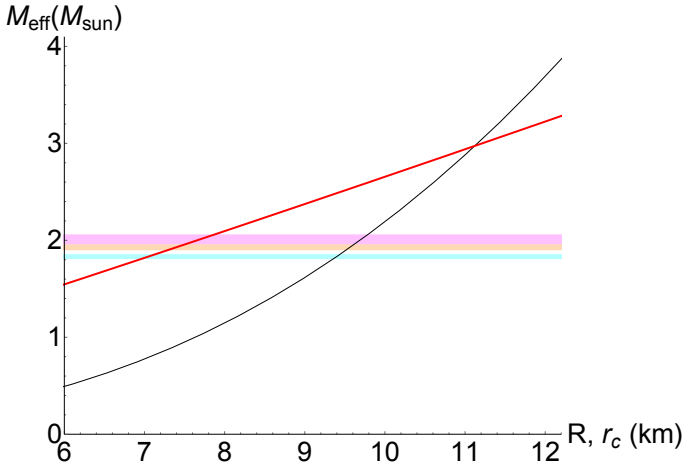

Figure 12.7: Effective mass M_{eff} *vs* matter radius R (black curve) and light-ring radius r_c (red curve) for static spherical objects of uniform matter density. The shaded bands are the masses of the most massive pulsars for which precise determinations have been possible to date: Magenta: PSR J0348+0432, Orange: PSR J1614-2230, Cyan: PSR J1946+3417.

12.7 Light-Rings, "Gravastars" and "Black Holes"

From Eq. 12.26, using ω_0 and k_0 from Eq. 12.18 and M_{eff} from Eq. 12.25, the propagation velocity v_c of a light wave at radius r from the center of a stationary massive body is:

$$\begin{aligned} v_c(r) &= \frac{\omega(r)}{k(r)} = c_0\left(1-\frac{k_0\chi\sqrt{\rho}}{r_n}\right)\left(1-\frac{\omega_0\chi\sqrt{\rho}}{c_0\, r_n}\right) \\ \frac{v_c}{c_0} &= \frac{\tanh(R)\big((r-R)\coth(R)+1\big)\left(r+R-R^2\coth(R)\right)}{r^2} \end{aligned} \tag{12.32}$$

This relation is plotted in Fig. 12.8:

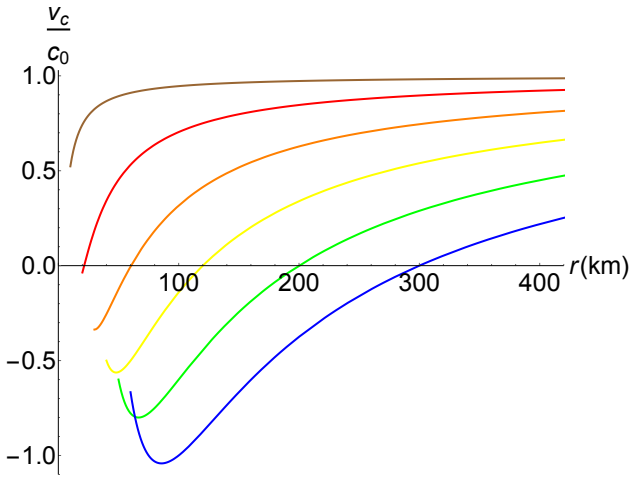

Figure 12.8: Velocity v_c of light Propagating in one direction in a circular path of radius r around a static spherical object of uniform matter density. Each curve is for an object of R_n=1(brown), 2(red), 3(orange), 4(yellow), 5(green), and 6(blue).

A great deal of care must be exercised in the interpretation of the light-velocity v_c as discussed in Section 7.6. It is the speed of a light wave propagating in *one direction*. Such a wave has a momentum $\hbar k$ that couples to the Compton wave-number of any local massive objects. The back-reaction from that coupling increases the propagation vector k for any given value of frequency ω, thereby lowering the speed of propagation below the local scalar potential c.

If we were to create a standing wave of the same frequency at the same location, for example in the Fabry-Parot cavity of a laser, the standing wave, having no net momentum, would have no net vector coupling to the massive object, and its dispersion relation would, instead of Eq. 12.32, be:

$$\frac{\omega(r)}{k(r)} = c_0\left(1 - \frac{\omega_0\chi\sqrt{\rho}}{c_0\, r_n}\right) = c_0\left(1 - \frac{k_0\chi\sqrt{\rho}}{r_n}\right) = c(r) \tag{12.33}$$

The scalar potential c never goes negative, as illustrated in Fig. 12.1, and energies of massive bodies are, by the dispersion relationalways greater than $k_0 c$ and hence never go negative, even in the most extreme gravity.

However, near sufficiently massive objects the speed of a one-way propagating wave of light (or gravitational radiation) can be brought to zero, as we see in Fig. 12.8. Engineers are familiar with the interaction of light with unique states of matter which have a similar effect on light propagation, where the "effective index of refraction" becomes negative. No disaster befalls us in these circumstances, and the interested reader can find amusing results under the heading **negative index** [54] [47].

In the present context, from Eq. 12.32, in G4v there will be a **horizon** where the one-way propagation velocity approaches zero at $r = r_H$:

$$\begin{aligned} &v_c \to 0 \quad \text{where} \quad \left(1 - \frac{k_0\chi}{r}\right) = 0 \\ &r_H = k_0\chi \quad \Rightarrow \quad r_{Hn} = k_0\chi\sqrt{\rho} = R_n^2\,\coth(R_n) - R_n \end{aligned} \tag{12.34}$$

where the final result comes from Eq. 12.17.
Using M_{eff} from Eq. 12.25, this relation is plotted, along with the light-ring radius, in Fig. 12.9:

The detailed observational consequences of objects with particular effective masses will, no doubt, be the subject of a great deal of controversy for many years. At present we only point out that Fig. 12.9 suggests the occurrence of three classes of ultra-dense objects:

$M_{\text{eff}} < 2.97 M_\odot$ Neutron Stars

$2.97 M_\odot < M_{\text{eff}} < 66.2 M_\odot$ Single-Light-Ring Stars

$M_{\text{eff}} > 66.2 M_\odot$ Double-Light-Ring Stars

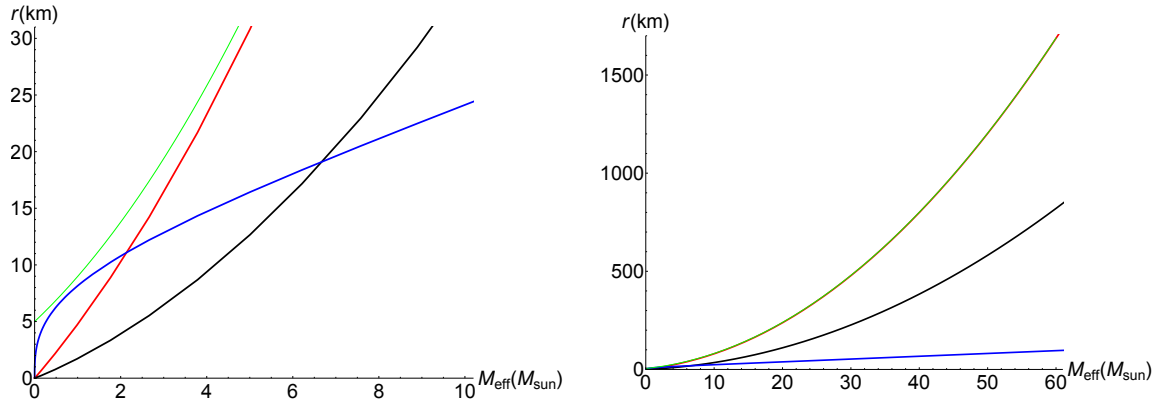

Figure 12.9: Light-ring radius r_c (red) from Eq. 12.29 and the (green) approximation of Eq. 12.30. The horizon r_H (black) is from Eq. 12.34, and (blue) is the matter surface $r = R$.
All plotted *vs* effective mass $M_{\rm eff}$ for static spherical objects of uniform matter density.

The light-ring will have a resonance at frequencies ω_{lr} where the phase around the ring is an integral number n cycles. From Eq. 12.27

$$\begin{aligned} \phi = \frac{\omega_{lr}}{c_0}\frac{2\pi r_c}{\left(1-\frac{k_0\chi}{r_c}\right)\left(1-\frac{\omega_0\chi}{c_0 r_c}\right)} &= n2\pi \\ f_{lr} = \frac{\omega_{lr}}{2\pi} = \frac{n\,c_0}{2\pi r_c}\left(1-\frac{k_0\chi}{r_c}\right)\left(1-\frac{\omega_0\chi}{c_0 r_c}\right) & \end{aligned} \tag{12.35}$$

Using ω_0 and k_0 from Eq. 12.18, r_c from Eq. 12.29, this relation becomes:

$$\begin{aligned} f_{lr} &= \frac{c_0 n\sqrt{\rho}\coth(R_n)\left(\sqrt{X}+1\right)\left(\sqrt{X}+R_n\coth(R_n)\right)}{2\pi(R_n\coth(R_n)-1)\left(\sqrt{X}+R_n\coth(R_n)+1\right)^3} \\ \text{where}\quad X &= {R_n}^2\coth^2(R_n) - R_n\coth(R_n)+1 \end{aligned} \tag{12.36}$$

In the "black hole" limit, where $M_{\rm eff} \gg 2.1M_\odot$, the normalized matter radius R_n, the light-ring radius r_c of Eq. 12.30 and the fundamental ($n = 1$) resonant frequency of Eq. 12.36 approach:

$$\begin{aligned} M_{\rm eff} \approx 7M_\odot\,(R_n-1) \quad &\rightarrow \quad R_n \approx \frac{M_{\rm eff}}{7M_\odot}+1 \\ r_{cn} \rightarrow 2R_n^2 - 1.5R_n \quad &\text{so} \quad r_c \rightarrow\approx 20\left(\frac{M_{\rm eff}}{7M_\odot}+1\right)^2 - 15\left(\frac{M_{\rm eff}}{7M_\odot}+1\right)\text{km} \\ f_{lr} \rightarrow \frac{c_0\sqrt{\rho}}{2\pi {R_n}^2} &\approx \left(\frac{7M_\odot}{M_{\rm eff}+7M_\odot}\right)^2 \times 1194\text{ Hz} \end{aligned} \tag{12.37}$$

where we have used $M_{\rm eff}$ and $\sqrt{\rho}$ from Eq. 12.24, Eq. 12.25 and discussion thereof.
The fundamental resonant frequency $f_{lr} = \omega_{lr}/2\pi$ is plotted in Fig. 12.36:

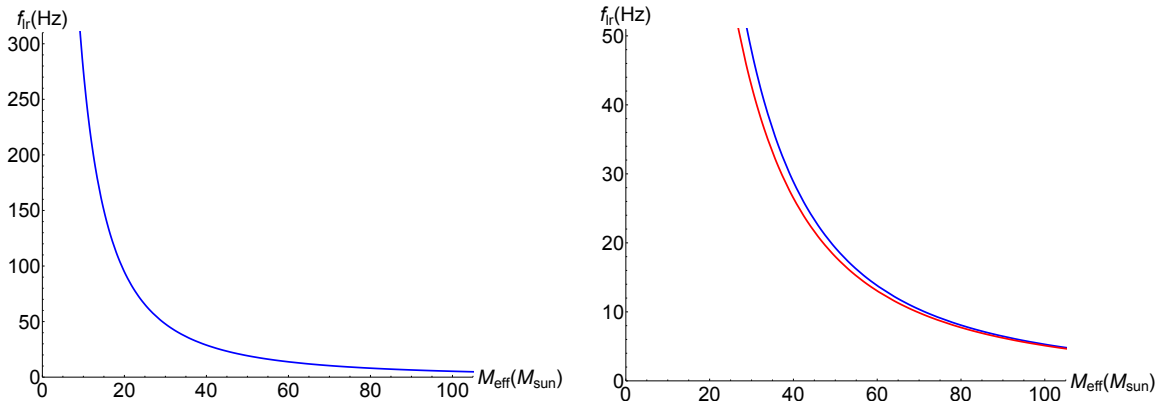

Figure 12.10: Light-ring fundamental resonant frequency f_{lr} *vs* effective mass M_{eff} for static spherical objects of uniform matter density. The blue curves are from Eq. 12.36 with $n = 1$; the red curve is the high-M_{eff} approximation of Eq. 12.37.

Because the light ring is non-dispersive, it can support an arbitrary number of harmonics. In particular, if the massive object is the result of a binary merger, the light ring of the combined object can support a "binary traveling pulse" as the remnant signature of the original objects.

Chapter 13

Conclusions

G4v recovers classical mechanics from a relativistically correct wave view of Quantum matter.

In the process G4v demonstrates that the observed behavior of matter is consistent with Mach's principle, and with the notion that the entire inertia and rest energy is due to the gravitational four-potential of the Universe.

G4v shows how the "mass" of a macroscopic object arises from the dispersion relation of its underlying quantum elements, and allows us to understand how energies, both nuclear and atomic, scale with gravitational potential.

I have highlighted the historic experiments that first showed clearly the coupling of gravitational scalar and vector potentials to the energy and momentum of Quantum matter waves.

In the process, G4v has become a simple approach to gravitation calculations beyond the Newtonian limit.
This approach has been applied to the frame-of-reference effects highlighted by Gravity Probe B, to the delay and deflection of light by massive bodies, to predicting the orbits around arbitrarily massive bodies, and to the gravitational redshift. In all these "standard tests of GR" G4v has obtained exactly the same expressions as those obtained by GR, to the first order beyond Newton.

The attributes of a simple G4v cosmology show, in broad brush, remarkable similarity to many GR based conclusions.

G4v predicts several results that are markedly different from those of GR:

1. The difference in speed of light between standing waves and propagating waves, which has probably already been observed in the carrier-envelope offset frequency of optical cavities, and should be studied in detail to quantify the effect of gravitational vector interaction.
   This experiment will show immediately whether G4v is right or wrong!
   It is discussed in Section 7.6, and I am personally dedicated to finding a way to do it!

2. G4v predicts a vector polarization in gravitational-wave radiation patterns, in addition to the diagonal-tensor-element polarization predicted by linearized GR[33]. GR predicts no vector contribution. My arXiv:1503.04866 posting did not include the tensor modes, which reference [33] predicts to be 4 times the amplitude of the G4v vector modes. The resolution of the three observatories that captured data from the historic GW170817 Neutron-star-merger sighting[38][37] was not sufficient to distinguish tensor+vector from pure tensor polarization. As more signals emerge from an increasing number of advanced gravitational-wave observatories, these predictions can be compared.

3. The two theories show very different results for the interior of ultra-high-density massive bodies such as neutron stars and black holes. Only time will tell if any of these predictions can be compared.

As I have pointed out at the end of many chapters, there is a great deal of work to be done before G4v can hold its own in a world where a vast number of extremely talented scientists rely on GR as an everyday language with which to describe gravitation. G4v has the advantage of great simplicity, both conceptual and mathematical, and of unification with electromagnetism and the Quantum nature of matter, but, as it stands, it is limited by not including tensor elements of the gravitational potential. I believe that a 4×4 tensor potential version, keeping the other desirable G4v attributes, is a feasible extension, but it is beyond my mathematical capabilities.

Finally, no theory is the ultimate theory: Each is just a step in the never-ending human quest to understand nature. My message to students is: There is Far More to be discovered than has already been discovered.
The exciting finds have seldom been on the beaten path. Develop your own intuition about How Nature Works. Mathematics is for making concepts precise and quantitative, but you must have the concept first!

As Einstein expressed it:

> As for the search for truth,
> I know from my own painful searching, with its many blind alleys,
> how hard it is to take a reliable step, be it ever so small,
> toward the understanding of that which is truly significant.

Bibliography

[1] Anderson, J. D., Esposito, P. B., Martin, W., Thornton, C., and Muhelman, D. Experimental Test of General Relativity Using Time-Delay Data from Mariner 6 and Mariner 7. *Astrophys. J. 200* (1975), 221–233.

[2] Barbour, J., and Pfister, H., Eds. *Mach's Principle*. Birkhäuser, 1995.

[3] Bergman, P. G. *Introduction to the Theory of Relativity*. Prentice Hall, New York, 1948.

[4] Berry, M. V. Quantum Phase Factors Accompanying Adiabatic Changes. *Proc. R. Soc. London, Ser. A 392* (1984), 45–57.

[5] Bertotti, B., Less, L., and Tortora, P. A Test of General Relativity Using Radio Links with the Cassini Spacecraft. *Nature 425* (Sept 2003), 374–376.

[6] Breton, R. P., et. al. Relativistic Spin Precession in the Double Pulsar. *Science 321*, 5885 (2008), 104–107. Available by subscription at: sciencemag.org.

[7] Callen, H. B., and Welton, T. A. Irreversibility and Generalized Noise. *Phys. Rev. 83*, 1 (1951), 34–40. Available at: lptms.u-psud.fr.

[8] Chou, C.-W., Hume, D. B., Rosenband, T., and Wineland, D. J. Optical clocks and relativity. *Science 329*, 5999 (2010), 1630–1633.

[9] Colella, R., Overhauser, A. W., and Werner, S. A. Observation of gravitationally induced quantum interference. *Physical Review Letters 34*, 23 (1975), 1472.

[10] Crabtree, G. W., Dye, D. H., Karim, D. P., Campbell, S. A., and Ketterson, J. B. Anisotropy of the Fermi surface, Fermi Velocity, Many-body Enhancement, and Superconducting Energy Gap in Nb. *Phys. Rev. B 35*, 4 (1987), 1728–1741.

[11] Damour, T., and Deruelle, N. General Relativistic Celestial Mechanics of Binary Systems II. The Post-Newtonian Timing Formula. *Ann. Inst. Henri Poincaré 44*, 3 (1986), 263–292. Available at: General Relativistic Celestial Mechanics...

[12] Davisson, C., and Germer, L. H. Diffraction of electrons by a crystal of nickel. *Physical review 30*, 6 (1927), 705.

[13] de Broglie, L. Ondes et Quanta. *Comptes Rendus 177* (Sep 1923), 507–510. Available at: in English (trans. by Brigitte and Barton Lane) and in French.

[14] Deaver, B. S., and Fairbank, W. M. Experimental Evidence for Quantized Flux in Superconducting Cylinders. *Phys. Rev. Lett. 7* (1961), 43–46.

[15] Demorest, P. B., Pennucci, T., Ransom, S. M., Roberts, M. S. E., and Hessels, J. W. T. Shapiro Delay Measurement of a Two Solar Mass Neutron Star. *Nature 467* (2010), 1081–1083. Available at: arxiv.org/abs/1010.5788.

[16] Doll, R., and Näbauer, M. Experimental proof of magnetic flux quantization in a superconducting ring. *Physical Review Letters 7*, 2 (1961), 51.

[17] Dyson, F. W., Eddington, A. S., and Davidson, C. A Determination of the Deflection of Light by the Sun's Gravitational Field, from Observations Made at the Total Eclipse of May 29, 1919. *Philos. Trans. R. Soc. London, Ser. A 220 issue 571–581* (1920), 291–333.

[18] Einstein, A. Zur Elektrodynamik Bewegter Körper. *Ann. Phys. T17*, 10 (1905), 891–921.

[19] Einstein, A. Gibt es eine Gravitationswirkung, die der Electrodynamischen Induktionswirkung Analog ist? *Vier. Gericht. Med. und Sanit. 44* (1912), 37–40.

[20] Einstein, A. Die Grundlage der Allgemeinen Relativitätstheorie. *Ann. Phys. T49*, 7 (1916), 769–822.

[21] Einstein, A. *The Meaning of Relativity: Four Lectures Delivered at Princeton University, May, 1921*. Methuen & Company Limited, 1922.

[22] Einstein, A. Lens-Like Action of a Star by the Deviation of Light in the Gravitational Field. *Science, New Series 84*, 2188 (1936), 506–507.

[23] Einstein, Albert. On the Influence of Gravitation on the Propagation of Light. *Annalen der Physik, 35*, 898–908 (1911), 906.

[24] Euler, L. *Methodus Inveniendi Lineas Curvas Maximi Minimive Proprietate Gaudentes, sive solutio problematis isoperimetrici lattissimo sensu accepti (Translation: A method for finding curved lines enjoying properties of maximum or minimum, or solution of isoperimetric problems in the broadest accepted sense).* Bousquet, Lausanne, Geneva, 1744, ch. Additamentum 2. A full discussion can be found at: Euler 1744.

[25] Feynman, R. P., Leighton, R. B., and Sands, M. *The Feynman Lectures on Physics*, vol. II. Addison-Wesley, Reading, 1964. Available at: FLP Vol. II.

[26] Freedman, W. L., et. al. Carnegie Hubble Program: A Mid-Infrared Calibration of the Hubble Constant. *Astrophys. J. 758*, 1 (2012), 1–10. Available at: Carnegie Hubble Program.

[27] Gravity Probe B. GPB Stanford. Available at: Gravity Probe B.

[28] Guo, J., McLemore, C. A., Xiang, C., Lee, D., Wu, L., Jin, W., Kelleher, M., Jin, N., Mason, D., Chang, L., et al. Chip-based laser with 1-hertz integrated linewidth. *Science advances 8*, 43 (2022), eabp9006.

[29] Hildebrandt, A. F. Magnetic Field of a Rotating Superconductor. *Phys. Rev. Lett. 12* (1964), 190.

[30] Holdridge, D. An Alternate Expression for Light Time Using General Relativity. In *Space Programs Summary 37-48, Vol. III.* Jet Propulsion Lab, 1967, pp. 2–4.

[31] Hubble, E. A relation between distance and radial velocity among extra-galactic nebulae. *Proceedings of the national academy of sciences 15*, 3 (1929), 168–173.

[32] Humphreys, E. M. L., et. al. Toward a New Geometric Distance to the Active Galaxy NGC 4258. III. Final Results and the Hubble Constant. *arxiv* (2013), 1–37. Available at: arxiv.org/abs/1307.6031.

[33] Isi, M., Weinstein, A. J., Mead, C., and Pitkin, M. Detecting Beyond–Einstein Polarizations of Continuous Gravitational Waves. *Phys. Rev. D. 91, I8* (Apr 2015), 82002–82021. Available at: arxiv.org/abs/1502.00333.

[34] Jaklevic, R., Lambe, J., Silver, A., and Mercereau, J. Quantum interference from a static vector potential in a field-free region. *Physical Review Letters 12*, 11 (1964), 274.

[35] Jones, D. J., Diddams, S. A., Ranka, J. K., Stentz, A., Windeler, R. S., Hall, J. L., and Cundiff, S. T. Carrier-envelope phase control of femtosecond mode-locked lasers and direct optical frequency synthesis. *Science 288*, 5466 (2000), 635–639.

[36] Lewis, G. N. On Four-dimensional Vector Analysis, and its Application in Electrical Theory. *Proceedings of the American Academy of Arts and Sciences 46*, 7 (1910), 165–181.

[37] LIGO Scientific Collaboration and Virgo Collaboration. GW170817: Observation of Gravitational Waves from a Binary Neutron Star Inspiral. *Phys. Rev. Lett. 119, 161101* (2017). Available at: www.ligo.org.

[38] LIGO Scientific Collaboration and Virgo Collaboration. Multi-messenger Observations of a Binary Neutron Star Merger. *Astrophys. J. Lett. 848:L12* (2017), 1–59. Available at: iopscience.iop.org.

[39] London, F. *Superfluids*, vol. 1. John Wiley, New York, 1950.

[40] Mach, E. *Die Mechanik in ihrer Entwicklung.* F. A. Brockhaus, Leipzig, 1883. Seven editions: 1883, 1888, 1897, 1901, ..., 1912.

[41] Mach, E. *The Science of Mechanics.* Open Court, La Salle, IL, 1893. English Edition. Four English editions, final 1919: Reprinted 1902, 1919.

[42] Marett, D. The Sagnac Effect: Does it Contradict Relativity?, 2012. Available at: The Sagnac Effect.

[43] McDonald, K. T. Radiated Power Distribution in the Far Zone of a Moving Charge, 2014. Available at: www.physics.princeton.edu/˜ mcdonald/examples/movingfar.

[44] Mead, C. A. *Collective Electrodynamics: Quantum Foundations of Electromagnetism*. MIT Press, Cambridge, MA., 2000, 2002. 2002 edition provides corrections, additions in the Epilogue, and reference to Gilbert Lewis.

[45] Mead, C. A. Gravitational Waves in G4v. *arxiv* (2015). Available at: arxiv.org/abs/1503.04866.

[46] Miller, M. C. Astrophysics: Weighing in on neutron stars. *Nature 467* (2010), 1057–1058.

[47] Moser, H. O., and Rockstuhl, C. 3D THz metamaterials from micro/nanomanufacturing. *Laser Photonics Rev. Rev. 6*, 2 (2012), 219–244. Available at: Laser Photonics Rev.

[48] Newton, I. *Mathematical Principles of Natural Philosophy*. H. D. Symonds, London, 1687. English translation by Andrew Motte (1846) (file size 50MB) at: Newton 1687, See pg. 81.

[49] Onnes, H. K. Further experiments with liquid helium. c. on the change of electric resistance of pure metals at very low temperatures etc. iv. the resistance of pure mercury at helium temperatures. In *KNAW, Proceedings* (1911), vol. 13, pp. 1910–1911.

[50] Onnes, H. K. *Further Experiments with Liquid Helium: G. On the Electrical Resistance of Pure Metals, Etc. VI. On the Sudden Change in the Rate at which the Resistance of Mercury Disappears*. 1911.

[51] Onnes, H. K. Further experiments with liquid helium. c. on the change of electric resistance of pure metals at very low temperatures etc. iv. the resistance of pure mercury at helium temperatures. In *Through Measurement to Knowledge: The Selected Papers of Heike Kamerlingh Onnes 1853–1926*. Springer, 1991, pp. 261–263.

[52] Özel, F., Dimitrios, P., Güver, T., Baym, G., C., H., and Guillot, S. The Dense Matter Equation of State from Neutron Star Radius and Mass Measurements. *arxiv* (2015). Available at: arxiv.org/abs/1505.05155.

[53] Özel, F., and Freire, P. Masses, Radii, and Equation of State of Neutron Stars. *arxiv* (2016). Available at: arxiv.org/abs/1603.02698 or Annual Review of Astronomy and Astrophysics, vol. 54, 401.

[54] Padilla, W. J., Basov, D. N., and Smith, D. R. Negative refractive index metamaterials. *Materials Today 9*, 7–8 (2006), 28–35. Available at: infrared.ucsd.edu.

[55] Planck Collaboration: et. al. Planck 2013 Results. XVI. Cosmological Parameters. *arxiv* (2013), 1–67. Available at: arxiv.org/abs/1303.5076.

[56] Reasenberg, R. D., Shapiro, I. I., MacNeil, P. E., Goldstein, R. B., Breidenthal, J. C., and Brenkle, J. P. Viking Relativity Experiment - Verification of Signal Retardation by Solar Gravity. *Astrophys. J., Part 2 - Letters to the Editor 234* (1979), L219–L221.

[57] Renn, J. *Genesis of General Relativity*. Springer, 2007. Note: A very insightful analysis of this period, with translation of many of the original papers into English, particularly Vol. 3.

[58] Riess, A. G. e. a. A redetermination of the hubble constant with the hubble space telescope from a differential distance ladder. *Astrophys. J. 699* (2009), 539–563.

[59] Riess, A. G., et al. A 3% Solution: Determination of the Hubble Constant with the Hubble Space Telescope and Wide Field Camera 3. *Astrophys. J. 730*, 2 (2011), 119–174. Available at: arxiv.org/abs/1103.2976.

[60] Sagnac, G. The luminiferous ether is detected as a wind effect relative to the ether using a uniformly rotating interferometer, 1913.

[61] Schliesser, A., Gohle, C., Udem, T., and Hänsch, T. W. Complete Characterization of a Broadband High-Finesse Cavity Using an Optical Frequency Comb. *Optics Express 14*, 13 (2006), 5975–5983.

[62] Sciama, D. W. On the Origin of Inertia. *Monthly Notices of the Royal Astronomical Society 113* (1953), 34–42. Available at: On the Origin of Inertia.

[63] Shapiro, I. I. Fourth Test of General Relativity. *Phys. Rev. Lett. 13*, 26 (1964), 789–791.

[64] Shapiro, I. I. Fourth Test of General Relativity: Preliminary Results. *Phys. Rev. Lett. 20*, 22 (1968), 1265–1269.

[65] Shapiro, I. I., Ash, M. E., Ingalls, R. P., Smith, W. B., Campbell, D. B., Dyce, R. B., Jurgens, R. F., and Pettengill, G. H. Fourth test of general relativity: new radar result. *Physical Review Letters 26*, 18 (1971), 1132.

[66] Smoot, G. F., Gorenstein, M. V., and Muller, R. A. Detection of anisotropy in the cosmic blackbody radiation. *Physical Review Letters 39*, 14 (1977), 898.

[67] Suyu, S. H., et. al. Two Accurate Time-Delay Distances from Strong Lensing: Implications for Cosmology. *Astrophys. J. 766:70* (2013), 1–19. Available at: iopscience.iop.org.

[68] Tate, J., Felch, S. B., and Cabrera, B. Determination of the Cooper-pair mass in niobium. *Phys. Rev. B 42*, 13 (1990), 7885–7896.

[69] Tausner, M. J. General Relativity and its Effects on Planetary Orbits and Interplanetary Observations. Tech. Rep. TK7855.M41.L741 no.425, MIT, 1966. Available from MIT Library (library.mit.edu) by request as call number TK7855.M41.L741 no.425. MIT privileges required.

[70] Thorne, K. S. Chapter VI.2 Gravitomagnetism, Jets in Quasars, and the Stanford Gyroscope Experiment. In *Near Zero*, Fairbank, J. D. and Deaver, B. S. and Everitt, C. W. F. and Michelson, P. F., Ed. Freeman, 1988, pp. 573–586.

[71] Vali, V., and Shorthill, R. Fiber ring interferometer. *Applied optics 15*, 5 (1976), 1099–1100.

[72] Werner, S., Colella, R., Overhauser, A., and Eagen, C. Neutron interferometry. Tech. rep., 1976.

[73] Werner, S., Staudenmann, J.-L., and Colella, R. Effect of earth's rotation on the quantum mechanical phase of the neutron. *Physical Review Letters 42*, 17 (1979), 1103.

[74] Wikipedia. Tests of general relativity. See Section: "Deflection of light by the Sun".

[75] Wilson, R., and Penzias, A. Isotropy of cosmic background radiation at 4080 megahertz. *Science 156*, 3778 (1967), 1100–1101.